Ecological resilience and the risk of land degradation in a dry Mediterranean rangeland

vorgelegt von
M. Sc.
Jennifer von Keyserlingk
ORCID: 0000-0003-2530-6316

an der Fakultät VI – Planen, Bauen, Umwelt
der Technischen Universität Berlin
zur Erlangung des akademischen Grades

Doktorin der Naturwissenschaften
- Dr. rer. nat. -

genehmigte Dissertation

Promotionsausschuss:

Vorsitzender: Prof. Dr. Martin Kaupenjohann
Gutachterin: Prof. Dr. Eva Nora Paton
Gutachterin: Prof. Dr. Birgit Kleinschmit
Gutachterin: Prof. Dr. Annegret Thieken

Tag der wissenschaftlichen Aussprache: 20. Juli 2021

Berlin 2021

Promotionsausschuss:

Vorsitzender:	Prof. Dr. Martin Kaupenjohann *TU Berlin; Institut für Ökologie; Bodenkunde*
Gutachterin:	Prof. Dr. Eva Nora Paton *TU Berlin; Institut für Ökologie; Ökohydrologie und Landschaftsbewertung*
Gutachterin:	Prof. Dr. Birgit Kleinschmit *TU Berlin; Institut für Landschaftsarchitektur und Umweltplanung; Geoinformation in der Umweltplanung*
Gutachterin:	Prof. Dr. Annegret Thieken *Universität Potsdam; Institut für Umweltwissenschaften und Geographie; Geographie und Naturrisikenforschung*

Diese Arbeit wurde im Rahmen des DFG-Graduiertenkollegs “Natural hazards and risks in a changing world“ (NatRiskChange) verfasst.

ABSTRACT

Land degradation, a negative trend in land conditions towards a less desirable ecosystem state caused by human activities, frequently happens once the ecological resilience of a system is critically reduced. Ecological resilience describes a system's ability to maintain its functional and structural integrity and persist without being pushed into another stable state under the influence of disturbance. In Mediterranean drylands, climatic events together with high human pressure are the main drivers of land degradation processes, such as erosion. Under the influence of climate change, the intensity and frequency of climatic triggers of land degradation, such as intensified climate variability and the occurrence of extreme hydro-meteorological events including droughts, is projected to increase distinctly in the Mediterranean region. Today, the immense damage caused by land degradation globally is well-recognized. However, coherent approaches for assessing and quantifying the extent of land degradation and associated damage over large areas, as well as for quantifying future risks, are still lacking.

In this thesis, the use of ecological resilience as a key concept to link land degradation assessment with quantitative risk analysis for natural hazards is suggested. Based on a systematic review of the discrepancies in existing land degradation risk assessment approaches, a conceptual risk-resilience model is proposed. Subsequently, ecological resilience to climate variability, particularly drought, is studied in a dry Mediterranean rangeland ('Randi Forest') located in southern Cyprus. Firstly, ecological resilience is spatiotemporally quantified, based on two resilience metrics: long-term resistance to climate variability, and recovery rate after drought. These two metrics are derived in a spatially explicit manner based on a 28-year Landsat NDVI time series analysis in combination with a change detection approach (BFAST) and breakpoint evaluation. Secondly, to deepen our understanding of what affects resilience in a Mediterranean dryland, the spatial variability of resistance to climate variability as well as of the recovery rate after drought are studied individually with regard to spatial distributions of grazing intensity and other environmental factors (terrain slope, aspect and mean NDVI). Thirdly, a combined resilience score based on resistance and recovery is derived to illustrate options for directly linking empirical, spatially explicit information on ecosystem resilience to land risk management goals. Finally, spatial dependencies between resilience categories are analysed.

The analysis revealed that high livestock grazing intensities as well as very low NDVI values (i.e. low green vegetation cover) were associated with high resistance, indicating a degraded, unresponsive ecosystem condition. Low grazing did not have a clear effect on resistance – it was suspected that under low grazing conditions other environmental conditions such as terrain effects control and limit vegetation dynamics. High NDVI values, as well as north-facing slopes also promoted high resistance, which, in this case, may be an indication of a healthy ecosystem state that is able to buffer climate variability well. Intermediate to high grazing levels as well as western/eastern orientation and average NDVI values promoted the occurrence of patches with low resistance, indicating areas with reduced resilience that may easily shift either to a degraded or a healthy state. Unlike expected, terrain slope had no effect on resistance.

Regression analysis showed that recovery rate after drought was positively affected by a northern orientation as well as by high NDVI values before the drought, and negatively related to grazing intensity. This indicates that overall favourable ecosystem conditions have a positive effect on recovery after drought. Further, on southern-oriented (but not on northern-oriented) slopes, terrain slope was negatively related with recovery, indicating a synergetic effect of slope steepness and southern orientation in their effect on recovery after drought. Finally, areas with low NDVI values before the drought were more sensitive to effects of a southern orientation than those with high NDVI values.

Based on resistance and recovery, a combined resilience score was developed. Resilience was spatially quantified for the Randi Forest study area using five distinct and easily interpretable resilience categories. The individual resilience categories were exemplarily linked to concrete land risk management goals based on the different phases used in the disaster risk management cycle (prevention, preparedness, response). As such, the approach contributes to relating land degradation research more closely to land risk management, as is already common practice for other natural hazards. Finally, an analysis of spatial dependencies between resilience classes showed that spatial resilience clusters exist in the Randi Forest study area, with spatial dependencies reaching up to 500 m. Data-based knowledge about the spatial location and extent of certain resilience clusters promotes a purposeful selection and prioritization of areas for specific land management actions and further field-based research on resilience and land degradation status.

In conclusion, results suggest that in a Mediterranean dryland resilience to climate variability, in particular drought, is modulated by livestock grazing, terrain effects and the amount of green vegetation cover. Particularly aspect and the amount of green vegetation cover seem to have major effect on resilience. On top of that, strong grazing promoted a degraded, unresponsive ecosystem state associated with low resistance and reduced recovery from drought. My results support the theory that anthropogenic land use affects ecological resilience to natural disturbances. Further, the derivation of a combined resilience score promotes the use of ecological resilience to link land degradation assessments with concrete land risk management goals and illustrates a practical approach to achieve this. The satellite data driven approach presented in this thesis has strong potential for resilience monitoring of ecosystems, for it can be applied on broad temporal and spatial scales in areas with low field data availability.

ZUSAMMENFASSUNG

Landdegradierung, eine durch menschliche Aktivitäten verursachte Verschlechterung des Ökosystemzustands, entsteht häufig, wenn die ökologische Resilienz eines Systems in kritischem Maße reduziert ist. Ökosystemresilienz beschreibt die Fähigkeit eines Ökosystems, seine funktionelle und strukturelle Integrität unter dem Einfluss von Störungen zu bewahren und fortzubestehen, ohne in einen anderen stabilen Systemzustand zu wechseln. In mediterranen Trockengebieten werden Landdegradierungsprozesse, wie z.B. Bodenerosion, vor allem durch klimatische Ereignisse in Kombination mit einer starken Beanspruchung durch den Menschen verursacht. Klimawandelszenarien prognostizieren, dass die Frequenz und Intensität der klimatischen Auslöser, die im Mittelmeergebiet zu Landdegradierung führen, deutlich zunehmen. So etwa ein Anstieg der klimatischen Variabilität insgesamt oder das Auftreten extremer hydrometeorologischer Ereignisse einschließlich Dürren. Heutzutage werden die enormen Schäden, die global durch Landdegradierung entstehen, allgemein anerkannt. Dennoch mangelt es an kohärenten Ansätzen, um das Ausmaß der Landdegradierung und der dadurch verursachten Schäden auf überregionaler Ebene festzustellen und zukünftige Risiken abzuschätzen.

In dieser Arbeit wird Ökosystemresilienz als Schlüsselkonzept vorgeschlagen, um Landdegradierungserhebungen mit der quantitativen Risikoanalyse von Naturgefahren zu verknüpfen. Auf der Grundlage einer systematischen Überprüfung der Diskrepanzen in bestehenden Ansätzen zur Risikoanalyse für Landdegradierung wird ein konzeptuelles Risiko-Resilienz-Modell herausgearbeitet. Anschließend wird Ökosystemresilienz gegenüber klimatischer Variabilität, insbesondere Dürre, in einem trockenen mediterranen Weideland (‚Randi Forest') in Südzypern untersucht. Zunächst wird die Ökosystemresilienz mit Hilfe von zwei Resilienz-Indikatoren raum-zeitlich quantifiziert: Langzeitresistenz gegenüber klimatischer Variabilität sowie Erholungsgeschwindigkeit nach einer Dürre. Basierend auf einer 28-jährigen Landsat NDVI-Zeitreihe in Kombination mit einer Bruchpunktanalyse werden diese beiden Indikatoren räumlich explizit quantifiziert. Um unser Verständnis darüber zu erweitern, welche Faktoren die Ökosystemresilienz in mediterranen Trockengebieten beeinflussen, werden in einem zweiten Schritt die räumliche Variabilität sowohl der Resistenz als auch der Erholzeit unabhängig voneinander in Zusammenhang mit der räumlichen Verteilung der Beweidungsintensität und anderen Umweltfaktoren (Geländeneigung, Hangexposition sowie mittlerer NDVI) untersucht. Im dritten Teil wird ein kombinierter Resilienzindex, basierend auf Resistenz und Erholungsgeschwindigkeit, berechnet, um Möglichkeiten zu illustrieren, wie sich empirische, räumlich-explizite Informationen über Ökosystemresilienz direkt mit Zielen des Land-Risikomanagements verbinden lassen. Zuletzt werden die räumlichen Abhängigkeiten zwischen den Resilienz-Klassen bestimmt.

Die Analysen ergaben, dass sowohl intensive Beweidung als auch sehr niedrige NDVI-Werte (i.e. eine geringe grüne Vegetationsbedeckung) mit einer überdurchschnittlich hohen Resistenz assoziiert waren, die in diesem Fall auf einen stark degradierten, trägen Systemzustand hindeutet. Geringe Beweidung hatte keine klare Auswirkung auf die Resistenz – bei geringer

Beweidung scheinen andere Umweltbedingungen wie Bodeneinflüsse die Vegetationsdynamik zu beherrschen. Hohe NDVI-Werte wie auch nord-orientierte Hänge begünstigten ebenfalls eine hohe Resistenz, die hier jedoch auf ein gesundes Ökosystem hinweisen könnte, das klimatische Störungen gut abzupuffern vermag. Mittlere Ökosystemkonditionen, i.e. mittlere NDVI-Werte, eine mäßige bis starke Beweidung sowie eine ost-/westliche Hangexposition, waren hingegen mit einer vergleichsweise geringen Resistenz assoziiert, was auf Bereiche mit verminderter Resilienz hindeutet, die sich leicht zu einem degradierten oder auch zu einem gesunden Ökosystemzustand entwickeln können. Anders als erwartet hatte die Geländeneigung keinen sichtbaren Einfluss auf die Resistenz.

Eine Regressionsanalyse ergab, dass die Erholungsgeschwindigkeit nach einer Dürre positiv von einer nördlichen Hangorientierung, von hohen NDVI-Werten vor einer Dürre und negativ von hohen Beweidungsintensitäten beeinflusst war. Das zeigt, dass sich insgesamt vorteilhafte Ökosystemkonditionen sowie geringer Beweidungsstress positiv auf die Erholungsgeschwindigkeit nach einer Dürre auswirken. Darüber hinaus hatte die Geländeneigung auf südorientierten Hängen (jedoch nicht auf nordorientierten Hängen) einen negativen Effekt auf die Erholungsgeschwindigkeit, was auf einen synergetischen Effekt zwischen Geländeneigung und Hangexposition hindeutet. Schließlich waren Bereiche mit sehr niedrigen NDVI-Werten vor der Dürre sensitiver gegenüber den negativen Effekten einer südlichen Hangexposition.

Im letzten Teil der Arbeit wurde ein kombinierter Resilienzindex, basierend auf Resistenz und Erholungsgeschwindigkeit, entwickelt. Mit Hilfe dieses Index wurde die Resilienz im Randi Forest Studiengebiet räumlich quantifiziert, dargestellt in fünf verschiedenen, leicht interpretierbaren Klassen. Darüber hinaus wurden die einzelnen Resilienzklassen exemplarisch mit einzelnen Phasen des Risiko-Kreislaufs aus dem Katastrophenmanagement verknüpft (Vorbeugung, Bereitschaftserhöhung, Bewältigung) und somit eine direkte Verbindung zu Zielen des Land-Risikomanagements hergestellt. Auf diese Weise trägt meine Arbeit dazu bei, Forschungen zur Dynamik der Landdegradierung enger mit Ansätzen des Land-Risikomanagements zu verknüpfen, wie es auch in Bezug auf andere Naturgefahren üblich ist. Eine räumliche Analyse der Resilienzklassen hat ergeben, dass es im Randi Forest Studiengebiet eine räumliche Clusterung gibt, mit räumlichen Abhängigkeiten zwischen den verschiedenen Resilienzklassen bis zu 500 m. Ein datenbasiertes Wissen über die räumliche Verteilung und das Ausmaß bestimmter Resilienzcluster fördert die zielgerichtete Auswahl und Priorisierung von Gegenden für spezifische Maßnahmen im Landmanagement, sowie für weitere feld-basierte Forschung.

Zusammenfassend weisen die Ergebnisse meiner Arbeit darauf hin, dass die Resilienz eines trockenen mediterranen Weidelandes gegenüber klimatischer Variabilität und speziell Dürre von der Beweidungsintensität, Geländeeffekten und dem Ausmaß der grünen Vegetationsbedeckung abhängt. Insbesondere die Hangexposition und der Grad der grünen Vegetationsbedeckung scheinen einen deutlichen Einfluss auf die Resilienz zu haben. Darüber hinaus zeigen die Resultate an, dass sehr starke Beweidungsintensität einen degradierten Systemzustand fördert, verbunden mit hoher Resistenz und langsamer Erholungsgeschwindigkeit, in dem die Vegetation nicht mehr auf klimatische Variabilität

reagieren kann. Meine Ergebnisse unterstützten die Theorie, dass menschliche Landnutzung die Ökosystemresilienz gegenüber natürlichen Störungen beeinflusst. Ferner treibt die Ableitung eines kombinierten Resilienzindikators die Möglichkeit voran, ökologische Resilienz zu nutzen, um Landdegradierungs-Analysen mit spezifischen Zielen des Land-Riskomanagements zu verknüpfen, und illustriert einen konkreten Weg, dies zu erreichen. Der hier präsentierte satelliten-basierte Ansatz besitzt ein hohes Potential zum Resilienz-Monitoring von Ökosystemen, da er sich auf räumlich und zeitlich großen Skalen auch in Gebieten mit geringer Felddatenverfügbarkeit anwenden lässt.

TABLE OF CONTENTS

LIST OF FIGURES

LIST OF TABLES

1 INTRODUCTION

1.1 ECOLOGICAL RESILIENCE IN CONTEXT OF THE RISK OF LAND DEGRADATION

Land degradation adversely affects ecosystems and people globally. In a current report of the Intergovernmental Panel on Climate Change (IPCC) it is defined as 'a negative trend in land condition, caused by direct or indirect human-induced processes including anthropogenic climate change, expressed as long-term reduction or loss of at least one of the following: biological productivity, ecological integrity or value to humans' (IPCC, 2019). It occurs over a quarter of the world's terrestrial ice-free area and has already begun with the Agricultural Revolution during Neolithic time, between 10,000 to 7,500 years ago (IPCC, 2019). Based on long-term trends of biomass productivity, Le et al. (2016) identified degradation hotspots over 29% of the global terrestrial land area, affecting about 3.2 billion people directly who reside there. However, the total number of affected people is likely to be higher, because the off-site effects of land degradation are considered to be even higher than the local effects (i.e. due to losses of global ecosystem services such as carbon sequestration and biodiversity) (Nkonya et al., 2016). Nowadays, the immense global damage potential of land degradation is well-recognized, yet there is still a lack of studies on the economics of land degradation (UNCCD, 2013). Estimates of the global annual costs of land degradation vary greatly, ranging between US$17.58 billion and US$9.4 trillion (Nkonya et al., 2016). The Millennium Ecosystem Assessment (MEA) revealed that approximately 60% of examined ecosystem services are being degraded (MEA, 2005a).

The processes of land degradation are diverse, encompassing soil degradation processes, such as wind- and water erosion or salinization, as well as biotic degradation, such as a loss of natural vegetation cover and/or of biodiversity or the woody encroachment of previously grass-dominated savannas. Land degradation processes can also act on the water balance, e.g. waterlogging of dry areas, or drying of continental waters or wetlands. Figure 1 illustrates different processes of land degradation. Land degradation processes operate on various temporal and spatial scales and are closely interlinked. Once degradation processes start at one level of the ecosystem, they usually entail other processes. Feedbacks between biotic and abiotic ecosystem components can lead to cascading effects that may result in sudden, sometimes irreversible non-linear transitions of the ecosystem state (Turnbull et al., 2008; Karssenberg et al., 2017).

Figure 1. Examples for different land degradation processes. Top left: strong overland flow after high intensity rainstorm event (New Mexico – SW USA). Top right: gully erosion in southern Cyprus. Bottom: shrub encroachment in a previously grass-dominated savanna in Namibia (picture adopted from Rohde and Hoffman (2012).

Unsustainable agriculture and clearing of land are considered as the main drivers of land degradation (UNCCD, 2009; IPCC, 2019). In combination with unsustainable land use, climate variability is another main driver of land degradation processes, especially in water-limited environments (UNCCD, 1994, 2009): unsustainably managed drylands often cannot recover well from drought, but tend to lose their biological and economic productivity (UNCCD, 2009). Other examples are short intensive rainfall events that can trigger severe gully erosion, the effects of which persist for decades (Showers, 2005); air temperature as well as water-availability affect the frequency and severity of wild-fires, which in turn affect vegetation cover and composition. Climate change exacerbates the rate of many ongoing degradation processes due to increasing temperatures, changing rainfall patterns with an increased frequency and/or intensity of heavy rainfall events as well as an increased frequency and severity of droughts and heat waves (IPCC, 2019). In reverse, several land degradation processes are also drivers of climate change:

deforestation and loss of natural vegetation, increasing wildfires, degradation of peat soils and permafrost thawing are reducing land carbon sinks and increasing emission of greenhouse gases (IPCC, 2019). These examples highlight an interlinkage between processes and drivers of land degradation that occurs on various levels, and makes it challenging to differentiate clearly between the two. In this work, I follow the approach of the IPCC, which defines processes of land degradation as the direct mechanisms degrading the land and drivers as the indirect conditions, which promote degradation processes, e.g. climate change pressure or changes in human land use (IPCC, 2019, p. 354).

Drylands are water-limited ecosystems, including all dry subhumid, semi-arid, arid or hyper-arid ecosystems (MEA, 2005b). Their bio-physical features in combination with anthropogenic pressure make drylands particularly vulnerable to land degradation (Reynolds et al., 2007). According to the UN, 70% of the world's drylands or 3.600 million hectares are already degraded, excluding hyper-arid areas (UNCCD, 2009). This trend is likely going to expand due to climate change and human population growth. Mediterranean drylands are characterised by aridity ranges that combine high human pressure with high vulnerability to degradation (Safriel, 2006). In addition, their highly variable intra- and interannual climate regime, including frequent droughts and intensive rainfall events, promotes land degradation processes such as erosion. In the Mediterranean, the degree of aridity, but particularly climate variability and frequency of extreme hydro-meteorological events is projected to increase due to climate change (IPCC, 2013, 2014). Compared to central and northern Europe the consequences of climate change projected for southern Europe by the IPCC are particularly drastic from an anthropogenic perspective: the provision of ecosystem services is projected to decline across all service categories. For all other European sub-regions both losses and gains in the provision of ecosystem services are projected in response to climate change (stated with *high confidence* in IPCC, 2014). A loss of ecosystem services in response to climate change corresponds exactly to the definition of land degradation – a loss of the land's value to humans (i.e. ecosystem services) caused by anthropogenic effects (IPCC, 2019).

Since drylands are often not productive enough for worthwhile arable farming, they are frequently used as pastureland. The FAO estimates that 26% of the world's ice-free land is used for livestock grazing, supporting about one billion people (mostly pastoralists in South Asia and sub-Saharan Africa) (FAO, 2012). Intensive livestock grazing has been shown to reduce the resilience of dryland ecosystems (Holling, 1996; Ruppert et al., 2015). For example, rangelands in savannas of southern Africa used for cattle grazing lose species diversity in favour of grazing resistant species, which are often less resilient to drought; this loss in diversity increases the likelihood for the system to flip into another system state dominated by woody shrubs (Holling, 1996; Dougill et al., 1999). Overgrazing reduces vegetation cover (Kawamura et al., 2005) and trampling further damages the soil, which strongly enhances the ecosystem's susceptibility to soil erosion (Zhou et al., 2010). Terrain also affects ecological resilience to climate variability: southern-oriented slopes, as well as steep slopes, are particularly vulnerable to soil erosion processes. In the northern hemisphere a southern orientation means a maximum exposure to solar radiation, which leads to particularly high evapotranspiration rates. On steep slopes, the

time for water infiltration into the soil is low, yielding high water runoff rates. In both cases, the conditions are unfavourable for vegetation. The combined effect of a loss of vegetation cover and soil erosion reduces the capacity of the ecosystem to resist and recover from drought (Mayor et al., 2013; Zhou et al., 2010). Figure 2 shows a degraded hillslope in a dry Mediterranean rangeland in southern Cyprus (located in the Randi Forest study area) suffering from frequent droughts and overgrazing by goats.

Figure 2. Degraded hillslope in the Randi Forest study area in southern Cyprus. Loss of natural vegetation cover with visible water erosion of the soil and clear signs of overgrazing (dwarf shape of shrubs and visible goat pathways indicate grazing).

In the face of continuing climate change, human population growth and an increasing over-exploitation of ecological resources several land degradation processes have been strongly intensified in the last century, and are projected to expand in many areas of the world (MEA, 2005a; IPCC, 2019). The Millennium Ecosystem Assessment states that 'over the past 50 years, humans have changed ecosystems more rapidly and extensively than in any comparable period of time in human history' (MEA, 2005a, p. 1). Thus, the potentially threatening nature of land degradation for people's livelihood becomes ever more perceivable. At present, 'land degradation represents – along with climate change – one of the biggest and most urgent challenges for humanity' (stated with *very high confidence* in IPCC, 2019, p. 348). This understanding brings forth the need to quantify and map the regional extend of land degradation in order to estimate the actual damage, but also to assess future risks of land degradation, thereby enabling land users to make informed decisions. Already the former has proven challenging; for the latter, a clear concept seems altogether lacking. In the state of the art chapter of this work, this issue is going to be addressed in detail. First, risk theory for natural hazards, based on the concepts developed within natural disaster risk research, is introduced. Second, land degradation is discussed as a natural hazard and approaches of land degradation

risk assessment are critically reviewed. Based on this review, ecological resilience is proposed as a key concept that has the potential to link land degradation assessment with quantitative risk analysis.

Ecological resilience describes a system's ability to maintain its structural integrity and persist without being pushed into another stable state under the influence of disturbance (Holling, 1973, 1996; Scheffer et al., 2015). Research has found convincing evidence that ecological regime shifts to less productive or less desired (i.e. degraded) states often occur in consequence of a loss of ecological resilience (Scheffer et al., 2001; Folke et al., 2004), or in other terms once a system is taken beyond its 'ecological resilience threshold' (Ibáñez et al., 2008, p. 181). Holling wrote that if ecological resilience is lost or reduced, 'a chance and rare event that previously could be absorbed can trigger a sudden dramatic change and loss of structural integrity of the system (Holling, 1973, p.21). Several studies report a threshold behaviour in ecosystem dynamics (e.g. Scheffer et al., 1993; Scheffer and Carpenter, 2003; Gao et al., 2011). Therefore, ecological resilience towards drivers of degradation processes directly relates to the dynamic aspect of land degradation, which has so far proved difficult to capture.

Remote sensing offers the possibility to infer aspects of ecological resilience from natural time series across large spatial and temporal scales even in otherwise data limited regions. Hence, with the increasing availability of remotely sensed data, several approaches to quantify resilience have emerged in scientific literature (see e.g. Washington-Allen et al., 2008; Frazier et al., 2013; De Keersmaecker et al., 2015; Schwalm et al., 2017). A frequently used tool to study ecosystem dynamics from space are vegetation indices, such as the Normalized Difference Vegetation Index (NDVI). The NDVI makes use of the unique spectral reflectance pattern displayed by photosynthetically active 'green' vegetation in the visible red and near-infrared spectral region when compared to other surfaces (Rouse et al., 1974; Myneni et al., 1995). The NDVI has been found to correlate with structural and functional characteristics of vegetation, such aboveground green biomass, basal cover, Net Primary Production (NPP) and Absorbed Photosynthetic Active Radiation (APAR) (Rouse et al., 1974; Tucker, 1979; Gamon et al., 1995; Pettorelli et al., 2005; Olofsson et al., 2007; Gaitán et al., 2013). In Mediterranean drylands, a reduction in vegetation greenness can indicate land degradation, which is often characterised by a loss of natural vegetation cover associated with an increase in bare soil (Tomaselli, 1977).

In this thesis, a methodological approach to spatiotemporally quantify two key aspects of ecological resilience to climate variability is developed based on long-term NDVI time series and a change detection method. The approach is applied to a grazed Mediterranean dryland located in southern Cyprus (Randi Forest study area, see Figure 2). Proxies for ecosystem resistance to climate variability (such as intra- and interannual rainfall variability and drought events) and recovery rate after drought are quantified spatially. In a next step the spatial variability of resistance and recovery are studied individually with regard to spatial differences in grazing intensity and environmental properties. Finally, the gathered information on resistance and recovery is used to create a combined resilience score in order to illustrate how empirical information on resilience can be linked to land risk management goals.

Contributing to the understanding of ecological resilience to climate variability in the context of land degradation dynamics in dry rangelands of southern Europe was the main motivation for this thesis. Further, illustrating the potential of ecological resilience as a key concept to link land degradation assessment to quantitative risk analysis, as an important step towards improving the quantification of future land degradation risk and for developing effective land risk management strategies.

1.2 RESEARCH OBJECTIVES

In the following, the four research objectives addressed in this thesis are introduced.

Objective 1: spatial quantification and mapping of ecosystem resistance to climate variability and recovery rate after drought in a dry rangeland of southern Cyprus, using proxies derived from satellite time series data by means of a change detection method and breakpoint analysis.

A methodological approach to spatially quantify two key aspects of ecological resilience (resistance and recovery) was developed and applied to a grazed rangeland in southern Cyprus. To this purpose, an existing change detection approach (BFAST) (Verbesselt et al., 2010a, 2010b) was adapted and applied spatially to a long-term Landsat NDVI time series. BFAST integrates the fitting of additive seasonal trend models to the data with an approach to detect changes within time series (Verbesselt et al., 2010a). Breakpoints in NDVI time series indicate abrupt changes in the additive seasonal and trend model, indicating effects of disturbance or land cover change (Verbesselt et al., 2010a). In this thesis, I interpret breakpoints in the time series as representing the response of vegetation to climate variability, including droughts. This is motivated firstly, by the knowledge that semi-arid drylands are water-limited systems; hence, vegetation dynamics are strongly climate-driven. Second, by the fact that no large-scale disturbance (except grazing) or land cover change was known by local land users in the study area. Finally, because BFAST has been reported to successfully capture drought induced trend changes (Verbesselt et al., 2010a; Huang et al., 2014) and has been already validated and tested for detecting vegetation changes in arid environments (Watts and Laffan, 2014; Browning et al., 2017).

Based on this reasoning, the relative number of breakpoints fitted within the NDVI time series was used as an inverted measure for vegetation resistance to climate variability. It was assumed that the higher the ecological resistance to climatic disturbances such as droughts, the lower the likelihood to experience breakpoints in the time series. As a proxy for recovery rate after drought, the linear trend fitted by the BFAST model after a known drought event was used. Maps showing the spatial distribution of resistance and recovery rate in the Randi Forest study area were produced.

Objective 2: analysis of the spatial distribution of resistance to climate variability over spatial gradients of grazing intensity, mean NDVI and topographic properties in a dry rangeland in Cyprus.

While the first objective aims at a spatially explicit, satellite-based quantification of two resilience indicators, the second and third objectives address the question how resilience to climate variability is modulated by livestock grazing and environmental factors.

For the second objective, I studied spatial density distributions of my proxy for resistance over spatial gradients of grazing, terrain slope and orientation, as well as mean NDVI. I expected that resistance to climate variability is affected by the ecosystem state: a healthy ecosystem should be able to buffer climatic variation well, and thus have a high resistance (phase C in Figure 3). On the other hand, a strongly degraded ecosystem that has reached an almost barren state, or in areas with rocky surfaces, the ecosystem cannot react to climate variability; while a drought would have little effect, the system also cannot benefit from years with high rainfall. In such an unresponsive ecosystem state, I also expected high resistance (phase A in Figure 3). In intermediate ecosystem conditions, resistance was expected to be low, indicating transient system behaviour (phase B in Figure 3). Resistance as used in this thesis is therefore not an indication of ecosystem health or sustainability. Rather, it purely relates to the system's resistance to disturbance within its current state, which can be a degraded or a healthy one.
Landsat pixels with high resistance were expected to show a bimodal density distribution with regard to ecosystem state (blue line, phases A and C), with maxima of data points concentrated in very healthy areas (i.e. associated with low grazing intensity, northern orientation, shallow slopes, high NDVI values) as well as in strongly degraded areas (i.e. associated with high grazing intensity, southern orientation, steep slopes, very low NDVI values). In contrast, most data points of pixels with low resistance (red line, phase B) were expected to be concentrated in intermediate ranges of ecosystem health.

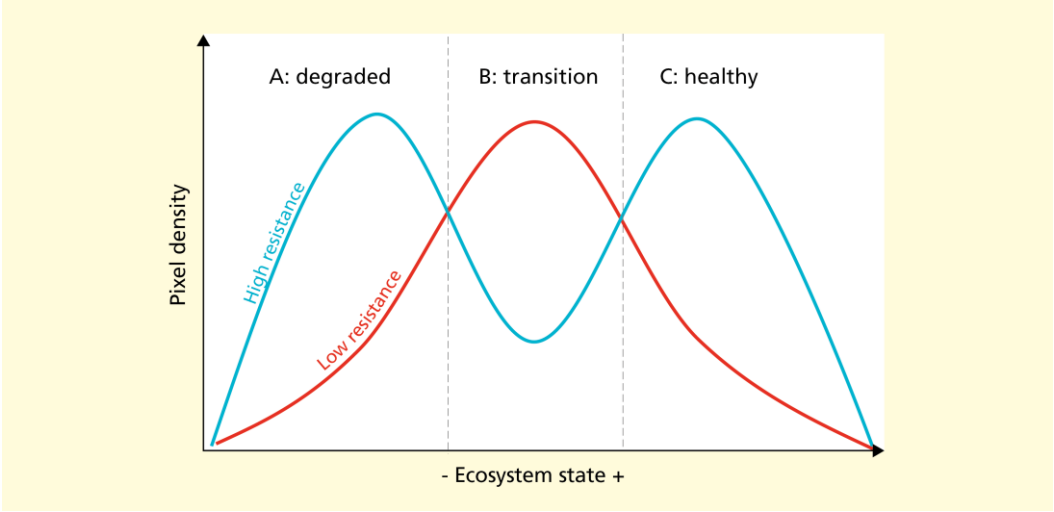

Figure 3[1]. Graphical hypothesis of resistance related to ecosystem state. The spatial density distribution of Landsat pixels representing high resistance were expected to show a bimodal pattern with regard to ecosystem state (blue line). Maxima were expected at a strongly degraded (phase A) as well as at a very healthy (phase C) ecosystem state. Pixels representing areas with low resistance (red line) were expected to be concentrated at intermediate ranges of ecosystem health, associated with areas in transition between states (phase B).

[1] This figure appears in similar form in von Keyserlingk et al. (2021).

My hypothesis about resistance (and later also recovery rate) with regard to ecosystem states is supported by López et al. (2013). Based on a study in the steppes of North Patagonia they suggested that in a healthy ecosystem state stability would be associated with high resistance in combination with a high recovery potential (termed 'resilience' in López et al. (2013)); beyond a critical threshold the ecosystem would become unstable, which would be associated with a reduction in resistance and recovery potential. In a highly degraded state the ecosystem would reach an indifferent stable dynamic equilibrium, which would be associated with enhanced resistance to a disturbance factor, but with a loss in recovery potential (López et al., 2013).

Objective 3: analysis of the effects of grazing intensity, mean NDVI and topographic properties on the spatial variability of the recovery rate after drought in a dry rangeland in Cyprus.

I expected all factors promoting degradation in my study area, namely a high grazing intensity, a southern orientation and steep slopes, to be negatively linked with the recovery rate of the vegetation after drought. Further, I expected that high vegetation cover before the drought, indicated by high NDVI values, would foster the ability to recovery. Hence, I expected a positive relationship between mean NDVI values before the drought and subsequent recovery rates.

This hypothesis is in line with suggestions for the relationship between recovery potential and degradation states by López et al. (2013), which I have cited in the previous segment dealing with objective 2.

To test the hypothesis, a regression approach was applied. First, modelling the relationships between recovery rate and grazing, as well as environmental factors individually; secondly, using a combined approach.

Objective 4: derivation of an exemplary resilience score, based on ecosystem resistance and recovery, which can be related to land risk management goals, followed by an assessment of the spatial dependencies between resilience classes.

This objective aims at integrating the previously obtained information on resistance and recovery in an applied context. To this effect, information on resistance and recovery were combined in an integrated resilience score. A resilience map for the Randi Forest study area in southern Cyprus was produced. Options to link each resilience category to land risk management goals were illustrated. Finally, spatial dependencies between resilience classes were analysed. Knowledge about the existence, extent and location of resilience clusters is important information for land managers aiming at resilience-based land management to reduce or react to the risk of land degradation.

1.3 OVERVIEW OF THE THESIS

The thesis is structured in a comprehensive state of the arts chapter, a method part, a combined result and discussion section, and conclusions.

The first part of the state of the art chapter (section 2.1) introduces quantitative risk theory for natural hazards and discusses land degradation as a natural hazard. A critical review of risk assessment approaches for land degradation is performed and ideas towards a land degradation risk assessment model funded on the concept of ecological resilience and the concepts of disaster risk research are presented. The second part of the state of the art chapter (section 2.2) deals with approaches to quantify ecological resilience and in that context introduces remote sensing and change detection methods.

The section 'material and methods' contains a detailed description of the Randi Forest study site in the broader context of land degradation in the Mediterranean ecozone (section 3.1). Further, all input data and pre-processing steps are described (sections 3.2 & 3.3). The methodological approach to extract proxies for resistance and recovery rate is presented, including a detailed description of the change detection approach (section 3.4). Finally, all data analysis steps are described (section 3.5).

The result and discussion chapter is structured in four subchapters (sections 4.1–4.4). Each presenting and discussing results related to one research objective of this thesis (see 1.2) in chronological order. Short conclusions summarize the main findings for each result subchapter.

The conclusions chapter begins with summarizing the main findings related to each research objective (section 5.1). Results are shortly discussed in the overall context of this thesis. In a second part (section 5.2), methodological limitations of the developed approach to quantify resilience are discussed, as well as limitations with regard to interpreting grazing effects on resilience. Finally, an outlook (section 5.3) into possible future research topics is given, followed by final remarks (section 5.4).

A list of abbreviations as well as a glossary are included to provide clarification of all used terminology for readers throughout the thesis (sections 8 & 9).

Parts of this thesis have been published as:

von Keyserlingk, J., de Hoop, M., Mayor, A.G., Dekker, S.C., Rietkerk, M., Foerster, S., 2021. Resilience of vegetation to drought: Studying the effect of grazing in a Mediterranean rangeland using satellite time series. Remote Sens. Environ. 255, 112270. https://doi.org/10.1016/j.rse.2020.112270

The article was prepared in close cooperation with Myrna de Hoop from Utrecht University. Footnotes indicate if figures, tables or substantial text parts of certain sections appear in similar form in that article. Individual elements that are based to more than 50% on work by M. de Hoop are marked additionally by footnotes.

2 STATE OF THE ART

2.1 LAND DEGRADATION IN THE CONTEXT OF DISASTER RISK RESEARCH AND QUANTITATIVE RISK ASSESSMENT FOR NATURAL HAZARDS

This chapter provides a background to the concepts of disaster risk research and risk assessment for natural hazards (2.1.1). Land degradation as a natural hazard is discussed (2.1.2). A critical review of selected studies assesses the discrepancies in current land degradation risk assessment approaches (2.1.3 & 2.1.4). Based on identified conceptual shortcomings, ideas for a comprehensive framework for a quantitative land degradation risk assessment are developed (2.1.5).

2.1.1 Introduction to risk theory for natural hazards

Natural hazards are natural processes or phenomena, such as floods, earthquakes, storms, droughts or volcanic activity that affect elements of human systems in a threatening manner (Alcántara-Ayala, 2002). In other words that 'may cause loss of life, injury or other health impacts, property damage, loss of livelihoods and services, social and economic disruption, or environmental damage' (UNISDR, 2009, p. 20). The extent to which hazards result in actual damage depends on the one hand on the spatial and temporal exposure of the elements at risk, on the other hand on the vulnerability of these elements. Vulnerability represents the predisposition of elements that makes them susceptible to damage (Cardona, 2003; UNISDR, 2009). In addition to the vulnerability of the human system (socio-economic aspects) also the vulnerability of the affected ecosystem has to be considered, particularly when it comes to land degradation. Both are closely interlinked and the need for a coupling of natural and human vulnerabilities has been stressed in several studies (e.g. in Alcántara-Ayala, 2002; Turner et al., 2003). When both types of vulnerability occur at the same time and place, natural disasters can occur (Alcántara-Ayala, 2002). A disaster is defined as 'a serious disruption of the functioning of a community or a society involving widespread human, material, economic or environmental losses and impacts, which exceeds the ability of the affected community or society to cope using its own resources' (UNISDR, 2009, p. 9). The possibility for future disasters is described by the term disaster risk (UNISDR, 2009; IPCC, 2012), which has been internationally established within the Sendai Framework of Disaster Risk Reduction 2015-2030 (UNISDR, 2015).

The risk terminology introduced above shows that risk is a concept based on a concomitance of hazard, exposure and vulnerability: 'one cannot be vulnerable if one is not threatened, and one cannot be threatened if one is not exposed and vulnerable' (Cardona, 2003). For a better understanding of risk and for effective risk reduction measures, it is important to differentiate clearly between hazard, vulnerability and risk (Cardona, 2003). However, in the past, the term risk was frequently used synonymously with hazard or vulnerability and varying approaches to **risk assessment** have evolved in different disciplines (Cardona, 2003). In the following, different approaches from natural, applied and social scientists are briefly summarized, based on a comprehensive overview given in Cardona (2003):

> **Natural sciences** traditionally focused on the physical causes of the hazard (e.g. earthquakes, floods, storms). In earlier days, risk was frequently expressed as the probability of hazard occurrence and graphically represented in the form of hazard maps (Plate and Merz, 2011). This approach resulted in a confusion between hazard and risk, for an intense natural event does not necessarily result in a (natural) disaster.
>
> In **applied sciences**, particularly in engineering**,** the focus lay on the effects of an event rather than on the event itself. Methods for damage quantification were established and the concept of physical vulnerability was promoted. This approach favoured a static concept of vulnerability, where vulnerability was interpreted as a fixed feature (i.e. mainly related to the degree of exposure of objects) rather than an ongoing condition or predisposition. Results were often presented in the form of vulnerability maps, damage matrixes or vulnerability indices.
>
> In **social sciences**, the focus lay on the perception of risk, aimed at understanding how individual people or societies perceive and react to a hazard. This approach introduced a different perspective on vulnerability, focussing on the capacity of entities, e.g., communities, to absorb and recover from the impact of a hazardous event. Here one has to take into account that a lot of the work on international disaster preparedness originates in humanitarian aid. Accordingly, results were used to develop prevention measures and disaster response measures, yet it did not aim for a quantification of risk.

(Cardona, 2003)

Towards the end of the 20th century, **quantitative risk assessment** approaches incorporating both hazard and vulnerability have been developed (e.g. by Kaplan and Garrick, 1981). Kaplan and Garrick (1981, p. 13) suggested that 'risk is probability *and* consequence'. This idea has been adopted by international disaster risk research and is nowadays well established in natural sciences, the insurance sector, as well as in decision making. The United Nations define risk as 'the combination of the probability of an event and its negative consequences' (UNISDR, 2009, p. 25); and disaster risk as 'the potential disaster losses, in lives, health status, livelihoods, assets and services, which could occur to a particular community or a society over some specified future time period' (UNISDR, 2009, pp. 9–10). Formally, risk R can be expressed as a function of hazard H, vulnerability V and exposure E with $R = f(H, V, E)$. Figure 4 exemplarily shows the risk conceptualization as implemented by the Intergovernmental Panel on Climate Change (IPCC) in a special report on managing the risk of extreme events and disasters (IPCC, 2012). (Compare also Figure 2.8 in UNDRR, 2019, p.66).

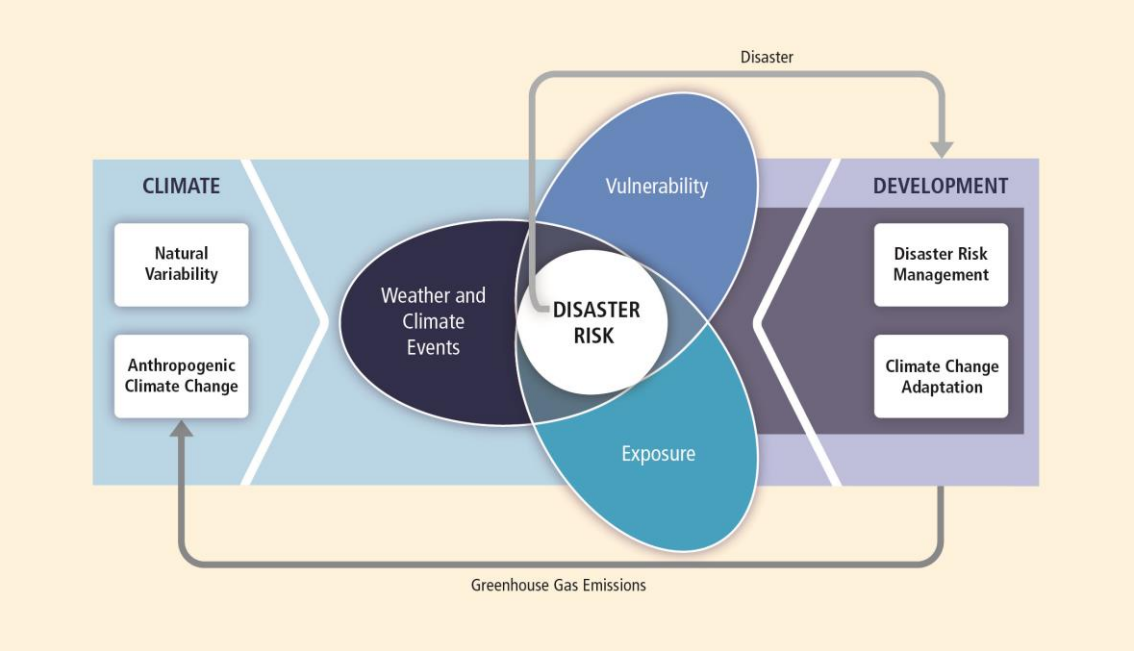

Figure 4. Natural disaster risk conceptualization of the IPCC (Figure 1-1 in IPCC, 2012, p. 31). Disaster risk results from a concomitance of hazardous weather and climate events, exposure and vulnerability.

The **hazard** is usually expressed as a probability of occurrence of an event with a certain magnitude at a given location and during a specified period of time. **Vulnerability** is expressed in form of potential damage affecting people, property or natural capital (Plate and Merz, 2001). It depends on the **susceptibility** (also called sensitivity) as well as the **resilience** of the affected elements. Sometimes, the physical **exposure** of the elements to the hazard is treated as part of the vulnerability (as e.g. in Merz and Thieken, 2004; Merz et al., 2007), sometimes separately (as e.g. in IPCC, 2012; UNDRR, 2019). The final risk can be derived spatially from a combination of a hazard and a vulnerability map (Plate and Merz, 2001); or, it can be represented in form of risk curves, where the annual frequency of events with a certain magnitude is plotted over the potential overall damage. The unit of risk is then given as the average number of damaged people or as the monetary damage expected per year (Plate and Merz, 2001). For very rare extreme events the hazard frequency is often represented in form of return periods (expressed e.g. as '50-year flood'), which are the inverse exceedance probability of an event with specific magnitude at a given place in the next year (Edwards and Challenor, 2013).

The goal of a quantitative risk assessment for natural hazards is to enable informed decision making, aiming at a minimization of potential losses. Risk assessment forms an important part of disaster risk management, which is an internationally established systematic approach for implementing strategies in order to avoid or lessen the adverse impacts of hazards and the possibility of disaster (UNISDR, 2009). The different stages of how to deal with natural disasters are frequently presented in form of disaster risk management cycles (Figure 5).

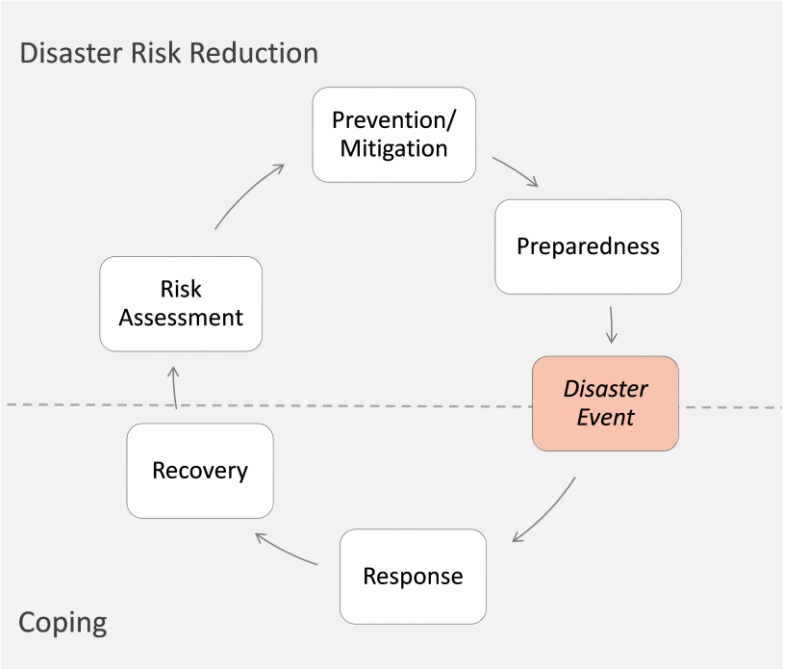

Figure 5. Disaster risk management cycle. Figure adapted from Plate and Merz (2001, Fig. 1.3, p. 32). English terms based on the internationally established terminology of the United Nations International Strategy for Disaster Risk Reduction (UNISDR, 2009).

After a natural disaster has happened, the response phase describes the mobilization of emergency services in order to reduce the direct negative impacts caused by the disaster and to meet the basic subsistence needs of the people affected (UNISDR, 2009). Next is a phase of recovery, dealing with restoration measures (ibid.). This part is often the most costly and protracted one (Plate and Merz, 2001). However, it also offers the chance to learn from the past and reduce disaster risk factors (Plate and Merz, 2001; UNISDR, 2009). Finally, there is a phase of disaster risk reduction, divided into prevention and preparedness. Both aim at a reduction of exposure and vulnerability to the natural hazard and at raising public awareness (Hellmuth et al., 2011). During disaster prevention measures are taken in order to prevent or mitigate adverse effects of hazards and related disasters (e.g. building dams, improving environmental policy and land management, improve coping capacities). Disaster preparedness lays the groundwork for the response (Hellmuth et al., 2011). It contains effective anticipation (early-warning) of hazard events and the knowledge of existing capacities for responding to and recovering from the impacts of likely imminent hazards (UNISDR, 2009).

2.1.2 Land degradation as a natural hazard

Opposed to acute natural hazards of short duration such as floods or earthquakes, land degradation is often a slow process, occurring on extensive temporal and spatial scales. The damage caused by land degradation often becomes visible only in the long-term, and is intermingled with effects of other climatic extreme events, which were often perceived as the imminent threat in the past such as droughts. In consequence, land degradation was not perceived as a stand-alone natural hazard for a long time and is still rarely considered in the context of natural disasters.

The immense damage potential of land degradation was first perceived in the world's drylands at the end of the 20th century. A prolonged drought in the Sahel region of sub-Saharan Africa in the 1970s and early 80s that led to the death of over 200 000 people and millions of livestock (UNCCD, 2020), provided the background for holding the first United Nations Conference on Desertification (UNCCD) in 1977 (Dregne, 2002). The conference officially introduced the term 'desertification' as a synonym for land degradation in drylands (Dregne, 2002; UNCCD, 2020). At first, drought was identified as the main factor for the human Sahel crises in the 1970s. Yet soon it became clear that drought was not the underlying factor, and that prior land management was a crucial point for the extent of the damage to the land (Dregne, 2002), i.e. it appeared to be a man-made loss in the land's ecological integrity which had made the land so vulnerable to droughts.

The notion that drought is often the mere trigger for human catastrophes, not the root cause, is a recurring notion in literature about drought risk: according to Felgentreff and Glade (2007) droughts only lead to severe loss in agricultural production and hunger crisis if they happen in fragile ecosystems, already weakened by land degradation, in combination with a socio-economic vulnerable population. Plate and Merz (2001) state that strongly degraded areas are particularly threatened by drought. Finally, in a recent report of the IPCC it says that the socio-economic impact of droughts arise due to a combination of natural conditions and human activities (IPCC, 2012); it is further stated that extreme impacts can arise even without extreme weather and climatic events (IPCC, 2012).

Nowadays, the global damage potential of land degradation is well-established. The IPCC recently described land degradation as one of the most urgent challenges for humanity (IPCC, 2019). Yet, its current global extent and severity is still not well quantified (IPCC, 2019). 'There is no single method by which land degradation can be measured objectively and consistently over large areas because it is such a complex and value-laden concept' (stated with *very high confidence* in IPCC, 2019, p. 348). Nevertheless, since the implementation of the UN Plan of Action to Combat Desertification (agreed in Nairobi in 1977), several assessments of the global cost of land degradation have been performed (UNCCD, 2013). The first estimate of the global cost of desertification (i.e. land degradation in drylands), published by UNEP in 1980, was US$26 billion per annum (UNCCD, 2013). Other studies followed. However, there is wide variation in the estimates of the global cost of land degradation. Nkonya et al. (2016) compared estimates of 12 studies and concluded that the estimated costs range from US$17.58 billion to as high as US$9.4 trillion. The authors argue that this large variation occurs firstly, due to different methodological approaches, and secondly, because some studies incorporated only selected biomes in their analysis, while others used a more comprehensive approach (Nkonya et al., 2016). Hence, results are not comparable among each other. Nkonya et al. (2016) assessed the annual global cost of land degradation due to land cover change resulting in loss of ecosystem services as well as degrading land management practices on cropland and grazing land as about US$300 billion. In this study, sub-Saharan Africa accounts for the largest share (22%) of the total

cost. Regarding rangelands, Kwon et al. (2016) quantified the annual global costs of losses in milk and meat production due to grassland degradation as about US$7 billion.

This short summary of estimated costs of land degradation should provide an impression on the large damage potential of land degradation. Further, the variety between different assessments points to the difficulties involved in estimating the cost of land degradation in a comparable manner. There is still a lack of research in peer-reviewed academic journals on the economics of land degradation (UNCCD, 2013). In the following, three general particulars (1)–3)) of land degradation as a natural hazard, which contribute to the difficulty of quantifying the extent of land degradation and the associated damage, are discussed. In section 2.1.3 existing approaches of land degradation risk assessments are then critically reviewed. Based on the identified conceptual shortcomings, a comprehensive framework for a quantitative land degradation risk assessment is proposed.

1) A matter of perspective: historical evolution of land degradation concepts and definitions

Over the last 30 years, definitions of land degradation have changed considerably, and consequently so have the approaches of its quantification. This lack of consensus has hindered a coherent approach for an assessment of land degradation. The conceptual evolution is exemplified by the differences in historical formal definitions of land degradation. In the following, a sample of authoritative definitions of land degradation is presented:[2]

FAO, 1979: ‘Land degradation is a process which lowers the current or potential capability of **soils** to produce.’ (FAO, 1979 in Nachtergaele et al., 2010, p.73)

UNCCD, 1994: ‘**Desertification** means **land degradation** in arid, semi-arid, and dry sub-humid areas resulting from various factors, including **climatic variations** and **human activities**.’

‘**Land degradation** in arid, semi-arid, and dry sub-humid areas is a **reduction or loss of the biological or economic productivity and integrity** of rainfed cropland, irrigated cropland, or range, pasture, forest, and woodlands resulting from land uses or from a process or combination of processes, including processes **arising from human activities** and habitation patterns, such as (i) soil erosion caused by wind and/or water; (ii) deterioration of the physical, chemical, biological, or economic properties of soil; and (iii) long-term loss of natural vegetation.’

LADA, 2011: ‘Land degradation is the **reduction in** the capacity of the land to provide **ecosystem goods and services** and to assure its functions over a period of time **for its beneficiaries**.’

IPCC, 2019: ‘Land degradation is a negative trend in land condition, caused by **direct or indirect human-induced processes** including anthropogenic climate

[2] Bold markings are added by myself to highlight keywords in the definitions.

change, expressed as long-term **reduction or loss of** at least one of the following: **biological productivity, ecological integrity or value to humans**.'

From a bio-physical focus on the soil in the 70s, the concept of land degradation has opened up towards a holistic perspective, focussing on the coupled human-environment system, which is providing ecosystem goods and services to the land users. Thereby, an economic perspective on the ecosystem was introduced. Yet, in the definitions by the UNCCD (1994) and the IPCC (2019), the ecological integrity is additionally valued by itself. The concept has evolved towards explicitly incorporating the drivers of land degradation, emphasizing the human responsibility but also the role of climatic variation and lately, climate change. The still widely used UNCCD definition from 1994 explicitly addresses the processes degrading the land in arid lands (soil erosion or deterioration and a loss of natural vegetation).

This broad range of historical perspectives on land degradation gives an impression of the complexity of the phenomenon and of the difficulties involved in an objective assessment of land degradation and the resulting damage. Up to today, all of these definitions are used within scientific literature, and often the perspective on land degradation is not explicitly stated within the research. This lack of consensus and often lack of transparency hinder the comparison of different assessments of land degradation, for usually they did not measure the same thing.

What all definitions have in common is that land degradation is not perceived as a fixed state, but as a process affecting the land in an adverse manner from an anthropogenic perspective. While it becomes clear that the consequences of land degradation are perceived as a threat for humanity, the question what exactly is perceived as the hazard, and how it can be measured, remains unanswered. In consequence, numerous 'land degradation indicators' have been developed in research. With increasing computational capacity and data availability these have become ever more detailed, aiming at capturing all features of land degradation: the geomorphic processes involved, the ecosystem state, the climatic and human drivers, the socio-economic situation of land users, etc. However, this development has not fostered a coherent approach for land degradation assessment.

2) Diversity of land degradation drivers and processes, acting on all temporal and spatial ecosystem scales

In the introduction we have seen that the processes of land degradation are diverse. They range from geological processes such as gully erosion to the salinization of the soil to seawater intrusion or shrub encroachment in grass dominated savannas. All of these processes act on individual temporal and spatial scales and the dominating processes vary locally. This makes general assessments of land degradation on large scales excessively difficult. The same holds true for drivers of land degradation. Finally, processes and drivers are often intermingled (IPCC, 2019). The result is that it is often not clear what should be measured – the current state of the ecosystem (e.g. vegetation coverage) or the rate of the processes involved (e.g. erosion rate) or the local intensity of the drivers (e.g. intensity of land use, population growth, etc.).

3) Land degradation: a permanent hazard or a discrete event?

Opposed to acute hazards of short duration such as floods or earthquakes, land degradation is often a creeping process. Land degradation processes can continue unnoticed for decades before damaging consequences become apparent. Yet, research has shown that they often follow non-linear dynamics and may unfold gradually as well as suddenly (Turnbull et al., 2008; Karssenberg et al., 2017). Ecological tipping points – points where the system rapidly reorganizes into an alternative system state (Kéfi et al., 2014; Scheffer et al., 2015) – can result in fast, cascading changes in ecosystems, even if external drivers change only gradually with time (Scheffer et al., 2001; Scheffer and Carpenter, 2003; Turnbull et al., 2008). This makes ecological regime shifts very hard to predict (Hastings and Wysham, 2010). At the same time, the existence of ecological tipping points makes land degradation particularly dangerous; once the ecosystem has been shifted to a degraded functional state, the process is often very difficult or very costly to reverse due to positive stabilizing feedback mechanisms (Tomaselli, 1977; Scheffer, 1990; Rietkerk and van de Koppel, 1997; Mäler, 2000; Roques et al., 2001). Furthermore, the consequences may even become apparent only after an ecological regime shift has already happened (Scheffer, 1990). The unique dynamical characteristic of land degradation – standing somewhere between a permanent hazard and a discrete event – clearly distinguishes land degradation from other, 'classical' natural hazards such as floods, earthquakes or storms. All of those are extreme events happening at discrete points in time and their impacts are immediately perceived. In consequence, the high damage potential of land degradation has long been concealed and methods for assessing future risks of land degradation are trailing far behind those that have been developed for acute hazards of short duration.

In conclusion, land degradation is an atypical natural hazard, driven by climate variability and anthropogenic factors. It encompasses a variety of processes that act on all spatial and temporal scales of the ecosystem. It is difficult to define land degradation as a discrete hazard in time and space and to analyse it as such. Yet, its high damage potential has become clear over the last decades and several approaches to assess the risk of land degradation have been developed in scientific literature. In the following, these approaches are critically reviewed.

2.1.3 Identification of shortcomings in land degradation risk assessment approaches

Land degradation describes a variety of processes that lead to a reduction of the land's biological productivity, integrity or value to humans (IPCC, 2019). Hence, the definition itself contains an explicit inclusion of biological and socio-economic damage resulting from these processes. This provides a direct link to the vulnerability concept as an expression of potential damage, resulting from a hazard, as it is used for risk assessment in the context of natural disaster risk research (described above). Curiously, however, to the present day no consistent framework for a quantitative assessment of land degradation risk appears to have been developed in the scientific literature.

The objective of this systematic review is to analyse the discrepancies in risk analysis related to land degradation towards a common understanding. In a second step, a comprehensive framework for a quantitative land degradation risk assessment is proposed.

Methodological procedure

A systematic literature search was conducted in the scientific database of the Web of Science (http://apps.webofknowledge.com; date of search: 25.01.2017) by using the title search criteria '("land degradation" OR desertification) AND Risk AND (Analys* OR Assess*)'. The keyword 'desertification' was included in addition to 'land degradation', because by definition it refers to land degradation in drylands (UNCCD, 1994), and the two terms are often used synonymously. The additional terms 'analys*' or 'assess*' were included, for if only the term 'risk' was used, the vast majority of results were not related to any conceptual risk framework, let alone to a systematic risk assessment approach. Rather, the term 'risk' was used with colloquial meaning. For the same reason, a title search was chosen over a topic search. The systematic search yielded 21 results, 19 of which were available in English language. This list of 19 studies (Table 1) is not intended to be exhaustive of all research performed on the topic; rather, it should provide an objectively chosen sample as a solid basis for the following literature review.

Identification of key issues

In a first step, the selected studies were grouped according to their risk concept. Table 1 provides an overview of the selected studies, summarizing their risk concept and overall approach. In a second step, the studies were discussed within thematic groups, based on identified key issues that are hindering coherent land degradation risk assessment.

*Table 1. Overview of selected studies for reviewing land degradation risk assessment approaches, including the risk concept and a summary of the overall approach**

Study	Risk definition provided	Risk concept / background	Approach
Rubio & Bochet (1998)	None	**No explicit concept** Risk assessment ~ Standardized evaluation system of desertification	Selection of indicators for desertification 'risk' assessment
Taguas, Carpintero & Ayuso (2013)	None	**No explicit concept** Risk is never explained	Soil erosion assessment; annual soil erosivity calculated based on precipitation
Vorovencii (2015)	None	**No explicit concept** Desertification risk ~ the negative consequences resulting from desertification	Land degradation status assessment for different time points
Vorovencii (2016)	None	**No explicit concept** Area at risk of land degradation ~ Areas with much degraded land	Land degradation status assessment for different time points + spatiotemporal trends
Salvati, Zitti & Ceccarelli (2008)	Implicit	**Vulnerability** Desertification Risk ~ Environmental vulnerability	Vulnerability assessment (based on socio economic data and comparing it to ESA approach based on bio-physical data); GIS analysis
Salvati et al. (2015)	Implicit	**Vulnerability** Desertification risk ~ Desertification	Vulnerability assessment vulnerability scores assigned based on bio-physical and socio-economic data; PCA- and cluster analysis
Garg & Harrison (1992)	Implicit	**Vulnerability/Susceptibility** Erosion risk ~ Susceptibility to soil erosion	Soil erosion vulnerability assessment (based on land use, gully density, slope); GIS analysis
Ladisa, Todorovic, & Liuzzi (2012)	Implicit	**Vulnerability/Susceptibility** Desertification Risk ~ Areas sensitive to or threatened by desertification	Vulnerability assessment GIS analysis; ESA approach (based on soil, vegetation, climate, land use, human pressure)
Ali & Kawy (2013)	Explicit	**Vulnerability/Susceptibility** Degradation risk = Soil rating x Topography x Climate rating; Risk ~ bio-physical susceptibility to soil erosion (without human effect)	Assessment of bio-physical vulnerability/susceptibility to erosion + present soil degradation status; difference between the two is assigned to human effects; GIS analysis
Ibanez, Valderrama & Puigdefabregas (2008)	Implicit	**Hazard / Vulnerability / Social sciences (Human-resource system)** Risk ~ Once the system is taken 'beyond its ecological resilience'	Theoretic assessment of stable system conditions and thresholds (based on economic decisions) leading to long-term desertification versus sustainability

Hai, Gobin & Hens (2013)	Explicit	**Hazard / Vulnerability / Social sciences** Risk = 'the chance of something happening that will have impacts on objects' Risk ~ 'Probability of **hazard** occurrence' x 'Potential **damage**'	Risk assessment Cause-effect model (Leopold matrix); semi-qualitative approach Risk value for specific socio-economic activities assigned based on the likelihood of occurrence of a potentially damaging cause and the degree of potential damage; based on expert-knowledge
Salvati & Zitti (2009)	Implicit	**Vulnerability / Future risk** Risk ~ Potentially desertified lands	Vulnerability assessment + spatiotemporal trends; based on spatial convergence in vulnerability index (ESA approach) over time; GIS analysis
Santini et al. (2010)	Implicit	**Vulnerability / Future risk** Risk ~ Present degradation status + rate of change	Desertification status assessment + temporal trend analysis GIS analysis, development of 'Desertification Risk Tool': based on 6 models describing vegetation productivity, soil fertility, erosion, seawater intrusion, grazing
Becerril-Pina et al. (2015)	Implicit	**Vulnerability / Future risk** Risk ~ Areas vulnerable to desertification because of negative temporal trends in relevant factors	Assessment of temporal degradation trends in vegetation, climatic and anthropogenic factors
Tombolini et al. (2016)	Implicit	**Vulnerability / Early-warning** Risk used in the context of early-warning related to spatial convergence in land vulnerability to degradation over time	Vulnerability assessment + spatiotemporal trends; based on spatial convergence in vulnerability index (ESA approach) over time; GIS analysis
Weinzierl et al. (2016)	Implicit	**Vulnerability / Early-warning** Risk ~ 'areas where a long-term decline in ecosystem function and land productivity is most likely to occur'	Risk/Vulnerability assessment 'Integrated Degradation Risk Index' based on topography, land cover, soil, land use, demography, infrastructure, climate; GIS analysis
Ubugunov, Kulikov & Kulikov (2011)	Explicit	**Natural disaster risk research** Risk = 'Probability of **hazard** occurrence' x 'Potential **damage**'	Risk assessment (quantitative) Based on total area of agricultural land, land affected by / exposed to desertification, land values, population numbers; on municipality level
Wang et al. (2015)	Explicit	**Natural disaster risk research** 'Desertification Disaster Risk' = Hazard x Exposure x Vulnerability x Restorability	Risk assessment GIS analysis; clear differentiation between individual risk components and final risk; bio-physical and socio-economic data
Akbari et al. (2016)	Explicit	**Natural disaster risk research** Risk = 'Desertification Severity' x 'Elements at Risk' x 'Vulnerability'	Risk assessment Bio-physical and socio-economic data used to create separate maps for the individual risk components and final risk

Ambiguity of the term risk

The process of searching for studies that conceptually address risk assessment related to land degradation or desertification first of all revealed that the term 'risk' is frequently used with the intention of alerting the reader to the seriousness of the problem of land degradation and to the extent of the associated damage for human livelihood, without any linkage to a conceptual risk framework. Hence, it proved challenging to develop a search strategy by which studies that at least in majority address risk within a conceptual context, could be efficiently extracted. The title search criteria described above proved to meet this goal. Still, four of the 19 studies namely (namely: Rubio and Bochet, 1998; Taguas et al., 2013; Vorovencii, 2015, 2016; see Table 1) do not provide any explanation of their conceptual understanding of risk, even though all of them refer to risk assessment for degradation or desertification in the title. The study by Rubio and Bochet (1998) aims at discussing and selecting suitable indicators for a desertification risk assessment. With the expression 'desertification risk assessment' they refer to an 'evaluation system of desertification'. In Taguas et al. (2013) the aim stated in the title – a land degradation risk assessment – does not connect to the rest of the article, which is concerned with the calculation of annual soil erosivity from precipitation records. While this approach takes into account that degradation is a process rather than a fixed state, it does not aim at estimating future risks. Within the text, the terms 'risk' or 'soil erosion risk' are used with the intention to highlight the potential negative consequences arising from soil erosion. The two studies by Vorovencii (2015, 2016) explicitly aim at a risk assessment. Again, risk assessment is interpreted as an assessment of desertification status (here based on satellite derived vegetation greenness, landscape pattern and surface albedo), which was repeated for several points in time. Additionally, in the study from 2016, the convergence to degraded land is assessed over time; yet, this is not included in their calculation of risk classes. The term 'risk' is used very frequently in both studies within various phrases, connected to desertification (e.g. 'the risk of exposure to desertification' (Vorovencii 2015, p.7), 'exposed to desertification risk' (Vorovencii 2015, p.9), 'measures for fighting against the land degradation risk' (Vorovencii, 2016, p. 15)), but also to drivers of desertification (e.g. 'the risk of destructuring' or 'the risk of overgrazing' (in Vorovencii, 2016, p.11, 13)). The differing ways in which 'risk' is used reveals that it is not related to any conceptual framework. Further, there is no clear distinction between hazard and risk and the hazard is not clearly identified. E.g. the hazard could be the desertification processes or it could be drivers of desertification such as overgrazing. The damaging consequences of desertification are clearly stressed as translating among others into a reduction or loss of the biological potential of the land ((Vorovencii, 2015). In summary, the studies that do not relate the term 'risk' to any conceptual framework use it with colloquial meaning with the intention to stress the threatening nature of land degradation. All of them appear to confuse a risk assessment with an assessment of the land degradation status or of certain degradation processes.

Confusion between risk and environmental vulnerability

15 of the reviewed studies use the term 'risk' within a conceptual, risk-related framework (see Table 1). Three of those can be related to the risk concept used within natural disaster risk

research (see 2.1.1) and are discussed separately at the end of this subchapter. The other 12 studies mostly did not provide an explicit conceptual risk definition (see Table 1), yet a conceptual framework could be implicitly discerned. However, the inherent risk concepts and terminology were not consistent among and within studies. Frequently, 'risk' is used synonymously with 'vulnerability' (namely in Salvati et al., 2008, 2015; Salvati and Zitti, 2009; Ladisa et al., 2012; Becerril-Piña et al., 2015; Tombolini et al., 2016). E.g. Salvati, Zitti & Ceccarelli (2008) use desertification risk synonymously with 'environmental vulnerability'. In Salvati et al. (2015) spatial vulnerability patterns are used to assess desertification risk. Furthermore, the term 'vulnerability' is recurrently used in substitution with 'susceptibility' or 'sensitivity' (e.g. in Ladisa, Todorovic & Trisorio Liuzzi, 2012). Garg & Harrison (1992) as well as Ali and Abdel Kawy (2013) use 'erosion risk' synonymously with 'susceptibility to erosion'. This ambiguity in terminology indicates that no consistent framework about the different risk components exists in land degradation literature and that they are not clearly distinguished from each other. The confusion of risk with vulnerability is frequently associated with an analysis implemented within a geographic information system (GIS), for instance the Environmental Sensitive Areas (ESA) framework (based on the EU funded MEDALUS (Mediterranean Desertification and Land Use) project) – one of the most common approaches to determine desertification risk (Salvati and Zitti, 2009). It has been applied by four of the studies reviewed here (namely: Ladisa et al., 2012; Salvati et al., 2008; Salvati and Zitti, 2009; Tombolini et al., 2016). In this methodology, an 'Environmental Sensitive Area Index' (ESAI) is calculated, based on four thematic indicators, representing soil quality, climate, vegetation and management practices / land use (Ladisa et al., 2012; Tombolini et al., 2016). Sometimes, socio-economic factors such as human pressure or demographic trends are added (here in Salvati, Zitti & Ceccarelli 2008; Ladisa, Todorovic & Trisorio Liuzzi, 2012). The ESAI is calculated as the geometric mean of these indices. The results are generally presented in spatially explicit risk maps identifying different classes of areas 'sensitive of desertification' ranging from 'non-affected' to 'critical' (e.g. in Ladisa, Todorovic & Trisorio Liuzzi, 2012). What appears striking is that the ESAI is explicitly called a 'risk index', e.g. by Salvati, Zitti & Ceccarelli (2008), and is commonly used to perform 'desertification risk assessment', while at the same time it is widely recognized as a measure of vulnerability to desertification (Salvati and Zitti, 2009; Tombolini et al., 2016). The naming of the index itself and its categories refer to environmental sensitive areas. This highlights the confusion of the terms risk, vulnerability and sensitivity.

Different perspectives on land degradation – no distinction between processes and drivers, cause and effect, hazard and vulnerability

What remains generally unclear is what the land is vulnerable to. Not only is there usually no distinction between hazard and vulnerability, but also the perspectives on land degradation vary among studies. While some studies focus on soil-related processes (e.g. Garg and Harrison, 1992; Ali and Abdel Kawy, 2013; Taguas et al., 2013), the majority of studies (e.g. Ibáñez et al., 2008; Becerril-Piña et al., 2015; Wang et al., 2015; Weinzierl et al., 2016) follow the more modern, holistic view on land degradation, including different components of the human-environment system (see overview of land degradation definitions in 2.1.2). Based on this

perspective, it has become common practice to look at the bulk impact of land degradation processes, rather than assessing the individual processes themselves (Ibáñez et al., 2008). According to Salvati & Zitti (2009, p. 960) the ESA approach does exactly match this requirement, because it 'does not focus on a specific process of land degradation (...) but quantifies the synergic impact of different factors potentially leading to land degradation'. Other 'risk indices' also follow a similar approach. E.g. Santini et al. (2010) combine vegetation, soil properties, soil erosion, seawater intrusion and grazing models to calculate a 'Desertification Risk Index'. Weinzierl et al. (2016) calculate an 'Integrated Degradation Risk Index' based on topography, land cover, soil, land use, demography, infrastructure and climate. While approaches such as this one indeed account in detail for many factors associated with land degradation, they create another problem: for when all factors are merged within one index, it becomes impossible to differentiate between drivers (e.g. climatic variation and land use) and processes (e.g. soil erosion rate, seawater intrusion) of land degradation. Additionally, the bio-physical susceptibility (e.g. topography, soil and vegetation properties) of the land itself cannot be disentangled. Lastly, expected damage cannot be quantified, for it is intermingled within the risk index. Yet, when aiming at estimating and reducing future risk for land degradation, a clear differentiation between drivers and processes is needed. Only then, a distinction between cause and effect, between hazard and vulnerability can be made and expected ecological or socio-economic damage can be quantified. Such a quantification can provide a basis for evaluating different risk reduction measures and take informed decision in land management.

Diverse approaches to distinguish between causes and effects

In the following, three studies that distinguish between causes and effects, yet without explicitly relating this to the risk concept used in natural disaster risk research, are discussed. The theoretic modelling study by Ibáñez et al. (2008) used system stability analysis to identify long-term land use conditions leading to desertification. Assuming constant climate and economic scenarios, they focus on the human-resource system. Resource exploitation is founded on economic decisions. They found that high profit scenarios are responsible for the extension of desertification. They clearly distinguish between the drivers (here: human activity) and the result (here: loss in provision of resources). Thereby, the authors indirectly interpret human overexploitation of resources as the hazard, and the loss in provision of resources, i.e. land degradation, as the potential damage (i.e. the vulnerability).

Another interesting, yet very different approach that clearly differentiates between cause and effect can be found in Hai et al. (2013). Here, a probabilistic understanding of risk is expressed and risk is defined as 'the chance of something happening that will have impacts on objectives' (Hai et al., 2013, p. 1546). The authors used a semi-qualitative approach focussing on cause-effect relationships that are arranged in a risk assessment matrix ('Leopold Matrix' after Leopold et al., 1971). Individual socio-economic activities that are potentially affected by desertification, such as rice or cotton cultivation, raising livestock or water supply, were collected together with a set of environmental and socio-economic factors associated with desertification (such as land use, topography, rainfall, population density, etc.) potentially affecting those activities. Risk

scores were calculated for each target activity based on categories of likelihood of occurrence of causes (i.e. 'hazards', ranging from 'very unlikely' to 'almost certain') in combination with ranks of consequence (i.e. 'vulnerability', ranging from 'no impact' to 'catastrophic'). Thus, the risk calculation is based on a combination of likelihood and consequence, and as such shows striking parallels to quantitative risk assessment. However, the assignment of the categories for likelihood as well as for consequence is not based on quantitative data. Rather, stakeholder knowledge and risk perceptions were used as main input to the risk matrix. Hence, the study relates to the social sciences approach. Risk scores are not used to quantify expected damage, but to determine which environmental and socio-economic factors pose most threat to socio-economic activities. As such, the approach of using a risk matrix still can assist management decision making, even though it lacks objectivity and precision.

Finally, the study by Ali & Abdel Kawy (2013) indirectly estimates the degree to which land use caused soil degradation. Soil degradation risk is calculated by multiplying a soil, a topographic and a climate rating in GIS, resulting in a risk map. They differentiate between the 'degradation risk', which they also call the 'susceptibility to degradation' (Ali and Abdel Kawy, 2013, p. 2774), and the 'degradation hazard', here meaning the actual presence of degradation processes (salinization, sodification, water logging). The difference between these two is attributed to human impact (positive or negative); i.e. land that has a low degradation risk, but is actually strongly degraded indicates land mismanagement, while land with a high degradation risk, but a low degradation status is managed beneficially. Thereby, inappropriate land use practices can be identified.

These three examples illustrate that a differentiation between cause (hazard) and effect (vulnerability) directly creates a link to decision making in land management. However, the diversity of approaches and lack of a shared risk concept and terminology hamper coherent land degradation risk assessment.

Temporal component of land degradation risk

Several studies (namely: Salvati and Zitti, 2009; Santini et al., 2010; Becerril-Piña et al., 2015; Tombolini et al., 2016; Vorovencii, 2016; Weinzierl et al., 2016) consider temporal trends in their analysis, thereby accounting for the dynamic nature of land degradation, as well as for the potential of future risk. Santini et al. (2010, p. 395) point out in their introduction that 'an area mildly degraded subject to an intense and rapid desertification process is more at risk when compared to an area at higher degradation level but stable over time'. They account for this by including temporal degradation trends in their risk calculation. Yet, in the end, the seriously degraded areas are assigned to the 'very high risk class', whereas critical areas at a 'precarious equilibrium between the natural environment and human activities' are assigned to the 'high risk class' (Santini et al., 2010, p. 406). This classification appears contradictory to their statement in the introduction. An integration of static and temporal components within one risk index (as in Santini et al., 2010 or in Weinzierl et al., 2016) makes it hard to disentangle future risk from the present degradation status. Another approach to account for the dynamic nature of risk is a spatiotemporal convergence analysis, as performed by Salvati and Zitti (2009),

Tombolini et al. (2016) and Vorovencii (2016). Here, spatial convergence of land degradation status or vulnerability is calculated over time to estimate future degradation trends, which is interpreted as risk. This approach indicates that risk is seen as something dynamic, differentiating from a degradation status assessment. Becerril-Piña et al. (2015) base their risk assessment purely on the temporal component of risk: they did not include any static factors such as terrain or soil properties, but analysed changes in temporal trends of land degradation factors (vegetation, climate and anthropogenic). In conclusion, while the incorporation of a temporal component in risk estimation is a necessary step, it does not necessarily lead to a clear differentiability between land degradation status and future risk. Furthermore, reducing risk to changes in temporal trends disregards other elements of land degradation risk, such as the vulnerability.

Land degradation risk assessment approaches related to the natural disaster risk research concept

The approaches attempting a land degradation risk assessment that can be linked to the natural disaster risk concept (namely: Ubugunov et al., 2011; Wang et al., 2015; Akbari et al., 2016; see Table 1) have in common that all of them include an explicit risk definition that clearly distinguishes hazard and vulnerability. The **hazard** is seen as consisting of anthropogenic factors, such as agricultural activities or livestock grazing, as well as natural factors, including climatic effects such as precipitation, evaporation and wind. Some properties of the land itself, such as vegetation coverage (in Wang et al., 2015) are also included here, but they also form part of the vulnerability (e.g. soil properties in Wang et al., 2015). In Ubugunov et al. (2011) the properties of the land itself are described as endogenous hazards whereas climate and human activities are described as exogenous hazards. At the same time Ubugunov et al. (2011) repeatedly use the phrase 'desertification hazard', indicating that the occurrence of desertification processes themselves is seen as the hazard. In line with this, they consider areas exposed to certain desertification processes (water erosion, deflation, salinization) in their risk analysis (see Table 1 in Ubugunov et al. (2011), p. 182). In Akbari et al. (2016) desertification severity is referred to as representing the hazard. However, the assessment of desertification severity is also referred to as the 'calculation of the risk' (p. 370). This shows that the terms 'risk' and 'hazard' are not clearly distinguished from each other in the text.

In the **vulnerability** term, potential damage is considered. In the three studies discussed here, vulnerability refers to a potential loss in ecosystem productivity, resulting in economic losses, i.e. by considering the fraction of agricultural land affected by land degradation as in Ubugunov et al. (2011), or by including the ratio of agricultural population as well as of the agricultural outputs to the gross domestic product (GDP) as in Wang et al. (2015). Additionally, the vulnerability term includes ecosystem properties, such as vegetation cover (in Akbari et al., 2016), and soil properties (in Wang et al., 2015), which make land vulnerable to degradation processes. This shows that vulnerability is approached on two levels: first, on the socio-economic level, and second, on the ecosystem level. In Wang et al. (2015) restorability is considered separately, yet purely in a socio-economic context (i.e. referring to the level of education and to a variety of measures for disaster prevention such as rehabilitation measures).

In Akbari et al. (2016) it does not become clear what the vulnerability term consists of. Vulnerability is described as a 'function of stability (resilience) and instability (vulnerability)', as well as a 'function of resilience and sensitivity of the elements at risk' (p. 369). The first definition appears to be inconsistent, for it defines vulnerability as a function of vulnerability itself. A vulnerability value is assigned based on socio-ecological conditions, but also on the presence of risk itself, for they write 'elements that are a higher risk classes will be more vulnerable' (p. 369, see also their table 4). This appears to be circular reasoning. With 'risk class' they seem to refer to the desertification severity – again confusing risk and hazard.

The dynamic component of land degradation risk is approached in contrasting ways. Akbari et al. (2016) do not consider a dynamic risk component at all. In Ubugunov et al. (2011), the inherently probabilistic nature of both hazards and vulnerability is explicitly acknowledged: risk is quantified as expected annual damage [$year^{-1}$]. Yet, at the same time, the authors understand desertification as a permanent hazard existing 'during the entire length of time of its action' (Ubugunov et al., 2011, p. 180) and keep the probability term constant over time. Thus, while the inclusion of a probabilistic term within a risk model is a novelty of this study, its implementation has obvious shortcomings. In Wang et al. (2015, p. 1712) the hazard term is described as the 'variation degree of natural disaster and human factors which caused the desertification disaster'. Even though no probabilistic term is explicitly included, risk is seen as something dynamical, depending on the variation of natural disasters. Yet, this dynamical idea is not coherently followed up in their analysis (except that some of the used input datasets are continuous, e.g. meteorological data, NDVI with 16-day resolution). Interestingly, in contrast to Ubugunov, Kulikov & Kulikov (2011), they describe desertification as a 'typical disaster risk event' (Wang et al., 2015, p. 1703), which suggests a discrete event in time.

In Ubugunov, Kulikov & Kulikov (2011) results of their risk analysis are presented quantitatively, giving direct estimates for the different administrative districts of the Republic Buryatia: in affected hectares/year for the physical desertification risk, in roubles/year for the economic risk and in number of affected persons/year. It is the only study where expected damages are quantitatively assessed. Both in Akbari et al. (2016) and in Wang et al. (2015) risk is presented in form of an index, with risk categories ranging from low to very high risk. Separate maps for the different components of risk (hazard, elements at risk, vulnerability (+ restorability in Wang et al., 2015), as well as final risk maps are produced. The study by Wang et al. (2015) is unique in clearly presenting which factors were included in which risk component (see figure 4 in Wang et al., 2015, p. 1713).

The approaches applying a natural disaster risk assessment to land degradation show, that even though they share a similar risk concept, the terminology is inconsistently used within and among studies. Vulnerability and hazard are still difficult to disentangle. Only in Wang et al. (2015) it is clearly discernible what factors the different components of risk are composed of. None of the studies presented a comprehensive solution for capturing the dynamic nature of land degradation adequately, as to allow projections of future risks. This highlights the difficulty

of including a probabilistic approach in land degradation risk assessment. Often the analysis falls short of the concept.

2.1.4 Discussion: what is the dilemma of current land degradation risk assessment approaches

The literature review leads to some initial conclusions: while approaches to calculate land degradation risk have evolved to include and capture ever more processes and factors involved in land degradation as well as in risk assessment in detail, the development of a coherent conceptual risk framework is trailing behind. At the same time, an urgent need to derive 'measures for fighting against the land degradation risk' (Vorovencii, 2016, p. 15) appears to be generally well-recognized. A quantification of risk is hampered by an overall discrepancy in what this risk contains. The critical review of 19 studies dealing with land degradation risk assessment approaches revealed that not even a consensus exists of what is perceived as the hazard. All in all, eight key issues could be identified, preventing a stringent and coherent risk assessment of land degradation up to today.

1) The term **'risk' is frequently used with colloquial meaning, with the intention of alerting and emphasizing the seriousness of the problem land degradation** and to the extent of potential damage for human livelihoods. This emphasizes that the perception of land degradation as threat to humanity is there, even though it is not connected to a formal risk concept.
2) **Risk assessment is often confused with degradation or desertification status or process assessment** (i.e. monitoring of land degradation). This confusion hinders a link to the risk management cycle in decision making and a projection of future risks.
3) **Risk assessment and vulnerability assessment are often confused and used synonymously**. Vulnerability is usually not linked to potential damage for the people (exceptions are: Hai et al., 2013; Ubugunov et al., 2011; Wang et al., 2015), but rather used as a descriptor for the land's likelihood of becoming degraded. This likelihood is assessed based on a combination of environmental susceptibility to degradation and the present land degradation status (+ past trends) as well as on climatic and human drivers. The confusion of risk-/vulnerability and susceptibility assessment makes it impossible to differentiate between present land degradation status and future risks.
4) **Potential damage** is mentioned frequently as a motivation or to raise attention to the urgency of the problem (similar to how 'risk' is often used). Yet, damage is rarely explicitly considered or quantified in the risk analyses (exceptions are: Hai et al., 2013; Ubugunov et al., 2011; Wang et al., 2015). Only one study (Ubugunov et al., 2011) quantified risk in form of expected annual damage.
5) **No consensus about the 'hazard' land degradation**. The definitions of land degradation have evolved in historical contexts. This is mirrored in land degradation risk assessment approaches. What is perceived as the threat (i.e. the hazard), ranges from pure soil related processes to attempts that include a large variety of processes adversely affecting the human-environment system. The fact that the hazard is usually not specified hinders the predictability of hazard occurrence.

6) **Risk terminology is not consistently used among and within studies**. The terms risk, hazard, vulnerability and susceptibility are often confused. Only a minority of studies (Ubugunov et al., 2011; Hai et al., 2013; Wang et al., 2015; Akbari et al., 2016) include an explicit risk definition. Even if a risk theory exists, it is not consistent between studies and often the analysis falls short of the concept.
7) **In the majority of studies there is no distinction between processes and drivers, cause and effect, hazard and vulnerability**. This hampers the development of quantitative risk projections as well as a link to decision making and land management. Even in those studies that explicitly include a hazard and vulnerability term, a clear differentiation between the two remains difficult (exception is: Wang et al., 2015).
8) **Temporal dynamics** are sometimes considered, but mostly not embedded within a theoretic risk framework. Land degradation is treated either as permanent or a discrete hazard. None of the approaches manages to account for the probability of hazard occurrence in such a way as to allow for future risk projections.

2.1.5 Towards a quantitative risk assessment for land degradation: ecological resilience as a concept to bridge the gap between land degradation dynamics and risk assessment

A first step towards a comprehensive risk assessment for land degradation would be to clearly follow one land degradation definition and use consistent risk terminology. Since a risk assessment is usually motivated by some threat perceived by people, a definition focussing on land degradation as a process leading to a reduction or loss in the ecological functioning or in the economic productivity of land, seems suitable. The latest definition by the IPCC provides this and I will follow it during this thesis: 'a negative trend in land condition, caused by direct or indirect human-induced processes including anthropogenic climate change, expressed as long-term reduction or loss of at least one of the following: biological productivity, ecological integrity or value to humans' (IPCC, 2019). The risk terminology developed by the United Nations International Strategy for Disaster Risk Reduction (UNISDR, 2009) is internationally established within disaster risk research (for details see 2.1.1), hence I suggest adopting it when addressing land degradation risk.

Second, it is necessary to clearly differentiate between drivers and processes. Only then a differentiation between hazard and vulnerability, between present degradation status and future risk becomes possible. The main drivers of land degradation processes are climatic factors and anthropogenic effects (see overview of land degradation definitions in 2.1.2). Yet, the specific processes involved and their drivers vary regionally. Therefore, I propose to identify the key land degradation processes, which reduce the land's ecological integrity, productivity or its value to humans as perceived by land users, on regional level. In a second step, the specific drivers of the involved processes should be identified. Thirdly, associated ecological and socio-economic impacts (damage) should be identified. Table 2 provides an exemplary overview of key degradation processes in selected biomes, their climatic and anthropogenic drivers, and associated impacts.

Table 2. Selected examples for degradation processes in different ecosystems, their drivers and associated damage.

Ecosystem type	Key land degradation processes	Drivers		Damage	Reference
		Climatic	Anthropogenic		
Mediterranean drylands	Soil erosion; loss of natural vegetation cover	Intensive rainfall events; droughts	Overgrazing by livestock; abandonment of previously cultivated land	Loss of ecological integrity; reduced livestock carrying capacity	Tomaselli, 1977
Semi-arid savannas	Shrub encroachment into grass dominated savannas	Mass recruitment of woody shrubs triggered by several consecutive wet years	Long-term, intensive livestock grazing; exclusion of wild herbivores (mixed feeders and browsers); suppression of wild fires	Loss of ecological integrity; reduced livestock carrying capacity; loss of touristic value for wildlife viewing	O'Connor, 1995; Scholes and Archer, 1997; Roques et al., 2001; Kraaij and Ward, 2006
Brazilian Cerrado	Overland flow; soil erosion; water degradation	High-intensity storms in rainy season; prolonged dry seasons	Agricultural transformation since the 1980s: clearing of natural vegetation in favour of monocultures	Loss of ecological integrity; water shortage during dry season; higher peak flow during rainy season; future reduction of agricultural productivity likely	Hunke, 2015
American and Canadian prairies in the Great Plains region ('Dust Bowl' during the 1930s)	Wind erosion	Dust storms; repeated droughts	Agricultural transformation from arid grassland to cultivated cropland	Loss of ecological integrity; loss of agricultural productivity; hunger; poverty; human displacement	McLeman et al., 2014

What all of these examples illustrate is that climatic drivers are usually the mere trigger of long-term land degradation, while gradual anthropogenic drivers are the underlying cause, i.e. the predisposing factor. I will exemplarily discuss this for Mediterranean drylands, whose productivity is frequently reduced by severe soil erosion processes. The main climatic drivers of soil erosion are intensive rainfall events in combination with droughts. These processes are natural in arid regions and can usually be buffered by intact ecosystems, which have historically evolved under these conditions and are naturally resilient (Imeson, 2012). However, if the ecosystem is stressed and transformed by livestock overgrazing, the ecological resilience of the ecosystem is reduced in such a way that augmenting feedbacks lead to long-term degradation

of the system. Overgrazing by livestock causes trampling damage and reduces vegetation cover, thereby continuously increasing soil exposure to intensive rainfall events and increasing soil compaction, which in turn reduces the infiltration potential of the soil (Barrow, 1991). This drastically increases the soil's susceptibility to erosion, leading to a loss in soil fertility and soil depths, which hampers the soil's water storage capacity. As a result, the ecosystem becomes more susceptible to drought, which reduces vegetation cover further. Less nutrients and water in the soil also reduce vegetation's ability to recolonize bare areas. In the long-term, the ecosystem is pushed to a different less desirable (i.e. degraded) functional state, consisting mostly of bare soil. In conclusion, only if an ecosystem is weakened by human intervention, natural geomorphological and biological processes such as erosion by wind and water become critical, pushing the ecosystem towards a different and less desirable degraded functional state. Another example is given in Scheffer et al. (2001), who describes that changes in land use have caused gradual eutrophication of Lake Apoka (Florida, USA), yet it was a hurricane in 1947, which wiped out aquatic plants, and probably triggered the final collapse to a turbid state (Schelske and Brezonik, 1992, in Scheffer et al., 2001). This characteristic of land degradation risk has been aptly described by Ibáñez et al. (2008), who stated that irreversible land degradation occurs once the system is taken 'beyond its ecological resilience threshold'. This perspective builds on the concept of ecological resilience, as introduced by Holling in the 1970s.

Holling discovered that ecosystems can have multiple stable states, also called basins of attraction. He defined **ecological resilience** as the 'ability of systems to absorb changes (…) and still persist' (Holling, 1973, p.17), without being pushed into an alternative basin of attraction. With this novel idea, he introduced an alternative perspective on resilience, focussing on the boundary conditions of basins of attractions, rather than on the stable state conditions around an equilibrium (Holling, 1996). He described stability as 'the degree of fluctuation around specific states' (Holling, 1973, p.17). In his view, ecosystems could be very stable, yet at the same time have a very low ecological resilience and the other way around. He argued that ecosystems with a high intrinsic environmental or climate variability are often characterised by very high fluctuations in combination with a high resilience to periodic extreme events. On the other hand, a gradual loss of functional diversity in managed ecosystems often goes along with high stability and, in the short-time, higher and more constant productivity; yet, Holling (1996, 1973) illustrated that this feature is often accompanied by a loss in ecological resilience, increasing the likelihood for the system to suddenly flip into a different, unproductive ecosystem state that is hard or even impossible to reverse.

I propose that the concept of ecological resilience has potential to bridge the gap between an assessment of land degradation dynamics and risk analysis. To explain this idea, I will build on the 'ball-in-a-cup' model (see Figure 6), by which means ecological resilience has been frequently illustrated (e.g. in Holling, 1973; Scheffer et al., 1993, 2001, 2015; Dakos et al., 2014). The valleys represent basins of attraction and the ball represents the system state. The overall size of the valleys represents the ecological resilience (Holling, 1973). An interesting feature of this conceptual model is that the shape of the valleys (henceforth called 'resilience landscape')

is not treated as a fixed property, but rather as an ongoing and changeable system condition (well-illustrated in Scheffer et al., 1993). Consequently, a transition from one to another basin of attraction can be twofold: either due to a fast exogenous disturbance pushing the ball above the resilience boundary; or due to a slow change in state variables or parameters diminishing the size of the valley (i.e. the ecological resilience) to such an extent, that even small stochastic fluctuations and natural environmental variability can easily transfer the system to another system state (Holling, 1973; Scheffer et al., 2001). Any combination of these two forces is possible.

Based on the current state of research on ecological regime shits (see extensive reviews on regime shifts in Scheffer et al., 2001 & Folke et al., 2004), I hypothesize that fast climatic drivers such as intensive rainfall events or droughts can generally be treated as triggers of land degradation, 'pushing the ball' towards another system state. Fast climatic drivers directly affect the frequency of geomorphic processes, such as erosion. In the context of land degradation risk analysis, I propose that these geomorphic processes can be treated as the hazards (compare also Gill and Malamud (2014) for thoughts on primary hazards triggering secondary hazards). Gradual anthropogenic drivers of land degradation on the other hand, like a persistent landscape transformation by livestock grazing, are slow drivers. Instead of 'pushing the ball', they affect the shape of the resilience landscape in such a way, that a transition to another state becomes more likely. That human actions indeed have the potential to reduce ecological resilience and that a loss of resilience increases the likelihood of regime shifts has been demonstrated in several studies (Holling, 1973; Gunderson, 2000; Scheffer et al., 2001; Folke et al., 2004; Vetter, 2009). Similarly, I would expect that long-term climatic trends or a change in the overall frequency of extreme events affect the resilience landscape in the long-term. These slow drivers, therefore, act on the ecological resilience, which is treated as part of the vulnerability term in the context of quantitative risk theory. Based on this connection between ecological resilience and vulnerability, and on the understanding of fast and slow drivers of land degradation, I propose a risk-resilience model for land degradation (Figure 6). This model provides a link between land degradation research and classical quantitative risk assessment developed within natural disaster risk research.

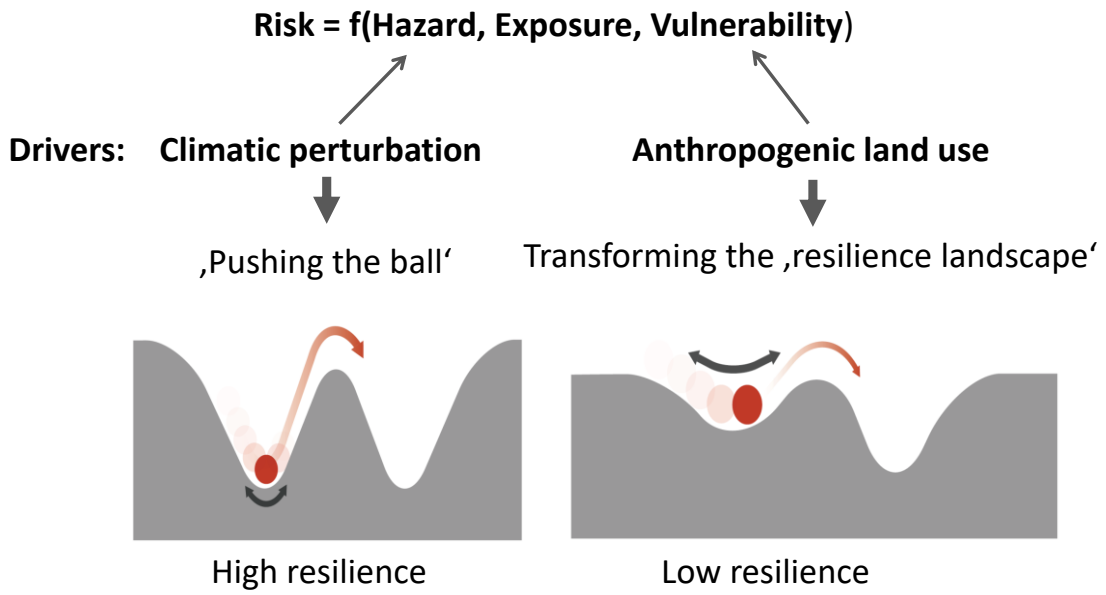

Figure 6. Conceptualization of the here proposed risk-resilience model for land degradation. Based on a combination of the 'ball-in-a-cup' model for ecological resilience (here taken from Popkin, 2014) and the classical risk function developed within natural disaster risk research.

A twofold perspective on fast and slow drivers of land degradation allows for a clear separation between fast drivers acting on the frequency of hazard occurrence, and slow drivers acting on the ecological resilience. Hence, such an approach would have the advantage of creating the possibility for a clear distinction between hazard and vulnerability in land degradation risk assessment.

A land degradation risk analysis founded on these conceptual ideas would essentially involve five steps:

1. Selection of a specific area or areas exposed to land degradation on local or regional scale or based on ecosystem type. The motivation why this area is perceived as threatened by degradation from the perspective of land users should be clearly stated. I.e. is it a loss of biological or economic productivity that is feared or already happening? This relates to the associated damage and the choice of risk metric.
2. Specification of critical geomorphic processes (e.g. erosion, overland flow, etc.) driving land degradation in the selected area. These processes are treated as the hazards in the subsequent risk analysis.
3. Identification of the fast climatic triggers of these hazards. Estimations for the frequency of occurrence of these climatic drivers can then be included in the risk analysis, allowing for a likelihood-based assessment of hazard occurrence. In addition, past trends in the geomorphic processes themselves could also be incorporated.
4. Assessment of bio-physical susceptibility (part of the ecological vulnerability) of the ecosystem towards the identified geomorphic processes. Whereas resilience is an ongoing condition, susceptibility describes relatively stable ecosystem properties, such as topography, soil and vegetation type or water quality.

5. Identification of gradual anthropogenic drivers as well as long-term climatic trends that affect the ecological resilience and hence the ecological vulnerability. Subsequently, different land management and climate change scenarios could be implemented within a risk model and their effects on the ecological resilience could be compared, allowing a direct link to decision making. This requires a quantification of ecological resilience, a challenge that is addressed in the main part of my thesis.

Such a procedure would allow us to quantify the area-specific land degradation risk resulting from specific natural hazards in combination with the underlying ecosystem vulnerability. The different risk components and suggested indicators are summarized in Table 3. In this model, the hazard occurrence depends on the frequency of climatic triggers and the adverse effects on the ecosystem (ecological vulnerability) are depending on the bio-physical susceptibility and on the ecological resilience, which in turn is affected by land use and climatic trends. For a given probability of hazard occurrence several land management and climate scenarios could then be compared (compare e.g. scenario-based approach for flood risk in Thieken et al., 2016) and the effect on the likelihood of an undesirable regime shift risk (i.e. loss of ecological integrity) could be estimated. Such a procedure would allow for empirically-based projections of land degradation risk, and a link to informed decision making in land management could be established.

Table 3. Identification of risk components and indicators for land degradation risk on ecosystem level. Based on the land degradation risk assessment concept suggested in this work.

Risk Component		**Sub-components**	**Indicators**
Exposure		Selected area of interest on local or regional scale; or spatial aggregation of areas based on the same ecosystem type	Spatial coordinates of area of interest, total size or % of agricultural land of the total area, depending on the goal of the risk analysis
Hazard		Specific key geomorphic degradation processes; e.g. shrub encroachment, overland flow, wind- and/or water erosion	Frequency of fast climatic events triggering these geomorphic processes (i.e. predicted number of extreme rainfall events based on past frequency distributions) + Predictions based on past rates and trends of the geomorphic processes themselves (i.e. trend in erosion rate)
Ecological Vulnerability	**Ecological resilience**	Ecological resilience to natural climate variability and extreme events, i.e. to fast climatic drivers triggering the key geomorphic degradation processes (hazards)	Quantification of ecological resilience to climate variability for different scenarios of slow land degradation drivers, i.e. land use and climate scenarios
	Bio-physical Susceptibility	Relatively stable ecosystem properties relevant for the susceptibility to the specific hazards	E.g. terrain slope steepness and aspect, soil type, vegetation type, water quality index

This work is not the first to connect the idea of ecological resilience to risk perception. E.g. in an extensive review on the application of resilience from 2000, Gunderson argues that if ecosystems behave in a surprising manner, for example if ecosystem suddenly shift to an alternative, non-desirable system state, resource crisis occur. According to Gunderson such ecosystem shifts occur when variation in large scale processes (such as extreme weather events), intersect with an often human-induced reduced ecological resilience of the ecosystem. However, to my knowledge, it is a novel approach to link ecological resilience explicitly to the quantitative risk analysis framework developed within natural disaster risk research.

The here proposed risk-resilience model for land degradation aims at providing conceptual ideas towards a comprehensive quantification of land degradation risk on the ecosystem level. It is aimed at the ecosystem level, yet provides the possibility for future complementation by including also socio-economic aspects of exposure and vulnerability, which are interlinked with those of the ecosystem and should be considered in subsequent research. The inclusion of socio-economic aspects would facilitate a risk quantification based on expected socio-economic damage. Treating the dynamic components of land degradation drivers twofold: probabilistic for fast climatic drivers, and scenario-based for slow anthropogenic drivers and long-term climatic trends, may present a way out of the dilemma of treating land degradation either as a permanent hazard – which yields little options for a probabilistic approach as exemplified in Ubugunov et al. (2011) – or a discrete, but unpredictable event in time. Furthermore, strengthening the focus on ecological resilience in land degradation risk analysis as a key element, could be a step towards accounting for non-linear ecosystem dynamics. It has been shown that sudden shifts in ecosystem states are generally preceded by a significant reduction in ecological resilience to small natural stochastic perturbations (Scheffer et al., 2015). This characteristic of ecological resilience offers valuable information for developing early-warning systems of non-linear critical land degradation dynamics.

2.2 Approaches to quantify ecological resilience

The last section revealed that the concept of ecological resilience may constitute a key element in the context of quantitative land degradation risk assessment. The following section deals with ways to quantify ecological resilience. The first part (2.2.1) gives insight into the theoretical background, while the second part (2.2.2) deals with remote sensing and change detection methods for quantifying ecological resilience.

2.2.1 Theoretical background to a quantification of ecological resilience

In the context of a fast changing world due to climate change, environmental disasters and anthropogenic influences, the focus in the study of ecological systems has shifted from a stable-equilibrium perspective to the non-equilibrium paradigm and to ecological resilience as described by Holling in the 1970s. Thereby, a system's ability to deal with disturbance and retain its function and structural integrity in a constantly changing world has become the centre of attention. Since the beginning of the 21st century resilience research has increased drastically. According to Folke (2016) the annual citations of resilience in the ISI Web of Science have jumped from below 100 in 1995 to more than 20000 in 2015. However, up to today the

interpretations of ecological resilience vary greatly in practice (Hodgson et al., 2015) and no consistent way of measuring ecological resilience has been established (Ingrisch and Bahn, 2018).

One popular aspect of resilience, which is relatively straight forward to measure, is the **recovery rate** (Pimm, 1984) of a system to an equilibrium after a disturbance. This has been termed 'engineering resilience' by Holling (Holling, 1996). If ecosystems have multiple stable states and are not generally close to equilibria, however, recovery rate alone is not a sufficient indicator of a system's ability to cope with change. For this reason, Holling (1996) argued to focus on ecological resilience instead, which deals with a system's likelihood for transitions to an alternative system state, induced by stochastic perturbations. Using the 'ball-in-a-cup' analogy (see Figure 6 & Figure 7a, b) the ecological resilience of a system corresponds to the overall size of the basin of attraction, representing the amount of disturbance that can be absorbed before the system is pushed into an alternative basin of attraction (Holling, 1973; Scheffer et al., 2001). The recovery rate, on the other hand, depends on the slopes on the sides of the cups.

The 'ball-in-a-cup' conceptualization of ecological resilience has fundamentally promoted a comprehensive understanding of non-linear ecosystem dynamics and resilience. However, for a long time, research on this topic has remained largely conceptual (Scheffer et al., 2015). Regarding application purposes, recent research has shown that the 'ball-in-a-cup' analogy has limited suitability (Hodgson et al., 2015). First of all, it is very difficult to prove that a natural system has multiple stable states (Scheffer and Carpenter, 2003). Secondly, measuring ecological resilience directly appears elusive (van Nes and Scheffer, 2007; Hodgson et al., 2015). A common understanding has emerged that ecological resilience has multiple components and cannot be captured by a single metric (Carpenter et al., 2001; Walker et al., 2004; Hodgson et al., 2015). In consequence, extensive research has focused on developing generic indirect indicators of ecological resilience (see e.g. Dakos et al., 2014; Kéfi et al., 2014; Scheffer et al., 2015). Several of the most promising of those indicators are related to a phenomenon called ‚critical slowing down' (Strogatz, 1994). Systems approaching a tipping point (a point where the system rapidly reorganizes into an alternative system state, represented by the hill tops in the 'ball-in-a-cup' model, Figure 7a, b) recover more and more slowly from perturbations (van Nes and Scheffer, 2007; Kéfi et al., 2014; Scheffer et al., 2015; van de Leemput et al., 2018). In mathematical stability analysis this means that the return rate to equilibrium goes to zero when a system approaches a bifurcation point (Scheffer et al., 2015).

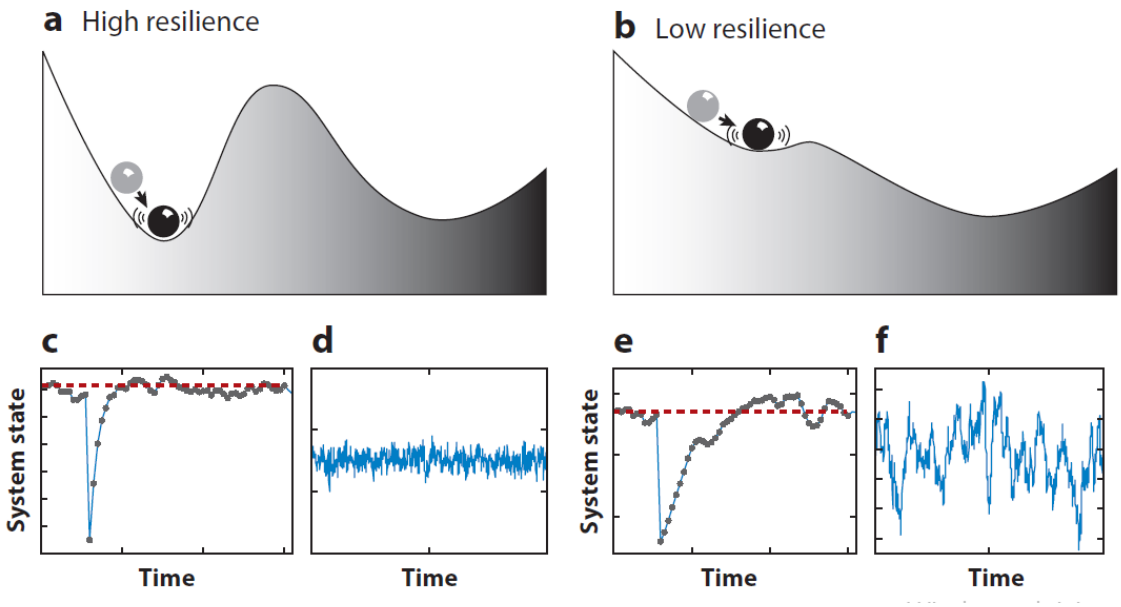

Figure 7. Illustration of critical slowing down as an indicator of low resilience. Recovery rates after a disturbance (c, e) become slower, if the basin of attraction is shallow (b) – i.e. system has low ecological resilience – than when the basin of attraction is deep (a) – i.e. system has high ecological resilience. Reduced recovery rate (e) leads to higher variation in natural time series (f compared to d). Figure adopted from Scheffer et al. (2015, Fig. 2, p. 152).

The slowness of a system can either be deduced directly from the recovery rate after experimental or natural perturbations; or indirectly, by measuring the degree of fluctuation induced by small stochastic disturbances (van Nes and Scheffer, 2007; Kéfi et al., 2014; Scheffer et al., 2015). If recovery rates become slower, the memory effect of the system increases, and thereby the degree of temporal autocorrelation and variance (Karssenberg and Bierkens, 2012; Scheffer et al., 2015). Interestingly, this finding also holds true for spatial autocorrelation and variance (Karssenberg and Bierkens, 2012; Kéfi et al., 2014). Originally, the theory of critical slowing down was conceived for systems fluctuating around an equilibrium due to small natural perturbations, once a tipping point is approached. However, van Nes and Scheffer (2007) demonstrated that the phenomenon is not restricted to small perturbations and becomes apparent already quite far from tipping points. It appears striking that recovery rate after a disturbance, what Holling, (1996) referred to as 'engineering resilience', has actually been found to be a remarkably good indicator of ecological resilience (van Nes and Scheffer, 2007). This is supported further by results from a global study of vegetation resilience by De Keersmaecker et al. (2015), which demonstrated that areas with low ability to recover after short-term disturbances are generally situated in locations that also have a high probability of switching to another system state. Thus, using recovery rate as a proxy for ecological resilience (the size of the basin of attraction) may allow for a unification of some aspects of resilience, which were originally perceived to be contradictory by Holling (Scheffer et al., 2015).

Another aspect of ecological resilience that has received increasing attention lately is **resistance**, the 'instantaneous impact of exogenous disturbances on the system state' (Hodgson et al., 2015). Resistance can be seen as a complementary property of recovery. While resistance deals with a system's ability to withstand disturbance in the first place, recovery describes a system's ability to return to its previous state after a disturbance. Resilience can be achieved via

resistance or recovery or both. In some cases even a trade-off between resistance and recovery has been proposed. Hodgson et al. (2015) illustrate such a trade-off with the example of elephants, whose life history has evolved towards making them resistant to disturbance. Yet, when disturbed their populations recovers only slowly, due to their long life-cycle and low reproductive potential.

Several recent studies emphasize the need to jointly consider recovery and resistance when measuring the resilience of ecosystems to disturbance (Hodgson et al., 2015; Nimmo et al., 2015; Ingrisch and Bahn, 2018). In the following empirical work, I focus on these two crucial aspects of ecological resilience: recovery rate and resistance. This choice does not aim for an exhaustive picture of ecological resilience, which is comprised of more attributes. E.g. Walker et al., (2004) identify four key aspects of resilience: latitude, resistance, precariousness and panarchy (see Fig. 1a in Walker et al., 2004); Hodgson et al., (2015) name resistance, elasticity, return time, precariousness, and latitude. However, based on the current state of research, I believe that recovery rate in combination with resistance yield a well-funded and robust approximation of ecological resilience.

2.2.2 Remote sensing and change detection: methods for quantifying ecological resilience[3]

At present, a great need for an operationalization of the concept of ecological resilience towards empirical measurement techniques and for land management exists (Cumming et al., 2005; Chambers et al., 2019). Approaches for a quantification of ecological resilience have been mostly based on mathematical models and simulated data in the context of approaching tipping points (e.g. in Kéfi et al., 2007; Karssenberg and Bierkens, 2012; Dakos et al., 2010, 2012; Kéfi et al., 2013; Karssenberg et al., 2017; van de Leemput et al., 2018). Yet, with the increasing availability of remotely sensed data, satellite-driven approaches have emerged (e.g. in Simoniello et al., 2008; Washington-Allen et al., 2008; Hirota et al., 2011; Frazier et al., 2013; De Keersmaecker et al., 2015; Verbesselt et al., 2016; Schwalm et al., 2017). Satellite data have the advantage of being consistently collected over time at a global scale. This makes it possible to monitor ecosystem dynamics repeatedly at a high cadence, instead of reverting to temporal snapshots, e.g. before and after a disturbance. According to Kennedy et al. (2014) a temporal consistency of observation is critical for understanding ecosystem dynamics.

Table 4 summarizes a selection of studies using different satellite-driven approaches to quantify ecological resilience. All studies I reviewed, except Hirota et al. (2011), used some measure for the recovery after a perturbation to quantify ecological resilience. Two studies (Washington-Allen et al., 2008 & De Keersmaecker et al., 2015) additionally considered the response magnitude of the vegetation to disturbance, a measure of resistance (called ‘amplitude’ in Washington-Allen et al., 2008). The way in which recovery is measured varies among studies. Simoniello et al. (2008) characterized resilience by analysing the persistence probability of positive recovery trends compared to negative ones in a time series. Frazier et al. (2013) analysed post-disaster ecological resilience in southwestern Louisiana, USA after Hurricane Rita in 2005. They calculated a spatially explicit ecological resilience index (ERI). The ERI is a binary

[3] Individual text passages in this section appear in similar form in von Keyserlingk et al. (2021).

measure of the ability of the system to recover, based on a pre-event baseline. Washington-Allen et al. (2008) measured the degree of recovery after and resistance to a disturbance based on mean-variance analysis of NDVI time series data. In a study from 2015, De Keersmaecker et al. developed a standardized indicator of short-term vegetation resilience (recovery) and resistance to drought and temperature anomalies on global scale. They based their metrics of resistance on the response magnitude of the vegetation to disturbance. Their measure of resilience is based on memory effect in the time series, which is related to the recovery speed after a disturbance. Verbesselt et al. (2016) used spatial patterns of slowness inferred from temporal autocorrelation (an indicator of slow recovery rates) in global NDVI time series of tropical forests. Finally, Schwalm et al. (2017) use recovery time – the time it takes for an ecosystem to revert to its pre-drought functional state – as metric for ecological resilience to assess global spatiotemporal patterns of drought recovery time. Hirota et al. (2011) used a deviant approach to quantify ecological resilience, based on remotely sensed estimates of tree cover in tropical and subtropical zones of Africa, Australia and South America. They empirically reconstructed the basins of attraction for forest, savanna and a treeless state to show how resilience changes over a precipitation gradient. Additionally, they used logistic regression models to estimate the likelihood of a biome to remain in its current state, given its rainfall. This study is the one coming closest to a direct quantification of the classical ecological resilience after the theory of Holling.

Table 4. Summary of selected satellite-based studies quantifying ecological resilience

Study	Ecosystem indicator	Satellite programme & spatial resolution	Area/Scale, Period	Measure of Resilience
Washington-Allen et al. (2008)	NDVI	Landsat MSS & TM (~60 m / 30 m)	Bolivian Altiplano, 1972–1983	**Magnitude of response to disturbance** (Amplitude) & **degree of recovery** (Malleability)
Simoniello et al. (2008)	NDVI	GIMMS-AVHRR (8 km)	Italy, 1982–2003	Persistence probability of positive **recovery trends** compared to negative ones
Hirota et al. (2011)	Tree cover estimates	MODIS (1 km)	Tropical and subtropical zones of Africa, Australia and South America	Empirical **reconstruction of the basins of attraction** & **likelihood of a biome to remain in its current state**, given its rainfall
Frazier et al. (2013)	Gross primary production (GPP)	MODIS (1 km)	Southwestern Louisiana, USA, 2000–2006	**Ability of the system to recover**, based on a pre-event baseline
De Keersmaecker et al. (2015)	NDVI	GIMMS (0.072°)	Global, 1981–2006	**Resistance**: **response magnitude** of the vegetation to disturbance & **Resilience**: indicator of memory effect in time series, related to the **recovery speed** after a disturbance.
Verbesselt et al. (2016)	NDVI & Vegetation Optical Depth (VOD)	MODIS (MCD43C4 product, 5.6 km) & AMSR-E, (0.25°)	Global, 2000–2011	Spatial patterns of slowness inferred from **temporal autocorrelation** (indicator of **slow recovery rates**)
Schwalm et al. (2017)	Gross primary productivity (GPP)	MODIS (0.5°)	Global, 2000–2008	**Recovery time**: the time it takes for an ecosystem to revert to its pre-drought functional state

All empirical studies I reviewed used a remotely-sensed indicator related to vegetation properties as response variable to study ecological resilience. Such indicators are based on mathematical transformations of reflectance measurements in different spectral bands, particularly the red and near-infrared bands (Gaitán et al., 2013). The most commonly used – and also the one I chose for the empirical part of my work – is the Normalized Difference Vegetation Index (NDVI), originally proposed by Rouse et al. (1973). The NDVI is a spectral measure of energy absorption of vegetation (Myneni et al., 1995) and correlates with functional vegetation characteristics such as aboveground green biomass (Rouse et al., 1974) and patterns of vegetation seasonality and productivity (Goward et al., 1985, 1987). It has been frequently applied to study vegetation dynamics, habitat degradation, as well as effects of disturbances such as drought in a range of environments (Pettorelli et al., 2005). NDVI variability was shown to agree with precipitation variability (Gaitán et al., 2013; Helman et al., 2014), and to correlate with drought in large areas of the world (Vicente-Serrano et al., 2013), which makes it suitable for studying vegetation response to climate variability. Another indicator used to quantify

ecological resilience is the Gross primary production (GPP), a measure of vegetation growth. It is based on the radiation use efficiency and measures the rate at which plant biomass is captured and stored from photosynthesis (Frazier et al., 2013) . However, it showed limited success in capturing interannual variation in dry conditions (Turner et al., 2006).

In the empirical part of this work, data from the Landsat satellite programme were used to study ecological resilience to climatic variation in an arid rangeland of southern Europe. The Landsat archive contains the longest record of global- scale medium spatial resolution earth observation data (Hansen and Loveland, 2012). Landsat 5 TM, 7 ETM+ and 8 OLI data are collected every 16 days at a spatial resolution of 30 meters (in the VIS, NIR and SWIR spectral bands). When two Landsat sensors are flying concurrently, satellite orbits are offset to allow 8-day repeat coverage of any Landsat scene. Their spatial scale make Landsat data especially suitable for addressing ecological questions (Kennedy et al., 2014) and allows for the detection of small changes (Zhu and Woodcock, 2014). However, their relatively low temporal frequency is a drawback, especially since the number of pixels available for the analysis of vegetation dynamics is reduced by cloud coverage. Furthermore, there is large variation in the regional annual coverage of Landsat 5 data due to technical problems with downlinking acquired data to the ground stations (Goward et al., 2006). In most places of the world outside the United States this variation yields a far lower frequency of available images, with several long data gaps, especially in the 80s and 90s. After the launch of Landsat 7 ETM+ in 1999 the number of acquisitions increased with the introduction of a global acquisition plan. Accordingly, some international ground stations switched their reception from Landsat 5 TM to Landsat 7 ETM+. However, several of them changed their operations again to Landsat 5 TM after the failure of the Landsat 7 ETM+ scan line corrector system in May 2003 (Kovalskyy and Roy, 2013). All in all, Landsat data offer the unique possibility to study ecosystems over time scales of several decades in relatively high spatial detail, however with limited temporal resolution.

Satellite time series offer the possibility to infer aspects of resilience from real world systems. Van Nes and Scheffer (2007) suggest estimating recovery rates after stochastic disturbances in natural time series as an alternative to experimental perturbations. However, especially in seasonal, climate driven time series of vegetation with large natural variation, it is difficult to distinguish between the intrinsic seasonal variation and a disturbance (e.g. see extensive review on change in grasslands in Henebry, 2019). To this effect, several change detection methods have been developed, which are able to detect abrupt changes (henceforth ‘breakpoints’) in time series, while accounting for seasonality and trends present in the data (Ben Abbes et al., 2018). One of these methods is the Breaks For Additive Seasonal and Trend (BFAST) method (Verbesselt et al., 2010a, 2010b, 2012). BFAST type approaches have been validated and tested for detecting and monitoring abrupt vegetation changes in forested landscapes (e.g. Verbesselt et al., 2010a, 2012; DeVries et al., 2015a, 2015b; Dutrieux et al., 2015), as well as in drylands (e.g. Watts and Laffan, 2014; Browning et al., 2017), and were found successful in detecting drought induced trend changes (Verbesselt et al., 2012; Huang et al., 2014). Even though the original BFAST method was developed for regularly spaced time series, adapted versions of the algorithm that are able to deal with missing data have been applied in several studies (Verbesselt

et al., 2012; de Jong et al., 2013; DeVries et al., 2016). Such approaches have the advantage of allowing for the integration of all available data, even if this results in an irregularly spaced time series. This feature makes them particularly suitable for time series analysis based on Landsat datasets, which have a relatively low temporal resolution.

In this work, I applied an adapted version of BFAST, based on DeVries et al. (2016), to a dense long-term Landsat time series of the NDVI, making use of all available data. BFAST model outputs were used as proxies for two key characteristics of ecological resilience: resistance and recovery. Several other studies have made use of a BFAST model to assess vegetation recovery after a disturbance. For instance, Katagis et al. (2014) made use of the BFAST algorithm to calculate post-fire vegetation recovery trends in a Mediterranean ecosystem, based on MODIS NDVI time series. DeVries et al. (2015a) applied the BFAST Monitor (see Verbesselt et al., 2012) approach to a Landsat time series to detect disturbance in tropical forest. Subsequently, they calculated if recovery to the previous stable state occurred or not, and if yes, the time duration until the onset of recovery. Zewdie et al. (2017) applied BFAST to study dryland ecosystem dynamics in Ethiopia, based on MODIS NDVI time series. They related positive trends after a disturbance to vegetation recovery (periods of greening) and negative trends to periods of browning. In the following, I use the slope of the linear trend fitted by the BFAST-type model to the segment succeeding a drought-associated breakpoint as a proxy for recovery rate.

As a relative inverted measure of ecosystem resistance to climate variability, I use the total number of breakpoints fitted by BFAST during the study period (1984–2011). This choice was motivated by studies that validated and tested BFAST type approaches, showing that breakpoints can be used to find drought induced trend changes (Huang et al., 2014; Verbesselt et al., 2012). Using the number of breakpoints as an inverted measure of ecosystem resistance is an innovative approach which, to my knowledge, has not been used in previous studies. However, one study by Watts and Laffan (2014) suggested, that analysing the spatial variability of the number of breakpoints within one comparable study area can give insight into stability properties of vegetation response at different locations. On the one hand, using the relative number of breakpoints to study resistance has the limitation that it is not disturbance specific, unless under controlled experimental conditions, which are difficult to realize for long-term observations on meso- to landscape scale. On the other hand, if applied within a defined study area under comparable disturbance regime (as in this work), it has the advantage of providing information on the vegetation response to repeated disturbance over a long historical time period, instead of being limited to a single disturbance event.

3 Material & Methods

All analysis was performed in R (R Core Team, 2017), except when otherwise indicated.

3.1 Description of the study area – the Randi Forest in Cyprus – a Mediterranean Dryland Ecosystem[4]

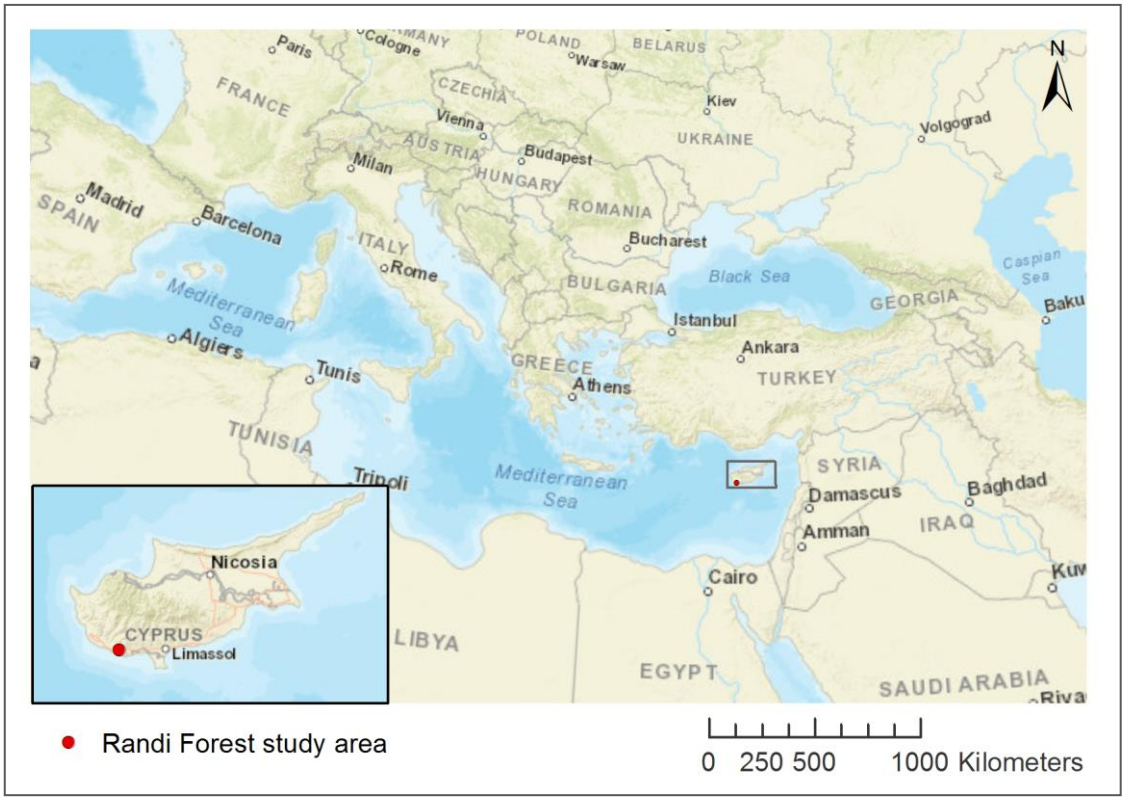

Figure 8. Cyprus in its region with close up to Cyprus with Randi Forest study area. Map produced in ArcMap 10.7.1. Credits/Sources: Esri, HERE, Garmin, USGS; Intermap, INCREMENT P, NRCan, Esri Japan, METI, Esri China, Esri Korea, Esri Thainland, NGCC, OpenStreetMap contributers, GIS User Community.

To study ecological resilience to climatic variation including drought, an exemplary Mediterranean dryland ecosystem in southern Cyprus ('Randi Forest'), near Pissouri town (34°40'20"N 32°38'50"O) was selected (Figure 8). Drylands include all dry subhumid, semi-arid, arid, or hyper-arid ecosystems (MEA, 2005b). Mediterranean drylands are particularly affected by land degradation (Safriel, 2006), for they combine high climate variability with intense human activities. Both of which are considered main causes for land degradation in drylands (UNCCD, 2009). Safriel (2006, p. 235) described the 'degradation of the biological productivity of drylands' as a function of the product of vulnerability and development pressure. He illustrated that in drylands human population and associated livestock density decreases with aridity, whereas vulnerability to degradation increases with aridity. According to Safriel (2006) Mediterranean

[4] Individual text passages in this section appear with slight adaptions in von Keyserlingk et al. (2021).

drylands are particularly prone to degradation for they cover to a large part exactly those intermediate aridity ranges, which combine high human pressure with high vulnerability to degradation.

The main feature of Mediterranean climate is its high intra-annual variability, with the alteration of a hot and dry summer and a rainy season in the cold month (Tomaselli, 1977). Winter rains are driven by cyclones advancing from Iceland (ibid.). They frequently appear in the form of high intensity rainfall events of short duration; thus, they are strong agents of water erosion (ibid.), especially if they fall on soil dried out from summer. Summers are characterised by high temperatures with almost no rainfall, lasting four month on average (ibid.). Aridity is more pronounced in the south-eastern part of the Mediterranean, where my study area is located, due to the effect of the Afro-Asian continental mass (ibid.).

In my study area in southern Cyprus, summer lasts from mid-May to mid-September (Republic of Cyprus: Meteorological Service, 2019). Winter rainfalls start in October, thus the hydrological year (in the following called 'h. year') in Cyprus is defined from 1st October to 30th September. During my study period (1984–2011), mean maximum daily temperatures in summer was on average 30°C (±1°C SD) (July and August) and 17°C in winter (January and February) (based on daily maximum temperature data from meteorological station at Pafos airport provided by Meteorological service of Cyprus). Mean annual precipitation was 396 mm (±92 mm SD) (based on daily precipitation data from Pissouri meteorological station provided by Meteorological service of Cyprus). Figure 9 provides a detailed summary of monthly mean rainfall and maximum temperature in the study area. In 2005 (h. year) a prolonged drought episode began continuing until 2008 (Michaelides and Pashiardis, 2008; Republic of Cyprus: Meteorological Service, 2019; see red triangles in Figure 9A). After four consecutive years with annual average rainfall well below the 1961–1990 average (and below the average during my study period – see red triangles in Figure 9A), the dams were almost empty in 2008 and Cyprus had to struggle with severe water shortage and agricultural drought (Michaelides and Pashiardis, 2008). This extreme water shortage is even more striking because the preceding three years (h. years 2002–2004) had been wet and the surface reservoirs filled with water (Michaelides and Pashiardis, 2008). In 2008 (h. year) the total amount of rainfall was 237.8 mm, which corresponds to 51% of its normal value. It is the second lowest value during the whole period of measurements in Cyprus (since the beginning of the 20th century) – the lowest ever recorded was during 1973 (h. year) (Michaelides and Pashiardis, 2008). In my studies, I chose this prolonged dry period (h. years 2005-2008) as an outstanding case to study vegetation recovery from drought.

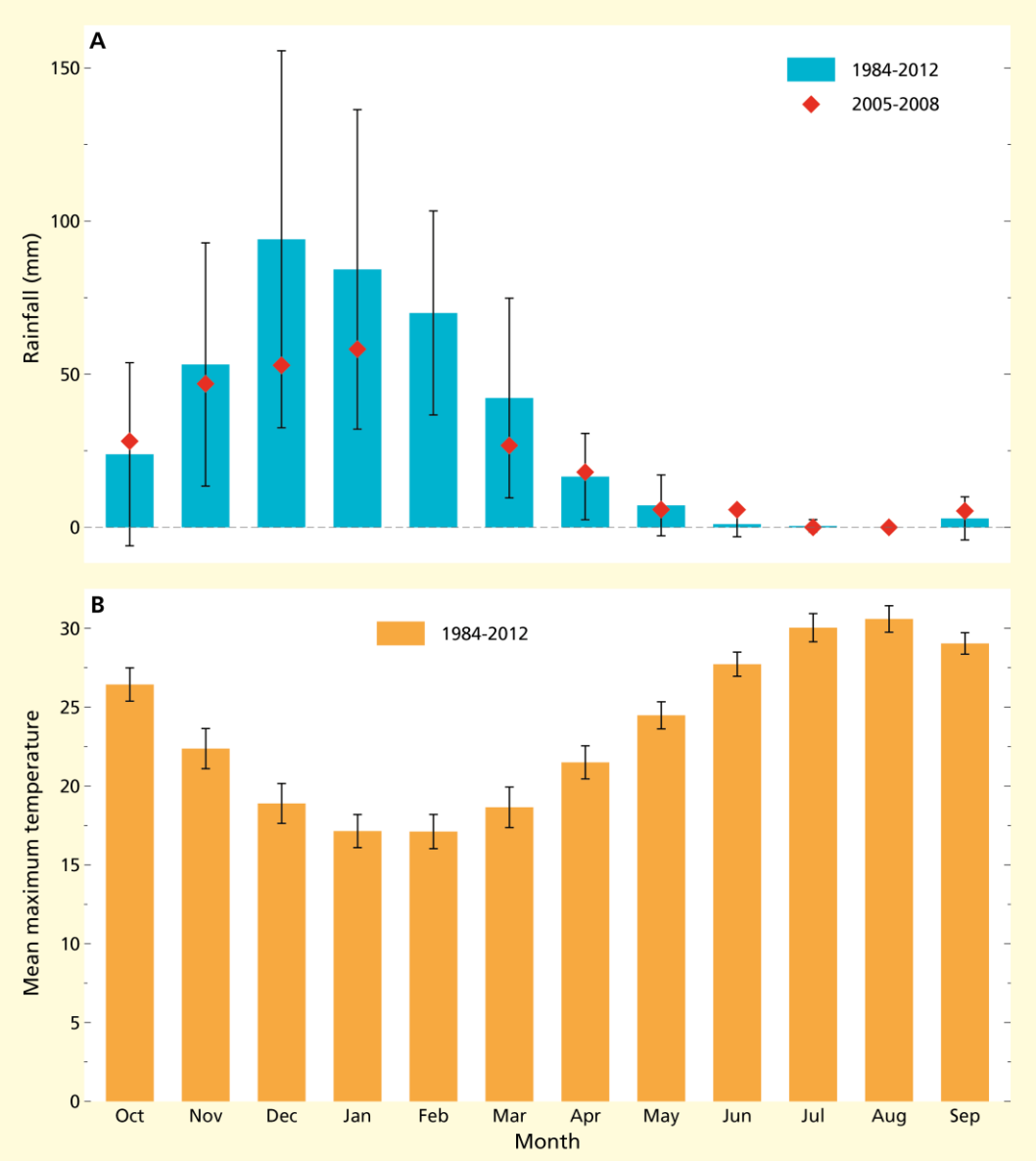

Figure 9[5]. Monthly mean rainfall (A) and maximum temperature (B) in the study area during 1984–2012 (h. years). Error bars show the standard deviation (±1SD). The red triangles in A represent the mean monthly rainfall for 2005–2008 (h. years). This time period represents the period of drought, which was used for the detection of drought breakpoints. Monthly mean max. temperature was calculated based on daily maximum temperature measured at meteorological station at Pafos airport. Monthly mean rainfall was calculated based on total daily rainfall measured at meteorological station at Pissouri. All data was obtained from the Meteorological Service of Cyprus.

Climate change is further enhancing the climatic stressors of land degradation in the Mediterranean basin. Already, Europe is warming faster than the global average (IPCC, 2013). The number of warm days and nights have *very likely* increased since the 1950s and there is indication for a general increase in the intensity and frequency of extreme precipitation, especially in winter (ibid). In the Mediterranean region, the frequency and intensity of drought has *likely* increased (IPCC, 2014). Throughout the 21st century, a continued increase in temperature is projected for Europe and the Mediterranean region (stated with *high confidence*, IPCC, 2013). In the Mediterranean region the warming will *likely* be more intense during

[5] This figure appears in similar form in von Keyserlingk et al. (2021).

summer, in combination with a *very likely* increase of warm spells and heat waves (ibid.). Annual mean precipitation will *likely* decrease in the region (ibid.). Climate projections further show a marked increase in meteorological droughts (stated with *medium confidence*) and heavy precipitation events (stated with *high confidence* in IPCC, 2014).

In Cyprus, climate change has already become apparent: average temperatures increased, while average annual precipitation decreased by -17% (559 mm to 462 mm) when comparing the first 30-year period with the last 30-year period of the 20th century (Republic of Cyprus: Department of Meteorology, 2019). The decrease in precipitation is attributed to a higher frequency of droughts in the second half of the 20th century (ibid.)

Drylands are particularly vulnerable to land degradation (Reynolds et al., 2007). This is due to a particularly high social-economic vulnerability in combination with very fragile ecosystems (Reynolds et al., 2007). Drylands are by definition water-limited ecosystems with low soil moisture, due to a combination of low rainfall and high evaporation rates (Safriel, 2006). This limitation in soil moisture results in a characteristically low biological productivity (ibid.), for there exist strong vegetation-soil moisture feedbacks (Tietjen et al., 2009). Low soil moisture limits plant growth and plant biomass, which leads to low amounts of plant litter (Safriel, 2006). This yields low soil organic content, which further reduces soil water holding capacity and soil microbial activity, which is in turn depended on soil moisture (ibid.). As a result, nutrient cycling is hampered, the soil structure loses complexity and the degree of soil development is reduced (ibid.). Vegetation, which has positive effects on soil moisture by increasing water infiltration, providing shading and reducing run-off (Tietjen et al., 2009), faces harsh conditions. These augmenting processes and feedbacks make the soil very vulnerable to water erosion (Safriel, 2006), which washes away nutrients and topsoil. Furthermore, shallow moisture penetration in the soil and fast evaporation of rainfall lead to an accumulation of salinity in the topsoil, which in the end can cause salinization (ibid.). It follows logically that a further decrease of vegetation cover due to livestock grazing or an increased frequency of droughts due to climate change proves a serious threat to these fragile ecosystems, which have evolved historically in and are well adapted to these challenging climate conditions (if undisturbed by humans).

The natural Mediterranean vegetation is typically sclerophyllous evergreen forest or dense maquis scrubland (Tomaselli, 1977). Vegetation is not considered to represent a stable equilibrium state, rather it is continuously in a stage of degradation towards less dense garrigue, or patches of bare soil – e.g. on steep sunny slopes or in wind-blown areas – or in a successional process of regeneration towards a forest (ibid.). These dynamics create a large variety of habitats promoting high biological diversity. Typical degradation stages are illustrated in Figure 10. Whereas degradation can happen very fast, regeneration of vegetation is slow and sometimes cannot happen spontaneously any longer (ibid.) – especially in drylands where augmenting vegetation-soil moisture feedbacks tend to stabilize a degraded ecosystem state once a tipping point is crossed. The main differences between forest, maquis and garrigue lies not so much in a change of the basic floristic composition, but rather in the vegetation structure (ibid). Maquis and garrigue both represent forms of *matorral*: ‘a stand of woody plants,

nanophanerophytes or chamaephytes, their size and habitus being either natural or artificial, resulting from degradation (cutting, burning, grazing)' (Sauvage, 1961, in Tomaselli, 1977, p. 358). Maquis consist of densely growing sclerophyllous shrubs with average height of 1-2 m, interspaced with small trees (İLseven, 2017). Garrigue is more discontinuous and occurs on dryer soil than maquis (Tomaselli, 1977).

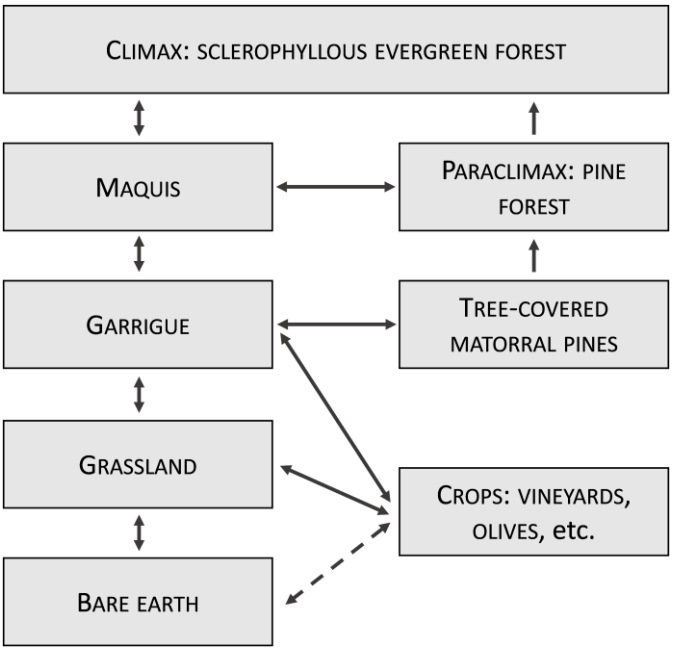

Figure 10. Pattern showing possible stages of degradation or progressive evolution of Mediterranean vegetation (adapted from Figures 2 & 3 in Tomaselli, 1977, p. 359).

The name 'Randi Forest' already indicates that the study area in Cyprus has historically been a forest. It used to be a pine forest, which was transformed to an open scrubland (maquis and garrigue) due to wood cutting during British governance in the 1930s (Daliakopoulos and Tsanis, 2014), which was succeeded by extensive livestock grazing. Most shrubs are sclerophyllous and thus well adapted to drought, such as *Calycotome villosa*, *Genista fasseleta*, *Rhamnus oleoides* (Daliakopoulos and Tsanis, 2014). Shrubs consist of both palatable (e.g. *Sarcopoterium spinosum*) and unpalatable (e.g. *Urginea maritima*) species. They are of varying height and sometimes interspaced with annual grasses, perennial herbs and individual trees, mainly: *Olea europaea*, *Ceratonia siliqua* and *Pinus species* (Daliakopoulos and Tsanis, 2014). In strongly grazed parts woody vegetation in the area consists mainly of small bonsai-type shrubs (Vallejo et al. (2014) and own observation during field visit). This shape is caused by the goats that feed on the outer palatable sprouts while avoiding the thorny inner parts. Palatable perennial herbs mainly grow within thorny shrubs, thereby being protected from grazing.

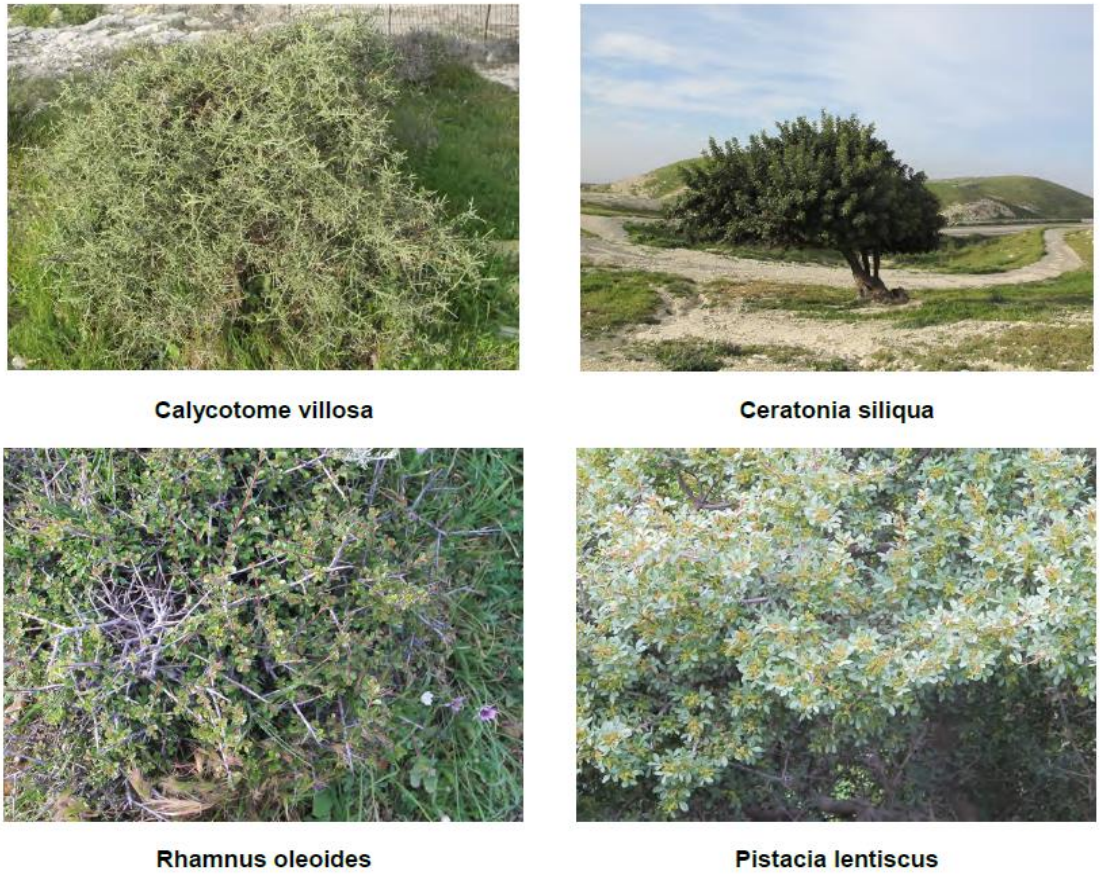

Figure 11. Typical vegetation in the Randi Forest study area. Figure adopted from Figure 89 in Daliakopoulos and Tsanis (2014, p. 92).

Today, the area is severely degraded (Vallejo et al., 2014; Daliakopoulos and Tsanis, 2014; Riva et al., 2017) with large patches of denuded and very thin, calcaric soil. Deep gully and rill erosion is frequently visible in the area, especially on south- to west-facing slopes, which are particularly exposed to the strong solar radiation. The main drivers of degradation are considered strong over-grazing (Daliakopoulos and Tsanis, 2014; Vallejo et al., 2014; Riva et al., 2017) combined with a trend of increasing aridity and higher frequency of droughts that has been observed in recent decades (Daliakopoulos and Tsanis, 2014; Republic of Cyprus: Meteorological Service, 2019). Figure 12 gives an impression of different degradation stages that can be observed in the study area.

Figure 12. Different degradation stages in the Randi Forest study area. From left to right: dense scrubland interspaced with herbaceous layer; discontinuous scrubland with bonsai-shaped shrubs that have been browsed by goats; strongly degraded hillslope.

The area is not owned by the shepherds, but they are commons open to all. It is grazed mostly by goats, but also some sheep. Since the 1970s grazing pressure has strongly increased, due to a growing tourism development and coastal urbanization in the Pissouri district, which reduced the total area available for livestock grazing. This development has led to strong overgrazing in the Randi Forest (Daliakopoulos and Tsanis, 2014). Even though today grazing pressure is reduced due to an abandonment of farms, the area shows little signs of recovery (Riva et al., 2017). Figure 13 shows a typical goat farm in the study area, with clearly visible goat pathways caused by trampling damage leading of the farm.

Figure 13. Goat farm in the Randi Forest study area with goat pathways leading of the farm.

The soils are derived from marls and are shallow Calcaric Regosols (IUSS Working Group WRB, 2015) with a light colour and high calcium carbonate content (60-70%). Elevation ranges from 65 m to 281 m above sea level. Most hillslopes range between 10° and 20° and are predominantly facing south-west (based on SRTM v3.0 digital elevation model).

The area of interest (Figure 14) contains seven farms. For all of these farms, detailed information on the past grazing regime was obtained during systematic interviews conducted by M. de Hoop in 2017. According to the farmers, the goats usually walk a maximum distance of 800 meters away from the farms. Therefore, everything within a 1000 m distance from the seven farms (using an extra buffer of 200 meter) was included. Between 2000 and 2006, a highway was built. To exclude disturbances by this road, the highway as well as the area south of the highway was excluded. Further, a circle with a radius of 800 m around a farm north of our study area was drawn. This region was excluded to eliminate the influence of this farm. This selection process resulted in the area of interest (Figure 14), covering 3.1 km^2 (3439 Landsat pixels).

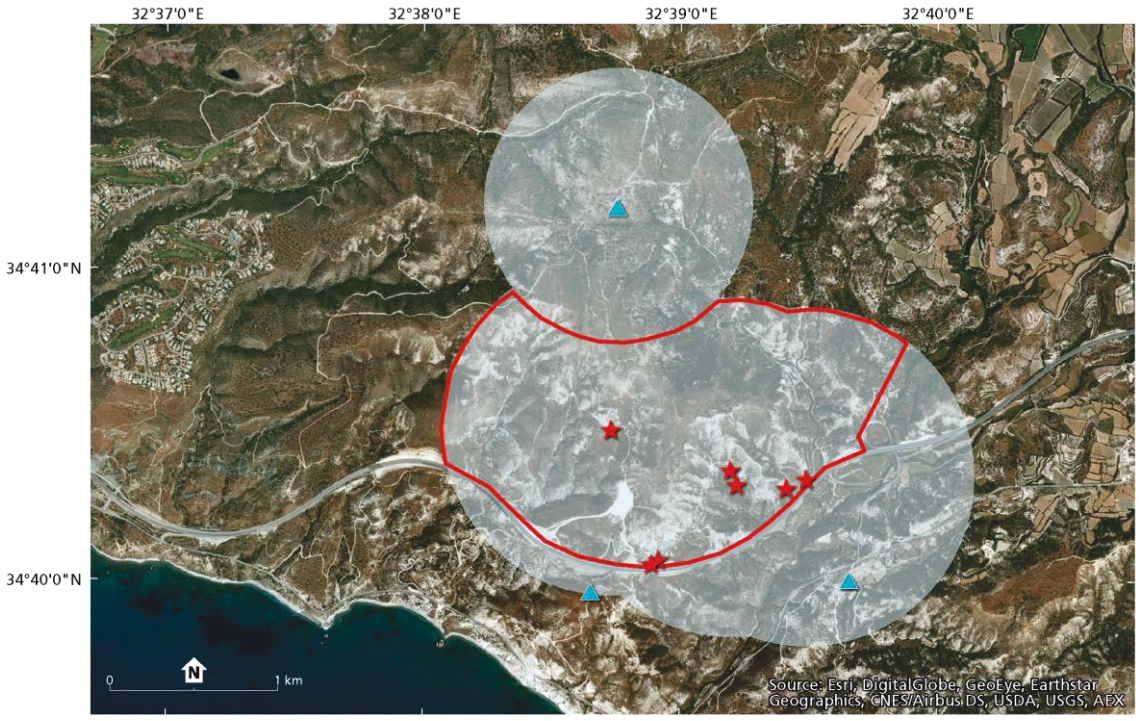

Figure 14[6]. Area of interest (3.1 km^2, 3439 Landsat pixels). Red stars show all 7 farms in the area of interest. Blue triangles represent farms outside the area of interest. Grey circles of 1000 m radius are drawn around the farms in interest to show the grazing area related to those farms. Final area of interest is outlined in red.

3.2 SATELLITE DATA ACQUISITION AND DATA PRE-PROCESSING[7]

To gain empirical insight into vegetation resilience, an extensive amount of remote-sensing data collected by the Landsat satellite programme (NASA / U.S Geological Survey) were processed and analysed. To this purpose, all available Landsat 5 and 7 data from the Thematic Mapper (TM) and the Enhanced Thematic Mapper Plus (ETM+) instruments were obtained. These datasets were chosen firstly, because the wavelength intervals of the bands required for the

[6] This figure appears in similar form in von Keyserlingk et al. (2021).
[7] Some text passages in this section appear with slight adaptions in von Keyserlingk et al. (2021).

calculation of the NDVI (namely the Red and Near Infrared (NIR)) of the TM and ETM+ sensors are almost identical. This allows inter-sensor comparability of the information collected by these bands, which is essential when aiming at time series analysis that is by nature highly sensitive to external error sources. Secondly, the Landsat 5 mission is the longest earth-observing mission in history. Combining TM and ETM+ data allowed me to analyse data over 28 years, between 1984 and 2011. Landsat 5 and 7 TM and ETM+ data are acquired at a spatial resolution of 30 meters, a temporal resolution of 16 days (except when two Landsat sensors flying concurrently), and collected decentralized via several ground stations around the globe. Both the archives from the U.S Geological Survey (USGS) and the European Space Agency (ESA) have acquired a comprehensive collection of Landsat scenes, which are available for free download. However, the data collections in neither archive are complete, and at the time of our study, at WRS-II path/row 176/36, most scenes from the 80s were only available in the ESA archive. I therefore downloaded all available Level-1 ground-terrain-corrected TM and ETM+ Landsat imagery (542 scenes in total) from the ESA archive for the time period 1984–2011. In 2003 the scan line corrector of the ETM+ instrument aboard Landsat 7 failed. These erroneous scenes were excluded. The downloaded data were atmospherically corrected to surface reflectance using the Landsat Ecosystem Disturbance Adaptive Processing System (LEDAPS, version 2.7.0) (Masek et al., 2006; Schmidt et al., 2013). All scenes were included independent of total cloud cover, but subsequently pixels affected by clouds, cloud shadow, snow and missing data were masked out on pixel level based on the 'QA' layers produced by LEDAPS.

Since geospatial shifts in the sub-pixel range were present in the data that would hamper multi-temporal analyses, all scenes were geospatially co-registered to a master scene using the software AROSICS in the programming language 'Python' (Scheffler et al., 2017). As geospatial reference for the co-registration, a cloud-free scene (LE71760362002225SGS00, surface reflectance, band 4), downloaded from USGS archive was used. A scene from the USGS archive was chosen, because the Landsat surface reflectance products are well geospatially aligned among each other, and I wanted to keep the option for including imagery downloaded from USGS in the analysis later on. Finally, several erroneous scenes were sorted out manually, e.g. scenes where the co-registration failed due to high cloud cover, or scenes that were shifted over the sub-pixel range. In total, 476 Landsat scenes (414 TM and 62 ETM+ scenes) were included in the analysis (Figure 15). On average there are 17 (±6.3 SD) scenes per year. There are no extensive data gaps in the time series, but temporal image density varies (Figure 15 & Figure 19F). In 1999 to 2002 image density is higher than the average, while in 1990 and 2003 very few images were available. As a result of the cloud masking on pixel level, the number of valid observations per pixel was lower than the overall number of included Landsat scenes and varied slightly among pixels (Mean=259 ±16 SD). All datasets were projected to UTM (Universal Transverse Mercator) coordinate system zone 36N (WGS 1984).

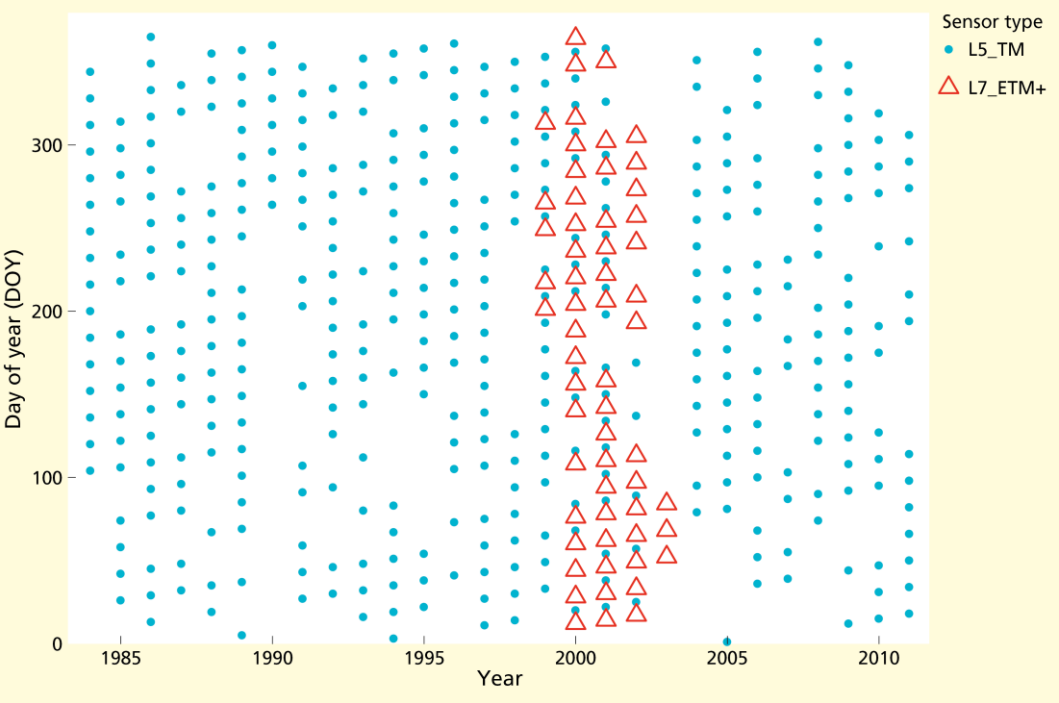

Figure 15[8]. Temporal distribution of all Landsat 5 TM scenes and Landsat 7 ETM+ scenes that were included in the analysis. Landsat 7 ETM+ scenes affected by the failure of the scan line corrector in 2003 (Landsat 7 ETM+ SLC-off) were excluded prior to the analysis and are not included in this figure.

3.3 Grazing intensity & Topographic properties[9]

Both aspect and terrain slope can affect the vegetation resilience to climatic variation. These topographic properties were obtained from properties from a digital elevation model provided by the Shuttle Radar Topography Mission (SRTM v3.0) at a spatial resolution of 1 arc-second. To align the elevation cells with the Landsat raster, a bilinear resampling was performed in ArcGIS 10.6.1. Thereafter, aspect (in degrees) and terrain slope (in %) were obtained with the ArcGIS Spatial Analyst Toolbox.

Grazing by goats affects the vegetation dynamics both directly, by reducing vegetation cover, and indirectly, by trampling. In this work, the combined effects were studied without differentiating between direct and indirect aspects. In 2017 local farmers in the Randi Forest were systematically interviewed by M. de Hoop to estimate the grazing intensity in the study area. The farmers explained that the goats can walk freely throughout the study area during several hours of the day. The animals prefer to stay close to the farm, so the estimated grazing intensity decreases with the distance to the farm. The farmers also explained that when the animals want to reach an area up- or downhill, they do not walk straight uphill. Instead, they have created walking paths along the hills, thereby increasing the distance to walk uphill. The interviews provided information about the number of animals for each of the seven farms around 1987 and 2007, respectively.

[8] This figure appears in similar form in von Keyserlingk et al. (2021).
[9] This section appears in similar form in von Keyserlingk et al. (2021). It is based largely on work by M. de Hoop, who has conducted the interviews with the local farmers and calculated the grazing intensity index.

This information from the local farmers was used to estimate the relative grazing intensity (livestock/m) for each 30x30 m pixel (x, y) with the path distance tool in ArcGIS. As input variables, the number of animals per farm (i) and the distance between the pixel and the farm were used:

$$Grazing\ intensity_{x,y} = \sum_{i=1}^{n} \frac{animals_i}{distance_{i(x,y)}} \qquad (1)$$

This calculation is in agreement with other studies (e.g. Manthey and Peper 2010), which show that grazing can be estimated by the inverse distance from a hotspot, which is in our case the farm. A vertical friction factor (symmetric inverse linear with the default slope of -1/45) was added to the distance to represent the extra 'friction' for the goats to walk up- or downhill as explained by the local farmers. The distribution of estimated grazing intensity is strongly right skewed. Therefore, all values above the 97.5% quantile were removed. These calculations resulted in estimations of the grazing intensities for both 1987 and 2007 (Figure 16). Estimates of 0-9 livestock/m are in the same range as found in another semi-arid rangeland by Manthey and Peper (2010). For the statistical analysis of the NDVI recovery trend, the grazing intensity values were log-transformed with $log\ (grazing\ intensity - 1)$, to approximate a normal distribution.

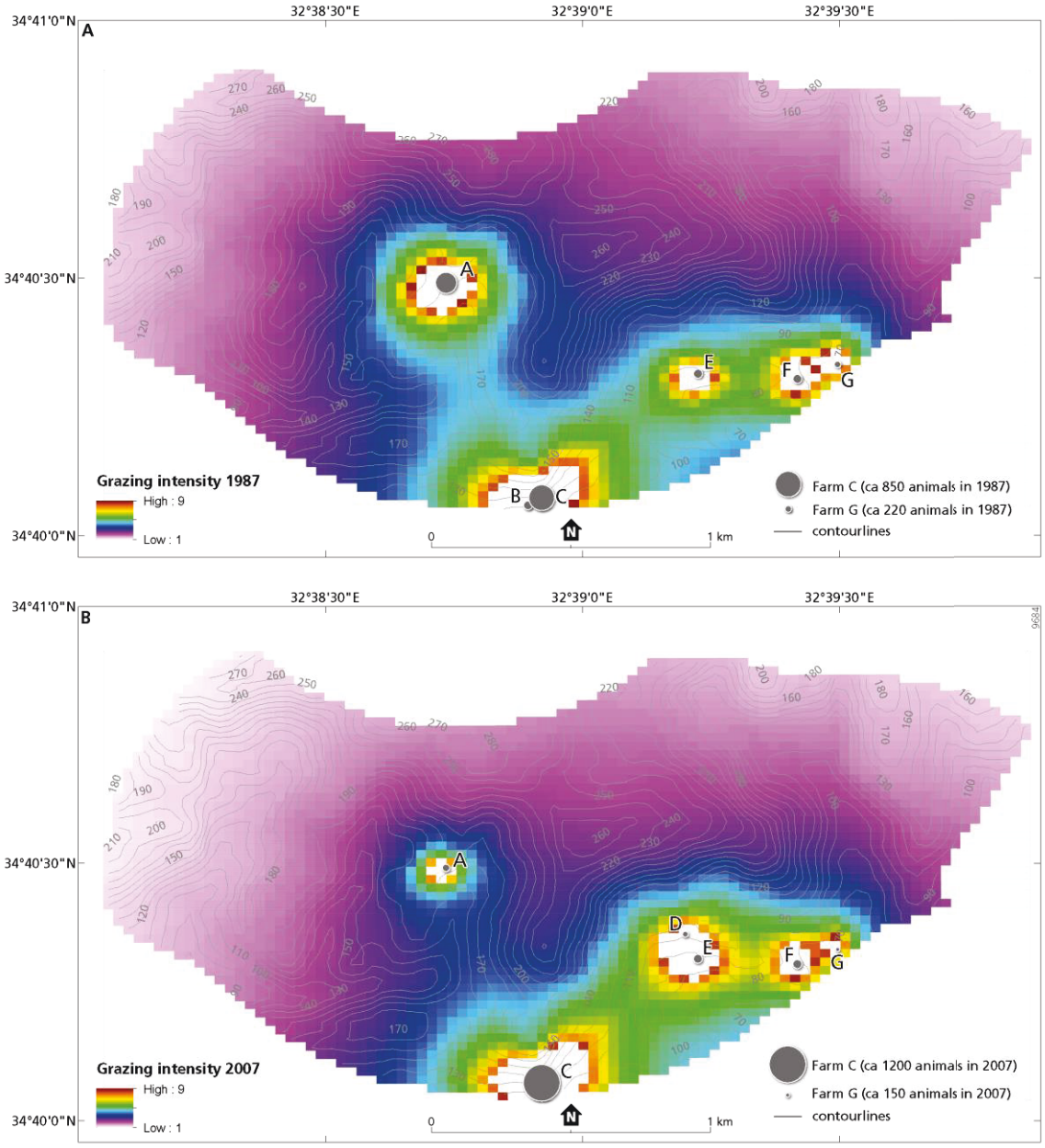

Figure 16[10]. Estimated grazing intensity for 1987 and 2007, based on the number of animals per farm, the inversed distance to the farm and the vertical friction factor (to account for the difficulty to walk up- or downslope). Grazing values above the 97.5% quantile are excluded. Circles depict goat farms with the size of the circle proportional to the estimated number of animals in the specific period. Please note that between 1987 and 2007 farm B was integrated in farm C. Therefore farm B does not appear in subfigure B.

3.4 Extraction of metrics for resistance and recovery using change detection in Landsat NDVI time series[11]

To study the ecosystem's resilience to climatic variation, I have decided on two key metrics: long-term vegetation resistance to climate variability and recovery rate after a drought (see

[10] This figure appears in similar form in von Keyserlingk et al. (2021). It has been provided by M. de Hoop, who has conducted the interviews with local farmers and calculated the grazing intensity index.
[11] Individual text passages in this section appear with slight adaptions in von Keyserlingk et al. (2021).

2.2.1 for details on motivation). To extract this information from remotely-sensed time series data, I made use of a change detection approach (BFAST), which enables to differentiate between natural seasonal variation and sudden, disturbance-driven effects. The original BFAST approach presented in Verbesselt et al. (2010a, 2010b) was designed for regularly spaced satellite time series. In my approach, I made use of all available Landsat imagery, which resulted in an irregularly spaced time series. Hence, I adapted the BFAST approach for this special situation, building on work by DeVries et al. (2016) and designing my own functions.

As a climate driven indicator of ecosystem dynamics the Normalized Difference Vegetation Index (NDVI) was chosen. The NDVI makes use of the strong reflectance contrast of green vegetation between the visible Red (0.63–0.69 µm in Landsat TM instrument) and Near Infrared (NIR) (0.76–0.9 µm in Landsat TM instrument) wavelength interval. Chlorophyll absorption reaches a maximum at about 0.69 µm, and is minimal in the adjacent NIR region (Myneni et al., 1995). Furthermore, the mesophyll leaf structure strongly scatters NIR. In the earliest reported use of the NDVI in the Great Plains study by Rouse et al. (1973), it has been found to correlate with aboveground green biomass. Later on, the NDVI has been interpreted as a measure of chlorophyll abundance and energy absorption of the vegetation (Myneni et al., 1995). Significant relationships between the NDVI and structural and functional characteristics of vegetation have been reported, such as basal cover, Net Primary Production (NPP) and Absorbed Photosynthetic Active Radiation (APAR) (Tucker, 1979; Gamon et al., 1995; Pettorelli et al., 2005; Olofsson et al., 2007; Gaitán et al., 2013). The NDVI is calculated based on the formula:

$$NDVI = \frac{(NIR - Red)}{(NIR + Red)} \qquad (2)$$

(Rouse et al., 1974). The value range of the NDVI is -1.0 to 1.0. On terrestrial surfaces with sparse to dense vegetation cover, its values usually range between 0.2 and 1, with values close to 1 indicating a large amount of photosynthetically active vegetation biomass in the area.

The NDVI calculation was based on an adapted version of the function ‘processLandsat’ in the package ‘bfastSpatial’ (Dutrieux and DeVries, 2004). The function was originally designed to grab the NIR and Red bands of Landsat images provided by the USGS archive. Since I made use of Landsat imagery downloaded from the ESA archive instead, which uses different terminology for the bands, and had further processed each band to surface reflectance (sr), I adapted the function to grab the processed sr-bands. Subsequently, an NDVI time series was created for each pixel of the study area.

Additive season-trend models were fitted to the time series data on pixel by pixel basis as described in detail in (Verbesselt et al., 2010b, 2012), using the R package 'bfast' (Verbesselt et al., 2010a, 2010b, 2012), where the data are decomposed into a linear trend and a harmonic, seasonal part. For each observation y at time t a season-trend model was fitted:

$$y_t = \alpha_1 + \beta t + \sum_{j=1}^{k} \gamma_j \sin\left(\frac{2\pi j t}{f} + \delta_j\right) + \varepsilon_t \qquad (3)$$

where α_1 is the intercept, β the linear slope, $\gamma_j, \ldots, \gamma_k$ the seasonal amplitudes and $\delta_j, \ldots, \delta_k$ the phases; f is the known frequency of the time series and ε_t the unobservable error term; k refers to the number of harmonic terms employed for the harmonic model, describing the seasonality in the data. Following Verbesselt et al. (2010b) and based on recommendations by Geerken (2009), three harmonic terms were used to capture the intra-annual variation in the data. By discarding harmonic components of a higher order, effects of high frequency noise are effectively eliminated. At the same time, phenological variation occurring within a four-month cycle or more (depending on the temporal resolution of the data) are captured, hence diagnostic phenological features in the NDVI time series are preserved (Geerken, 2009). Because the Landsat data were collected at irregular dates, a frequency (f) of 365 was used to convert the data to a daily time series for methodological reasons, following DeVries et al. (2016).

Extraction of metric for long-term resistance

To gain insight into long-term resistance (*lt*-resistance) of the vegetation to climate variability in the study area, I extracted the optimal number of breakpoints fitted by a change detection approach for the whole time series on a pixel by pixel basis. Using the number of breakpoints as an inverted measure for long-term resistance was motivated by the assumption that the higher the ability of the vegetation to resist climatic anomalies such as droughts, the lower the direct impact on the NDVI dynamics, and the lower the likelihood for the occurrence of a breakpoint in the time series. As such, resistance is not used synonymously to ecosystem health or sustainability. Rather, it relates to the resistance of the ecosystem to be disturbed from its current state, which may be positive or negative, depending on the ecological value of that state. Further, using the number of breakpoints in a time series as an inverted measure of resistance is only meaningful when seen in spatial relation to the general frequency of breakpoint occurrence in the whole study area. I.e. a number of one breakpoint during ten years does not directly tell us anything about the resistance of the ecosystem. Only when, for example, most other pixels show three breakpoints during the same time interval and under a comparable disturbance regime, a value of one breakpoint would indicate a high resistance relative to the rest of the area. The number of breakpoints, therefore, gives insight in the spatial variability of long-term resistance within the study area.

To detect breakpoints in the time series, I followed the 'breakpoint' approach originally described in Bai & Perron (1998) and implemented in the R package 'strucchange' by (Zeileis et al., 2002, 2003). First, an ordinary least squares (OLS) residuals-based Moving Sum (MOSUM)

test was performed to test for a deviation from structural stability in the harmonic-trend models fitted by equation (3). If the MOSUM test was significant (p-value <0.05), breakpoints were fitted. The optimal number of breakpoints was determined by minimizing the Bayesian Information Criterion (BIC) and the position of the breakpoints (breakdates and confidence intervals) were chosen by globally minimizing the residual sum of squares. The parameter 'h' in the function 'breakpoints' (Zeileis et al., 2002, 2003), which sets the minimum number of observations required between two breakpoints, was set to 0.15, based on recommendations in Bai and Perron (1998) as well as in Watts and Laffan (2013); the latter found an advantage of using h values of 0.2 or smaller. Based on a total of 476 scenes, $h = 0.15$ results in a minimum of 71 scenes (approximately 3.4 years, depending on temporal data availability and cloud-conditions) between two breakpoints. Within this interval only the most important breakpoint is detected. The total number of breakpoints and their time of occurrence for each pixel was extracted and saved for further analysis. The total number of breakpoints was used as an inverse proxy for long-term vegetation resistance to stochastic climatic variation.

Extraction of metric for the recovery rate after drought

As a proxy for the recovery rate after a drought, I used the slope fitted by the linear trend component of BFAST model (thereby excluding seasonal effects) following a drought-associated breakpoint in the time series, on a pixel by pixel basis. To this purpose, I selected all pixels that experienced a breakpoint in the hydrological years 2005 to 2008 (01.10.2004–30.09.2008). During this time period a majority (77%) of the pixels in the study area experienced at least one breakpoint (Figure 19D). This widespread occurrence of breakpoints throughout our study area cannot be explained by small-scale disturbances or local land use change, nor by temporal variation in data availability. A denser time series increases the likelihood to detect a breakpoint, yet it is not above average during the time period in question (Figure 19F). Climatic drivers, however, affected the area as a whole. The hydrological years 2005 to 2008 were relatively dry, including two major droughts (2006 and 2008) that were preceded by three successive wet years (from 2002 until 2004) (Figure 19E). I therefore assumed that the widespread occurrence of breakpoints throughout our study area between 2005 and 2008 was driven by drought. To make this assumption more robust, I calculated the relative change in the mean NDVI of the three years before and after the breakpoint. Only if the NDVI dropped by at least 10%, the breakpoint was designated as a 'drought breakpoint' and pixels were included in further analysis (81% of all breakpoint pixels). In the rare case that more than one breakpoint was found between 2005 and 2008 the first one was selected for further analysis. Additive season-trend models (3) were fitted to all segments separated by breakpoints, using the robust regression approach described in DeVries et al. (2016) that is particularly robust to outliers. The output of the adapted BFAST approach is shown exemplarily for three pixels with different dynamics in Figure 19A–C. Finally, the slope of the linear trend component (parameter β) in the segment following the breakpoint between 2005 and 2008 was extracted from the model parameters and used as a measure for the recovery rate of the vegetation after a drought (henceforth called 'NDVI recovery trend').

Extraction of metric for event-based resistance

In chapter 4.4 I used an additional measure for resistance, namely event-based resistance (*eb*-resistance) to drought. To that purpose, I extracted the relative difference in mean NDVI of the three years before and after the drought breakpoint, which occurred during the hydrological years 2005 to 2008.

The adapted BFAST approach applied in this work differs from the original BFAST method described in (Verbesselt et al., 2010a, 2010b) in several ways. In Verbesselt et al. (2010a, 2010b) the seasonal and trend components are fitted separately, and breakpoint detection and model fitting is performed in an iterative procedure. Breakpoints are fitted to the seasonal and trend component individually. In my adapted approach, a full season-trend model (equation (3) is fitted to the time series and then checked for structural stability to fit breakpoints to the time series. After breakpoints are fitted, additive season-trend models are fitted to all individual segments in the time series, following DeVries et al. (2016). The general procedure of detecting breakpoints based on a full season-trend model is similar to the BFASTmonitor approach described in Verbesselt et al. (2012), which was designed to monitor near real-time disturbance in time series. However, instead of checking only for one recent breakpoint in a time series based on a stable history period as in Verbesselt et al. (2012), the approach applied in this thesis checks for breakpoints within the whole time series and is not dependent on a stable history period. Fitting a full season-trend model to the data to check for breakpoints, instead of using an iterative procedure to fit the seasonal and trend components separately makes the approach a little less sensitive for the occurrence of breakpoints if those do not happen in the seasonal and trend component simultaneously (Haywood and Randall, 2008). However, great advantages are that it can be applied to irregularly spaced time series (Verbesselt et al., 2012), and requires much less computational power. The latter becomes particularly relevant when aiming at spatial analysis of large raster datasets, as done in this thesis.

All satellite data processing steps are summarized in Figure 17. The code for the adapted BFAST analysis and for extraction of the number of breakpoints and NDVI recovery trend can be found at 'https://github.com/jennifervk/resInd'. I designed the function 'resInd.R' to perform the adapted BFAST analysis for individual pixels for an irregularly spaced time series. The function 'resIndSpatial.R' implements this function spatially for a raster dataset. It is based on a similar approach as in the 'bfastSpatial' package (Dutrieux and DeVries, 2004).

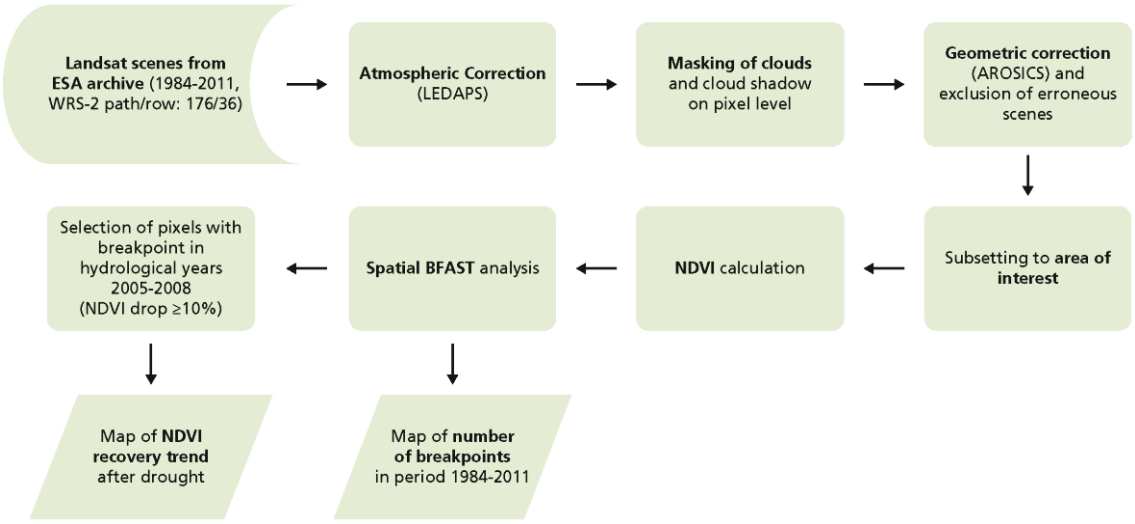

Figure 17[12]. Scheme of the satellite data processing steps.

The output of the adapted BFAST analysis, together with two high resolution satellite images taken in August 2003 and 2009 (before and after drought), is shown for three exemplary Landsat pixels (A, B, C) located in the south of our study area (Figure 18 & Figure 19A-C). The pixels show varying dynamics: pixel A is located on a southeast-facing slope with few shrubs, little grass cover and visible rill erosion (Figure 18). It has three breakpoints (i.e. low resistance), and a low NDVI recovery trend after the breakpoint in 2005 (Figure 19A). This combination indicates low ecological resilience. Compared to pixel A, pixel B has higher vegetation cover that also contains an herbaceous layer (Figure 18). It has only two breakpoints and shows a steeper recovery trend after the breakpoint in 2006 (Figure 19B). This combination indicates higher ecological resilience compared to pixel A (i.e. higher resistance and faster recovery). Pixel C mostly contains bare soil (Figure 18) and has no breakpoints (i.e. high resistance) (Figure 19C). This pixel represents the almost barren, unresponsive ecosystem state, for which I expected no or one breakpoint.

[12] This figure appears in von Keyserlingk et al. (2021).

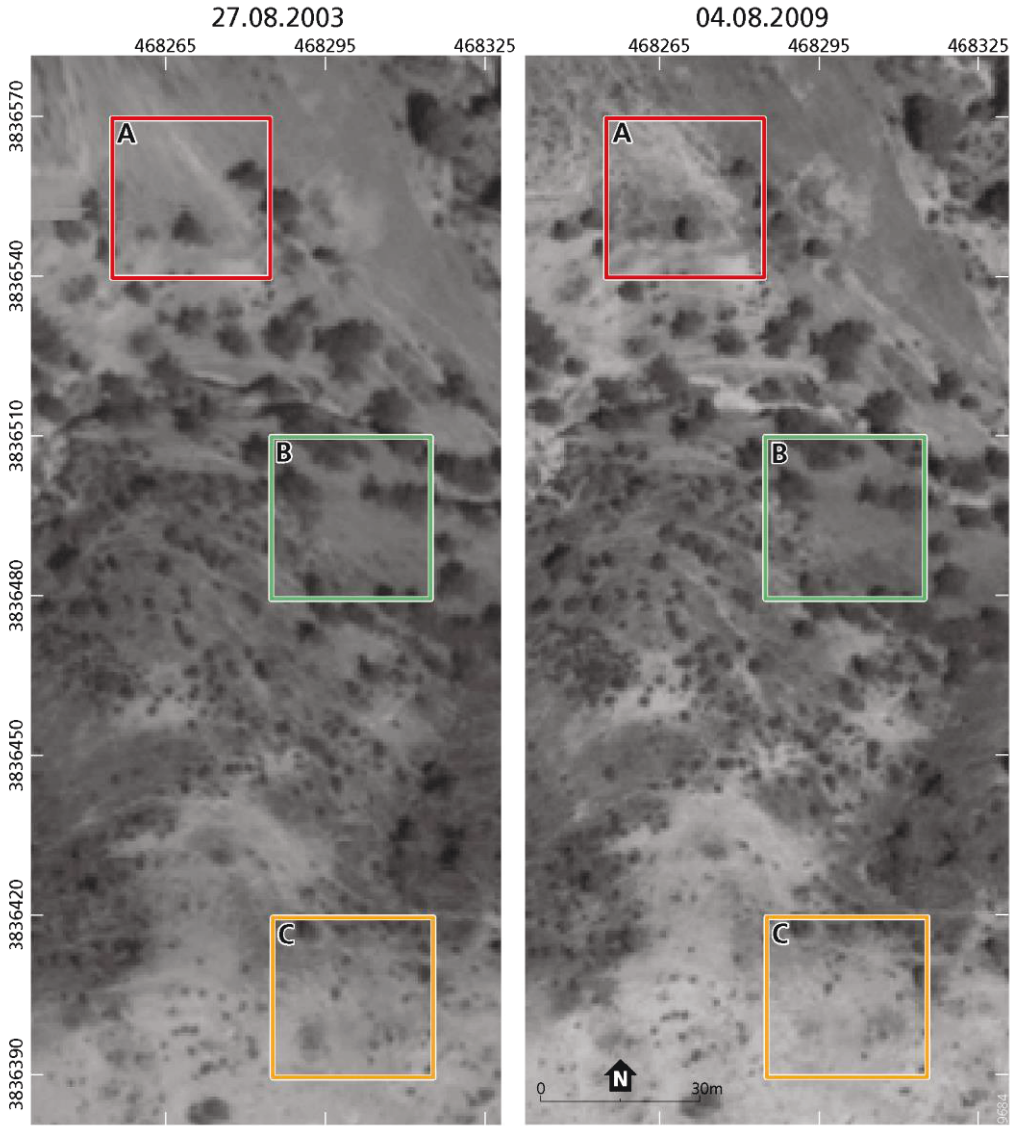

Figure 18[13]. Example 30x30 m Landsat pixels A, B & C. Two Quickbird images (panchromatic, spatial resolution: 0.6 m) taken on 27.08.2003 and 04.08.2009 (before and after drought). BFAST analyses for pixels A, B & C are shown in Figure 19 A-C.

[13] This figure appears in similar form in von Keyserlingk et al. (2021).

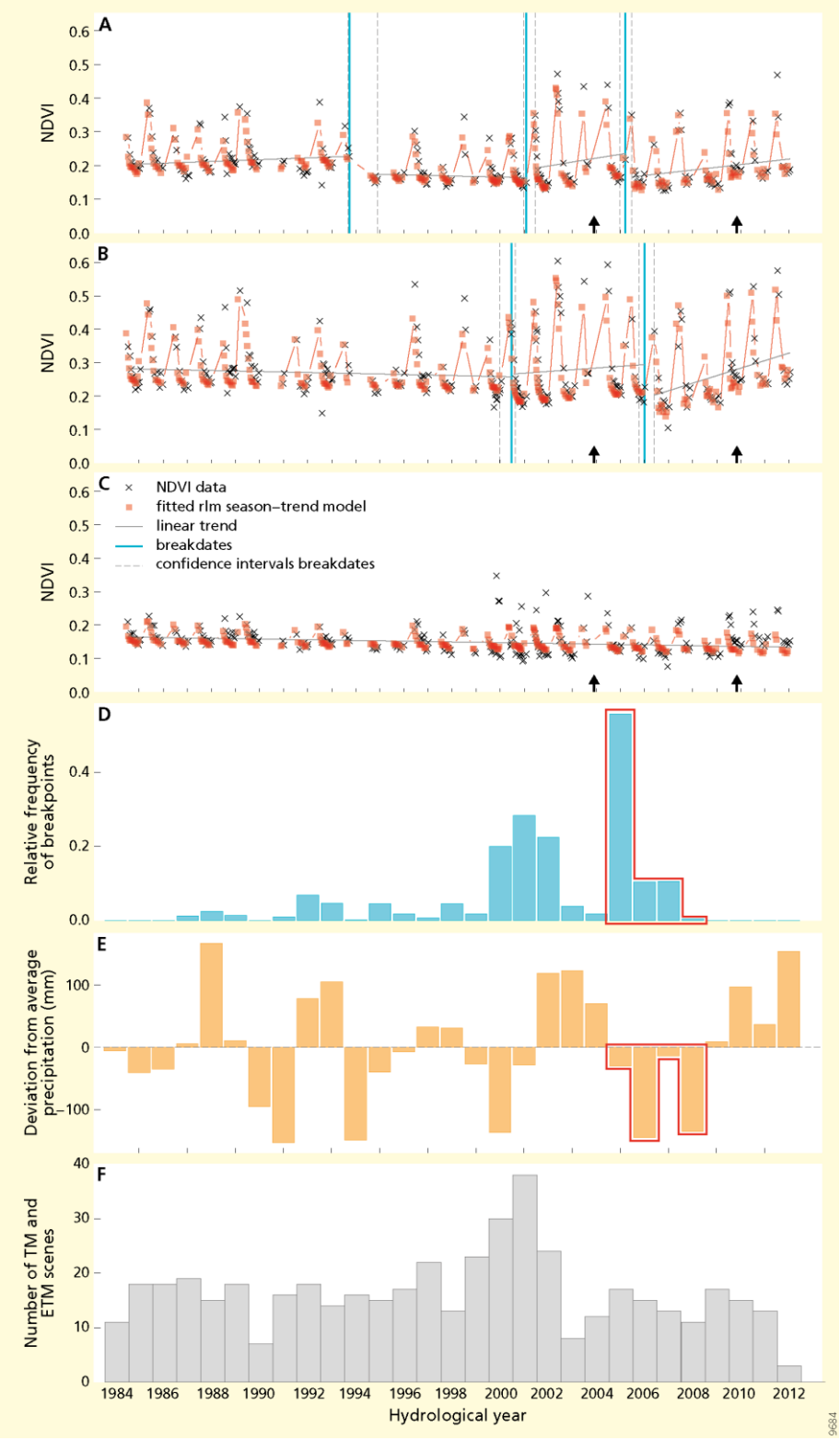

Figure 19[14]. (A–C) BFAST results for example pixels A, B, C. Black arrows indicate the time points of the Quickbird images shown in Figure 18. (D) Relative frequency of breakpoints. (E) Rainfall anomaly in the study area during 1984–2012 (h. years). Red borders around the bars in E and F indicate the period of drought (h. years 2005–2008) that was selected to study the NDVI recovery trend after a drought breakpoint. (F) Number of available TM and ETM+ (excluding SLC-off scenes) scenes included in the analysis. All scenes irrespective of cloud cover were included; clouds and cloud shadows were masked on pixel level.

[14] This figure appears in similar form in von Keyserlingk et al. (2021).

3.5 DATA ANALYSIS

3.5.1 Spatiotemporal quantification of resistance and recovery in the Randi Forest

As described above, I used a time series based approach in combination with a change detection technique to extract metrics for resistance to climate variability and recovery rate from drought. In order to gain insight into the spatial variation of resistance and recovery within the Randi Forest study area, the adapted BFAST analysis described in 3.4 was performed spatially for each of the 3439 Landsat pixels. This was achieved by using a parallel computing approach making use of up to 20 processing cores on a server computer provided by the German Research Centre for Geosciences (GFZ) with high computation power. For the spatial implementation of the adapted BFAST approach I designed the function 'resIndSpatial.R' (see: 'https://github.com/jennifervk/resInd').

The selected measures of long-term resistance and recovery rate from drought, namely: the total number of breakpoints during 1984–2011 and the NDVI recovery rate after a drought breakpoint that occurred between 2005 and 2008 (h. years) were extracted for each pixel. Results were stored in a large data frame in R (R Core Team, 2017), together with the x- and y-geographical coordinates of each pixel and other relevant information; namely: aspect, terrain slope, mean NDVI during 1984–2011, grazing intensity and event-based resistance. In a next step, geographic raster datasets were produced from this information and saved in the 'geotif' format in R. These files were exported to the software ArcGIS (10.6.1) where maps of the number of breakpoints and the NDVI recovery trend, together with the location and size of the farms in 1987 and terrain contour lines, were produced for the study area. Results are presented in section 4.1.

3.5.2 Analysis of the spatial variability of resistance along gradients of grazing and environmental properties[15]

To study the spatial relationship between grazing intensity, terrain slope, aspect, mean NDVI and long-term resistance spatially on a pixel by pixel basis, I sorted all pixels into breakpoint categories from zero to four. Pixels with five breakpoints were excluded, because only two pixels were in this category and they were considered as outliers. The mean NDVI was calculated based on all available observations between 1984 and 2011 for each individual pixel.

First, I calculated spatial Kernel probability density distributions of all explanatory variables (grazing intensity, terrain slope, aspect, mean NDVI) in the study area. In a next step, I repeated this calculation for each breakpoint category separately, in order to check if the spatial distribution of the individual breakpoint categories differed from the overall distribution of the explanatory variables in the study area. The underlying assumption was that a random sample of pixels should not deviate considerably from the overall distribution of the studied variables; if a distinct deviation can be observed, it was assumed to be caused by some mechanism related to the spatial variation in that variable. A two-sample Kolmogorov-Smirnov test (henceforth "KS-test") was performed to test against the null hypothesis that the breakpoint categories were

[15] This section appears in similar form in von Keyserlingk et al. (2021).

drawn from the same underlying continuous distributions as the overall distributions of the respective variables in our study area, using the R package 'stats' (R Core Team, 2017) at a significance level of $\alpha = 0.01$. To visually highlight the differences to the overall distributions of grazing intensity, mean NDVI, terrain slope and aspect, I divided the density of each breakpoint category (estimated at 1000 equally spaced points between the min. and max. data ranges), by the overall density of the studied variables in our study area, keeping the bandwidth for estimating the smoothing kernels constant. Thus, I created a 'Relative Density Breakpoint Index (RDBI)':

$$RDBI_i = \frac{DB_i}{DA} \text{ with } i = \{0, \ldots, 4\} \quad (4)$$

DB stands for the density of the respective breakpoint category (i) and DA for the overall density of the studied variables in the study area. A value of one signifies no difference to the overall distribution of the studied variable; a value larger 1 signifies an overrepresentation of the breakpoint category at this data range and a value below 1 an underrepresentation. Results for this part are presented in section 4.2.

3.5.3 Regression analysis of recovery rate from drought in relation to grazing and environmental properties[16]

To study the spatial relationship between recovery rate from drought (measured as NDVI recovery trend), grazing, topographic properties and the mean NDVI in the three years before the drought-breakpoint, generalized linear regression analysis were applied with the 'gls' function in the 'nlme' package in R (Pinheiro et al., 2018). Scaled factors were used to obtain the β-values. Spatial autocorrelation is present in the data. Six autocorrelation structures were tested within the 'gls' function, namely exponential, gaussian, spherical, linear and rational quadratic. In all cases, the rational quadratic models had the lowest AIC values and was therefore used for the analysis. First, a simple linear regression approach was applied. Second, all factors were combined in a multiple regression approach, in order to account for interactions between the factors. Results for this part are presented in section 4.3.

3.5.4 Reclassifications of resistance and recovery for resilience score

All analysis was performed in ArcGIS (version 10.7.1).

In chapter 4.4, the previously obtained spatial information on resistance to climate variability and recovery rate from drought is used to create a combined resilience score that can be linked to land risk management goals. The applied context of the resilience score requires that information on resilience is presented in an easily comprehensible manner. The individual resilience classes should be clearly distinguishable from each other and allow for a direct linkage to the different risk-phases of the risk management cycle (Figure 5) that has been proposed in natural hazard theory. To meet these goals, I limited the maximum number of resilience classes

[16] This section appears in similar form in von Keyserlingk et al. (2021). It is based largely on work by M. de Hoop, who has – in close cooperation with myself – performed the statistical regression analysis of the NDVI recovery trend.

to five. This required a reclassification of the metrics for resistance and recovery rate into two discrete subclasses each (low and high resistance and recovery), resulting into four possible combinations. An extra fifth resilience class was created to capture areas that are suspected to have reached a permanently degraded and unresponsive ecosystem state. In this work, such a state is indicated by low recovery rates in combination with very high resistance.

All reclassification was performed using the Natural Break algorithm (Jenks and Caspall, 1971) within ArcGIS ('spatial analyst' toolbox). This method was designed to find natural clusters within data and to maximise the difference between classes, which suits my goal of creating clearly distinguishable resilience classes.

The input for recovery rate from drought was the linear NDVI recovery trend fitted by the BFAST model after a drought breakpoint, which occurred between the hydrological years 2005 to 2008. For those pixels in the study area (37% of total), which did not experience a drought breakpoint (i.e. a breakpoint associated with a drop in NDVI of at least 10%) during this time period, the recovery rate was approximated by using the mean NDVI over the years 1984 to 2011. To this purpose, mean NDVI was classified as 'low' (NDVI: 0.1–0.23) or 'high' (NDVI: 0.24–0.37). Pixels with a relatively low mean NDVI were assigned to the 'low recovery' class, and pixels with a high mean NDVI to the 'high recovery' class. This procedure was motivated by the finding that the recovery rate was highly correlated with the mean NDVI in section 4.3 – a connection that is also visible in the similar spatial patterns of the NDVI and recovery classes in Figure 25 & Figure 26.

The input for resistance was twofold: firstly, the total number of breakpoints fitted by the change detection approach throughout the 28-year study period was used as an inverse proxy for long-term resistance (*lt*-resistance). Secondly, the relative magnitude of the drop in NDVI around the drought breakpoint was used as proxy for event-based resistance (*eb*-resistance). If no breakpoint occurred during the time periods used for the calculations of *lt*-resistance and *eb*-resistance, respectively, the pixels were sorted into an 'unresponsive/stable' class, which was specifically created in addition to 'low' and 'high' resistance.

Results for the reclassification of recovery rate, resistance and mean NDVI are presented in chapter 4.4.

3.5.5 Variogram fitting to resilience classes to assess spatial dependencies

In order to assess the extent of spatial dependencies between the resilience categories that have been assigned in chapter 4.4, variograms were fitted to the data. Variograms depict the spatial autocorrelation between data points and thereby give an impression on how similar neighbouring data points are. The analysis was performed in R (version 3.6.1, R Core Team, 2019) using the package 'gstat' (Gräler et al., 2016; Pebesma, 2004).

First, experimental variograms were calculated; second, models were fitted to the experimental variograms. This procedure was performed for the resilience score that was based on *lt*-resistance as well as for the resilience score based on *eb*-resistance. In both cases, an exponential model was chosen over a spherical and a gaussian model by minimizing the residual sum of squares. The nugget, the 95%-sill and the effective range were extracted (Table 11). The effective range is the distance where the model first levels out. Exponential models reach their

sill asymptotically, thus the effective range is the distance where the variogram reaches 95% of its sill (Pebesma, 1992). The effective range describes the extent of the spatial dependencies in the data. Data points separated by distances closer than the range are spatially autocorrelated, whereas data points further away from each other are not spatially related. The nugget depicts the variation in the data, which cannot be explained by the inherent spatial dependency; it is either due to measurement error or to spatial sources of variation at distances smaller than the sampling interval – in my case given by the 30 m-scale of the Landsat data.

4 Results & Discussion: Analysis of ecological resilience in a semi-arid rangeland in Cyprus

This chapter presents and discusses the results related to the four research objectives in chronological order (sections 4.1–4.4). Each subchapter is structured into a result section, a discussion section and a brief conclusion.

4.1 Spatiotemporal quantification and mapping of ecosystem resistance and recovery rate from droughts in the Randi Forest[17]

This section deals with the pixel-based quantification of long-term resistance to climate variability and recovery rate from drought. Results are presented and discussed spatially for the Randi Forest study area. Both resistance and recovery are seen as two key indicators of ecological resilience (see section 2.2.1). The chosen indicators for long-term resistance and recovery rate from drought are the number of breakpoints fitted to Landsat NDVI time series (1984–2011) by a change detection approach, and the linear NDVI recovery trend following a drought breakpoint that occurred during the hydrological years 2005–2008. The motivation for choosing these indicators for resistance and recovery, as well as the methodological procedure, can be found in sections 3.4 & 3.5.1.

4.1.1 Results

Quantification of long-term resistance to climate variability

Between 1984 and 2011, zero to five breakpoints were fitted to the pixels in the study area (3439 pixels in total) (Figure 20). 41.64% pixels had two breakpoints, followed by one breakpoint (29.11%), three breakpoints (18.58%), zero breakpoints (6.40%), four breakpoints (4.22%) and five breakpoints (0.06%). The pixels with five breakpoints were considered to be outliers and were excluded from further analysis of resistance.

The spatial distribution of the number of breakpoints in the study area shows a large variability (Figure 21A). Some breakpoint categories (0, 3, 4) visually appear more clustered, and others (1, 2) more evenly distributed in the whole area.

[17] Most parts of this section appear with some adaptions in von Keyserlingk et al. (2021).

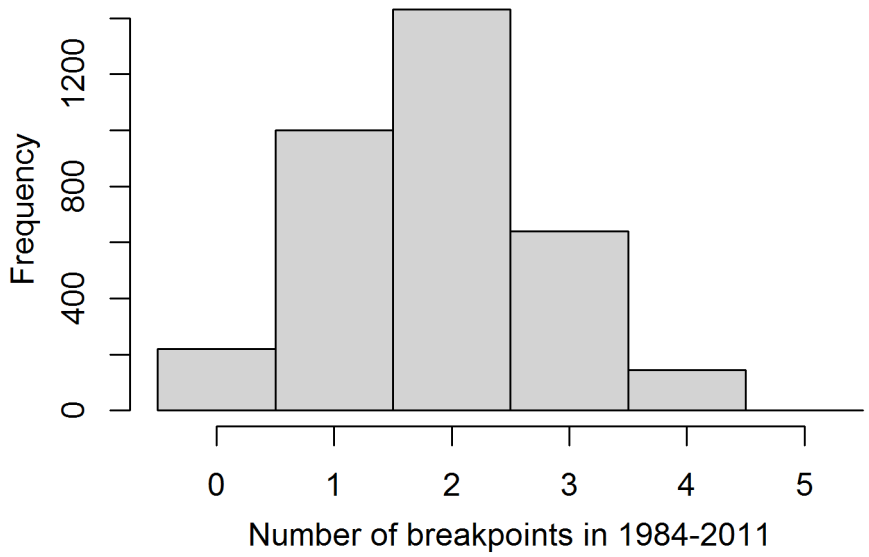

Figure 20. Spatial frequency of pixels with 0–5 breakpoints (BP) during 1984–2011 fitted by the BFAST change detection approach to Landsat NDVI time series in the Randi Forest study area. Total area: 3439 pixels; 0 BP: 220 pixels; 1 BP: 1001 pixels; 2 BP: 1432 pixels; 3 BP: 639 pixels; 4 BP: 145 pixels; 5 BP: 2 pixels.

Quantification of recovery rate from drought

In the relatively dry hydrological years between 2005 and 2008, 77% of the pixels in the study area experienced at least one breakpoint (Figure 19D). Of those breakpoints, 81% were associated with a relative decrease in NDVI of at least 10%. Following this decrease in NDVI, nearly all pixels (99.7% of the pixels experiencing a decrease in NDVI of at least 10%) showed a positive NDVI recovery trend, although there was a large spatial variability in the magnitude of the NDVI recovery trend (Figure 21B).

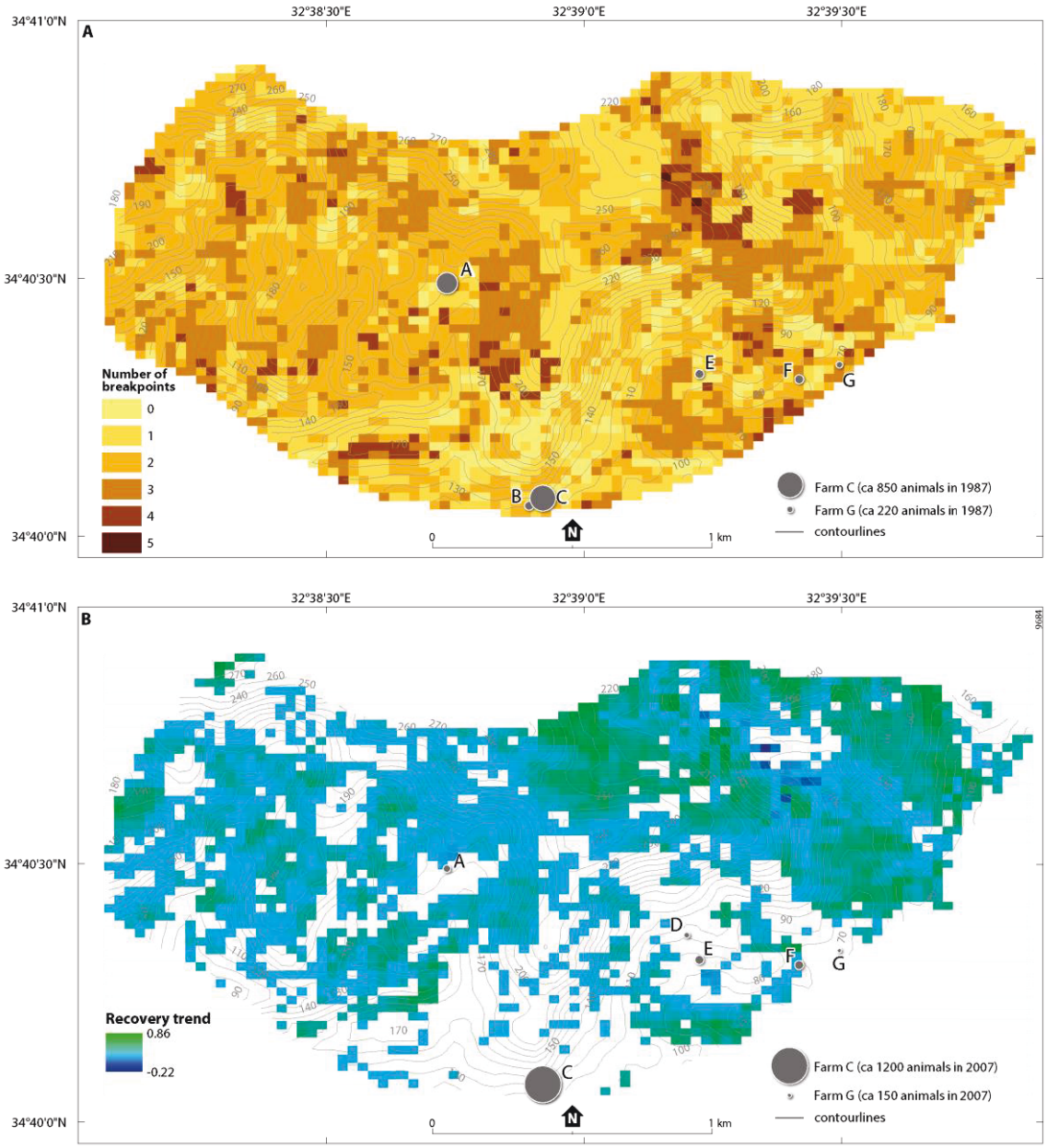

Figure 21[18]. (A) Number of breakpoints fitted by BFAST on pixel basis in the period 1984–2011. Circles depict goat farms with the size of the circle proportional to the estimated number of animals in 1987. (B) NDVI recovery trend ($\frac{\Delta NDVI}{day} \times 10{,}000$) *for pixels that experienced a drought breakpoint during the prolonged dry period in the hydrological years 2005–2008. Results are only shown for pixels that experienced a relative decrease in NDVI of at least 10% using average NDVI of the three years before and after the breakpoint. Circles depict goat farms with the size of the circle proportional to the estimated number of animals in 2007. Please note that between 1987 and 2007 farm B was integrated in farm C. Therefore farm B does not appear in subfigure B.*

4.1.2 Discussion

The objective of this result section was a spatiotemporal quantification of two key ecological resilience metrics: resistance and recovery. A change detection approach was applied on pixel-by-pixel basis to derive proxies for resistance and recovery from long-term Landsat NDVI time series. Resistance to climate variability was measured as the inverse of the total number of

[18] This figure appears in similar form in von Keyserlingk et al. (2021).

breakpoints fitted to the time series. Recovery rate from drought was measured as the NDVI recovery trend after a drought breakpoint, derived from an adapted BFAST model.

Resistance

Between 1984 and 2011, zero to five breakpoints were fitted to the pixel-based NDVI time series in the study area. Based on the frequency distribution of breakpoints in the study area (Figure 20), I considered two breakpoints as average resistance, more than two breakpoints as relatively low resistance (compared to the average) and less than two breakpoints as relatively high resistance to climate variability. Two of 3439 pixels located in the north-east of our study area showed five breakpoints, which appeared to me a suspiciously high number. A closer examination of these pixels based on high resolution Quickbird imagery revealed that small-scale land use change had occurred between 2003 and 2009, appearing like the opening of a soil dumping site. This artificial disturbance probably caused an additional breakpoint in the time series that was not related to climatic variation. The 5-breakpoint category was thus considered to be an outlier (2 of 3439 pixels) and excluded from further analysis. This example illustrates a methodological limitation of using the number of breakpoints as an inverse measure of resistance towards a selected source of disturbance (in this case climatic variation). Unless performed in a controlled experimental set-up, other small-scale disturbances can always cause additional breakpoints in the time series. However, given the large number of pixels studied, I believe that individual small-scale disturbances would not substantially affect the overall distribution of breakpoints within the area. Due to a detailed knowledge of the history of the area, I am further aware that no large-scale land use change that could have affected the area as a whole has occurred during the study period.

When interpreting the number of breakpoints as an inverse measure of resistance, it has to be taken into account that resistance is not used synonymously to sustainability or ecological status. It rather depicts the ability of the ecosystem to withstand change within its current state. High resistance can thus be considered a positive characteristic, when it occurs in a desirable, vegetated state, but also as something hindering regeneration towards a healthy state, if occurring in a degraded, almost barren state. I suspected that pixels with zero breakpoints could be related to such an unresponsive, severely degraded state, associated with very low NDVI values. Low resistance could either indicate a transient ecosystem state that can easily tip into another basin of attraction (i.e. related to low ecological resilience), or characterise a very flexible ecosystem that changes easily, but is also able to recover fast.

In the Randi Forest study area, the frequency of pixels with relatively high resistance (0 or 1 breakpoint: 36%) exceeded those with relatively low resistance (3 or 4 breakpoints: 23%) to climatic variation during 1984–2011. These results indicate that the majority of the area is able to withstand change well – either due to an ability to buffer climatic variation such as droughts – or due to an unresponsive, degraded ecosystem state. The large spatial variability in the spatial distribution of the breakpoint categories points to some spatial sources of variation in those environmental variables controlling resistance to climate variability. However, local clustering

could also point to small-scale land use changes that triggered additional breakpoints in the time series, as has been the case for the 5-breakpoint category.

Recover rate after drought

During the prolonged period of drought in 2005–2008, 63% of the pixels in the study area experienced a breakpoint associated with a drop in NDVI of at least 10%. Of those, 99.7% displayed a positive NDVI recovery trend afterwards. This finding indicates that a majority of the area was affected by this drought, but at the same time showed a positive recovery afterwards. The exact rate of recovery varied largely within the area, indicating some underlying environmental mechanisms.

4.1.3 Short conclusion

Overall, results indicate that the Randi Forest study area has a positive drought recovery potential and that areas with high resistance to climate variability exceed those with low resistance. Further, results revealed that both resistance and recovery show large spatial variability in the Randi Forest study area. How the spatial variability of resistance and recovery can be explained by underlying spatial distributions of grazing intensity and environmental factors will be addressed in section 4.2 and 4.3, respectively.

4.2 Analysis of the spatial variability of resistance in relation to topographic properties, mean NDVI and grazing intensity[19]

This subchapter addresses how the spatial variability of long-term resistance to climate variability, measured as inverse of the number of breakpoints during 1984–2011, was related to the spatial distribution of grazing intensity and environmental factors in the Randi Forest study area.

I analysed spatial density distributions of grazing intensity, mean NDVI, terrain slope and aspect for all pixels combined, and for the different breakpoint categories separately (Figure 22E–H). A two-sample Kolmogorov-Smirnov test was applied to test the distribution of each breakpoint category for deviations from the overall distribution (including all pixels) of the respective variable (Table 5). If the studied variable has no effect on resistance, no deviation from the overall distribution would be expected for the individual breakpoint categories.

To visually highlight deviations from to the overall distribution of grazing and environmental factors, a 'Relative Density Breakpoint Index' (RDBI) was calculated (Figure 22I–L). If the distribution of a breakpoint category does not deviate from the overall distribution, the index fluctuates around the value 1. A value above 1 indicates an overrepresentation of a breakpoint category in this data range, which cannot be explained by the overall distribution of the studied variable; a value below 1 indicates an underrepresentation.

[19] Most parts of this section appear with some adaptions in von Keyserlingk et al. (2021).

Density always relates to the data distribution within each individual breakpoint category. It follows, that densities cannot be directly compared between groups. To give insight into the absolute numbers within each breakpoint category, frequency distributions were calculated (Figure 22A–D).

Methods are described in detail in section 3.5.2.

4.2.1 Results

The frequency distributions (Figure 22A–D) show that the 1- and 2-breakpoint categories dominate over all data ranges of grazing intensity, mean NDVI terrain slope and deviation from south. This is because they are the most common breakpoint categories in the study area (compare Figure 20).

A detailed analysis of the individual spatial density distributions of each breakpoint category, relative the overall distribution of the studied explanatory variables (including all pixels, see dashed black line in Figure 22E–H) revealed that the relative density distributions of the individual breakpoint categories discernibly differ in shape (Figure 22E–H). Some follow the shape of the overall distribution of the studied variables, others deviate clearly from the latter, indicating that their behaviour in relation to that variable is not random. The distribution of the 2-breakpoint category did not differ significantly from the overall distributions of any of the here selected explanatory variables, which fits to the impression that this category appears randomly spread in space (Figure 21A).

The distribution of grazing intensity in the study area is right skewed, with most values being concentrated in the low-to medium grazing ranges (Figure 22A&E). This is because the high grazing values correspond to areas in the vicinity of farms (compare Figure 16). To account for this when interpreting results, I used the 25% and 75% quantile to differentiate between low (<1.8), medium (1.8–2.8) and high (>2.8) grazing intensities. The 1- & 2-breakpoint categories followed the overall distribution of grazing in the study area. However, the distributions of the 0-, 3- and 4-breakpoint categories differed significantly from the overall distribution (KS test, α=0.01; Table 5). This difference is visible in Figure 22E&I. Relative to the overall distribution of grazing intensity, the 0-breakpoint category is particularly overrepresented at high to very high grazing levels, corresponding mostly to areas in the vicinity to farms. In Figure 22E the bimodal pattern of the 0-breakpoint category with regard to grazing is striking, particularly when relating it to my hypothesis of a bimodal distribution of high resilience related to ecosystem state. However, the first peak at low grazing intensities may be caused simply by the high frequency of pixels at this grazing range and disappears when taking the overall distribution of grazing into account (Figure 22I). The 3-breakpoint category is slightly overrepresented at high grazing levels and the 4-breakpoint category is overrepresented at different ranges from medium to high grazing levels.

The distribution of mean NDVI appears bell-shaped. The distributions of the 0-, 1- and 3-breakpoint categories differed significantly from the overall distribution of mean NDVI in our study area (KS test α=0.01; Table 5). Relative to the overall distribution of mean NDVI (Figure 22

F&J), the 0-breakpoint category is strongly overrepresented at low NDVI levels (< 0.2), the 1-breakpoint category at extremely low (< 0.16) as well as extremely high (> 0.27) NDVI values, and the 3-breakpoint category at medium NDVI values.

For the topographic properties, only aspect showed significant results. The distributions of the 1- and 3-breakpoint categories differed significantly from the overall distribution of aspect (measured as deviation from south) in our study area (KS test α=0.01; Table 5). The 1-breakpoint category was overrepresented on northern slopes, the 3-breakpoint category on western/eastern slopes (Figure 22H&L).

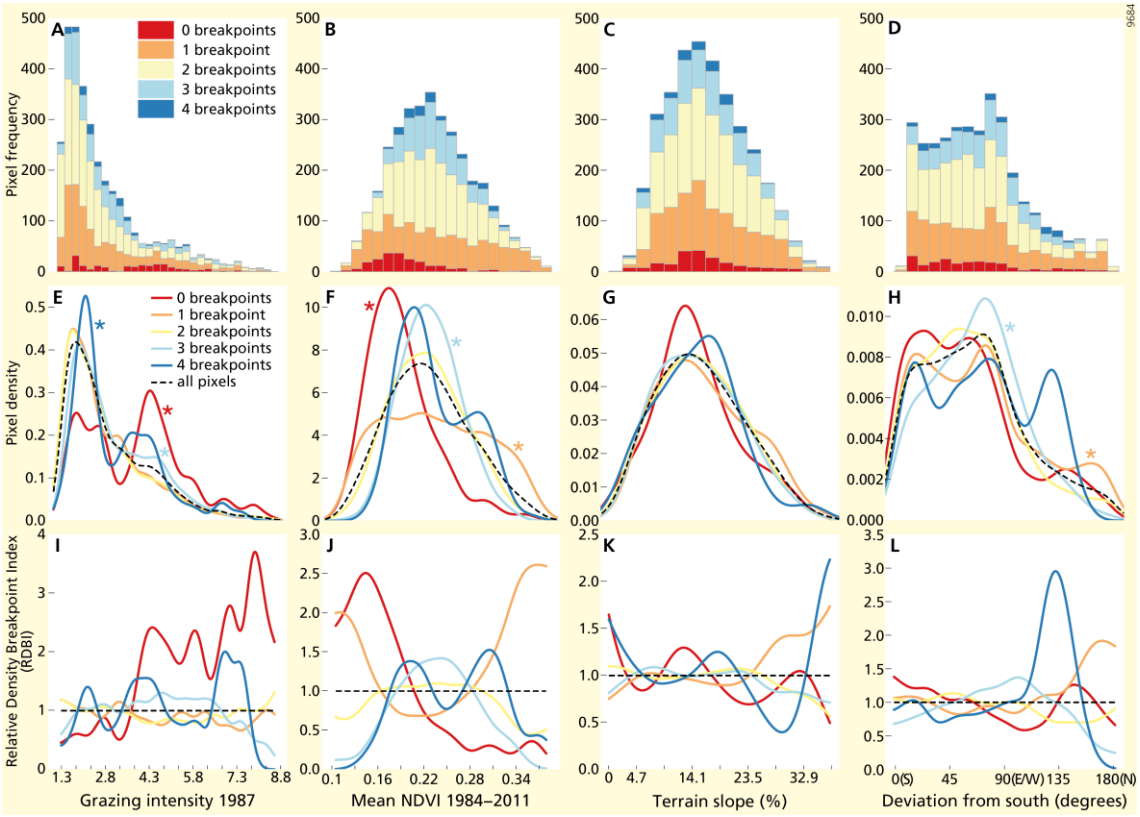

Figure 22[20]. Spatial distribution of breakpoint categories over grazing intensity 1987, mean NDVI 1984–2011, terrain slope and deviation from south. Number of pixels in each breakpoint category: 0 breakpoints: 220, 1 breakpoint: 1001, 2 breakpoints: 1432, 3 breakpoints: 639, 4 breakpoints: 145, total: 3439. (A–D) Stacked frequency histogram of breakpoint categories showing absolute numbers of pixels. (E–H) Kernel density estimations for each breakpoint category separately and for all pixels combined (bandwidth=0.27 (E), 0.01 (F), 2.50 (G), 9.91 (H). Breakpoint categories for which the KS test indicated a significant deviation (α = 0.01) from the overall distribution are marked with a star. (I–L) Relative Density Breakpoint Index ($RDBI_i$): the densities of the breakpoint categories $i = \{0,\dots,4\}$ divided by the overall density of grazing intensity, mean NDVI, terrain slope and deviation from south. Note that the RDBI is a relative measure that only applies to the distribution of the data within each category in relation to the overall distribution of the studied variable.

[20] This figure appears in similar form in von Keyserlingk et al. (2021).

Table 5[21]. Results from a two-sample Kolmogorov-Smirnov test performed with the R package 'stats' (R Core Team, 2017). Significant p values at α = 0.01 are highlighted in grey. The spatial probability distributions of each breakpoint category were calculated and compared to the overall spatial distributions of grazing intensity 1987, mean NDVI, terrain slope and deviation from south in our study area. A significant p value indicates that the two distributions do not share the same underlying continuous distribution. D is calculated as the maximum vertical difference between the cumulative distribution functions of the two samples. Since the breakpoint categories are sub-samples of the overall distributions there are ties present in the data. Hence the p values are an approximation. To account for this and to make our results robust, we used a conservative significance level of α = 0.01.

Breakpoint category	Grazing intensity 1987		Mean NDVI 1984–2011		Terrain slope		Deviation from south	
	D (max Δ)	p value	D (max Δ)	p value	D (max Δ)	p value	D (max Δ)	p value
0	0.3	<0.001	0.348	<0.001	0.095	0.049	0.104	0.024
1	0.058	0.013	0.116	<0.001	0.052	0.028	0.059	0.009
2	0.046	0.03	0.037	0.133	0.019	0.847	0.045	0.036
3	0.087	0.001	0.116	<0.001	0.035	0.539	0.077	0.003
4	0.151	0.004	0.135	0.012	0.08	0.34	0.125	0.026

4.2.2 Discussion

My second objective was to study the spatial distribution of resistance in relation to controlling factors for vegetation resilience: grazing, mean NDVI, terrain slope and aspect. The spatial distribution of breakpoint categories related to grazing and environmental factors in our study area partially agreed with my hypothesis. I expected a bimodal pattern for the density distribution of high resistance (0- & 1- breakpoint categories) related to the expected ecosystem state. Potentially healthy areas (thought to be associated with low grazing, high NDVI, northern orientations, shallow slopes), as well as potentially strongly degraded areas (e.g. with very low NDVI, high grazing, steep southern slopes) were expected to be associated with an overrepresentation of pixels with high resistance. Intermediate to harsh conditions were expected to be associated with an overrepresentation of pixels low resistance (3- & 4-breakpoint categories), indicating an ecosystem in a transient state.

As expected, high NDVI and/or a northern orientation (i.e. favourable conditions) were associated with an overrepresentation of pixels with high resistance (few breakpoints). In this situation, high resistance appears related to a healthy ecosystem that is able to buffer climatic variation well. Potentially strongly degraded areas, with medium to high grazing intensities and/or low NDVI values were also associated with an overrepresentation of pixels with high resistance. In this case, high resistance may indicate an unresponsive ecosystem state. Intermediate conditions (intermediate to high grazing intensity and/or intermediate NDVI values, and/or western/eastern orientation) were associated with an overrepresentation of pixels with low resistance (many breakpoints).

Contrary to my expectations, a southern orientation did not significantly promote high resistance (related to potentially degraded state). In addition, terrain slope had no effect on resistance in my study area. This result was surprising, for I had expected that steep slopes would

[21] Table adapted from von Keyserlingk et al. (2021).

promote the strongly degraded state, associated with high resistance. However, the finding fits to my results for recovery rate after drought (section 4.3) that also did not reveal a significant effect of terrain slope when studied individually. However, in that case terrain slope became relevant if studied in combination with aspect. The same might be the case for resistance. Regarding grazing, results suggest that while strong grazing promotes high ecosystem resistance (related to potentially degraded state) as expected, low grazing intensity does not necessarily promote high resistance (related to a potentially stable healthy state). This may be explained by other environmental conditions that control vegetation in the study area. Even if grazing is low, steep, southern slopes can limit conditions for vegetation growth, and thus affect resistance. This finding corresponds to results by Riva et al. (2017), who studied land degradation in southern Europe, among others in study sites in southern Cyprus (in an area partly overlapping with my study area in the Randi Forest) and Greece. The study found that under moderate grazing pressure other factors such as landscape features appeared to be better predictors of land degradation status than grazing pressure. On the whole, however, grazing showed a significant correlation with degradation patterns in the area (Riva et al., 2017). To further enquire interactions between grazing and terrain on resistance, an analysis of their joined effects on resistance would be an interesting next step, especially for low grazing intensity. This could also help to reveal an effect of terrain slope, supposing that grazing and/or effects of slope and aspect are synergetic.

The finding that strong grazing intensity and very low NDVI values were associated with an unresponsive ecosystem state, characterized by high resistance, is supported by results from studies by Schneider and Kéfi (2016) and Saruul et al. (2019). In a modelling study Schneider and Kéfi (2016) found that grazing increases the bi-stability domain of a desert and a vegetated state in a dryland ecosystem. The authors argue that strong grazing reduces ecological resilience, thereby making a transition to a stable, permanently degraded desert state more likely. This conjecture further fits to my finding of a slight overrepresentation of pixels with low resistance at medium and high grazing intensities. These pixels could represent areas in transition to a degraded state with reduced ecological resilience. However, to draw sound conclusions about the stability of ecosystem states, further analysis into stability behaviour would be required. Saruul et al. (2019) showed that highly degraded grazed grasslands in Mongolia had a higher resistance to natural disturbances than less degraded grasslands. However, in the same study moderately degraded grasslands displayed higher resistance and recovery than slightly degraded and undegraded ones. Saruul et al. (2019) ascribe their finding to positive effects of intermediate grazing levels on species composition and richness and relate it to the intermediate disturbance hypothesis. This is contrary to my findings: intermediate NDVI and grazing levels were associated mostly with a low resistance and also showed no improved recovery rates after drought (see section 4.3). In areas with very high NDVI however, as well as on northern-oriented slopes, I did find a significant overrepresentation of pixels with high resistance; these areas also showed high recovery rates after drought (see section 4.3), which might indicate that these locations were in a healthy ecosystem state. That intermediate levels of grazing did not seem to have any positive effects on ecosystem resistance or recovery in my case might be ascribed to

the fact that the area has been overgrazed for decades. Thus, the vegetation might not benefit from the continuation of even intermediate grazing intensities, and such areas were probably more than 'moderately degraded'.

In conclusion, the effects of grazing on resistance appears to depend on the ecosystem state as a whole: if highly grazed areas are associated with a permanently degraded and unresponsive state (in our case indicated by very low NDVI values), grazing seems to increase ecosystem resistance to climate variability. In this state the ecosystem cannot react to climatic variation any longer. By removing vegetation cover, grazing even more promotes this state. In my work, this is indicated by an overrepresentation of pixels with high resistance both at high grazing levels and very low NDVI values. However, if grazing is associated with intermediate levels of degradation, it can lower ecosystem resistance, creating areas at risk of transition to a permanently degraded state. In my case, this is indicated by an overrepresentation of pixels with low resistance at medium and high grazing levels, and intermediate NDVI values. Similar results are reported in a study by Whitford et al. (1999) and in De Keersmaecker et al. (2016). Whitford et al. (1999) studied resistance to drought over livestock induced stress gradients in a field study of a dry grassland ecosystem in New Mexico, USA. They found that resistance to drought and recovery were reduced in an intensely grazed ecosystem in comparison to a lightly grazed one. A study by De Keersmaecker et al. (2016) in the Netherlands showed that strongly grazed, species-poor grasslands exhibited lower resistance to climatic anomalies than species-rich semi-natural grasslands. They argue that grazing reduced species richness, which in turn reduced resistance. Ruppert et al. (2015) quantified resistance to drought and recovery using 174 long-term datasets from more than 30 dryland regions. They found that in perennial systems grazing had a slightly negative effect on resistance (-8% drop in resistance compared to ungrazed systems). Finally, if grazing has positive effects on the ecosystem state (e.g. associated with particularly high species richness as in Saruul et al. (2019)), it can promote resistance to remain in that 'healthy' state. In the Randi Forest study area I found indications for this in an overrepresentations of pixels with high resistance at very high NDVI values and on northern slopes, yet not related to low grazing intensities. This may be either due to synergetic interactions between grazing and terrain that were not accounted for in my analysis or related to the long history of overgrazing in the ecosystem.

4.2.3 Short conclusion

The analysis of grazing and environmental effects on long-term resistance revealed that strong grazing as well as very low NDVI values were associated with a highly resistant state that I assume to be in a degraded, unresponsive condition. Low grazing did not have a clear effect on resistance, while a high NDVI, as well as north-facing slopes promoted high resistance, which may be an indication of a healthy ecosystem state that is able to buffer climatic perturbations. Intermediate to high grazing levels as well as western/eastern orientation promoted the occurrence of patches with low resistance. These findings suggest areas with reduced resilience that can easily shift either to a degraded or a healthy state. To draw comprehensive conclusions

however, further research on the correlation between resistance and ecosystem state is required.

4.3 Analysis of the effect of grazing and environmental properties on drought recovery[22]

This subchapter addresses how the spatial variability of recovery from drought, measured as the linear NDVI recovery trend after a drought breakpoint during the hydrological years 2005–2008, can be explained by grazing intensity and environmental factors in the Randi Forest study area. To this purpose, a linear regression approach was applied (see methods in 3.5.3).

4.3.1 Results

Simple linear regression analysis

The simple linear regression shows a clear positive relation between the mean NDVI three years before the drought breakpoint and the NDVI recovery trend after the breakpoint (Figure 23A). This result indicates that 'greener' pixels recovered faster. Regarding terrain effects (terrain slope and aspect, Figure 23B&C), only aspect showed a significant relationship with the NDVI recovery trend. Namely, southern pixels had a low NDVI recovery trend, while the recovery trend significantly increased when the orientation turns towards north (Figure 23C). This relationship indicates that northern-oriented pixels recover faster. The grazing intensities for 1987 (Figure 23D) and 2007 showed a slightly negative relationship with the NDVI recovery trend.

Table 6. Simple regression between NDVI recovery trend and the independent variables

Independent variable	β	p-value
NDVI before breakpoint	0.287	< 0.001
Deviation from south (degrees)	0.242	< 0.001
Log grazing intensity 1987 (livestock/m)	-0.192	0.010
Log grazing intensity 2007 (livestock/m)	-0.149	0.042
Terrain slope (%)	0.003	0.932

[22] Most parts of this section appear with some adaptions in von Keyserlingk et al. (2021). Statistical results described in this section are based largely on work by M. de Hoop, who has – in close cooperation with myself – performed the statistical regression analysis of the NDVI recovery trend.

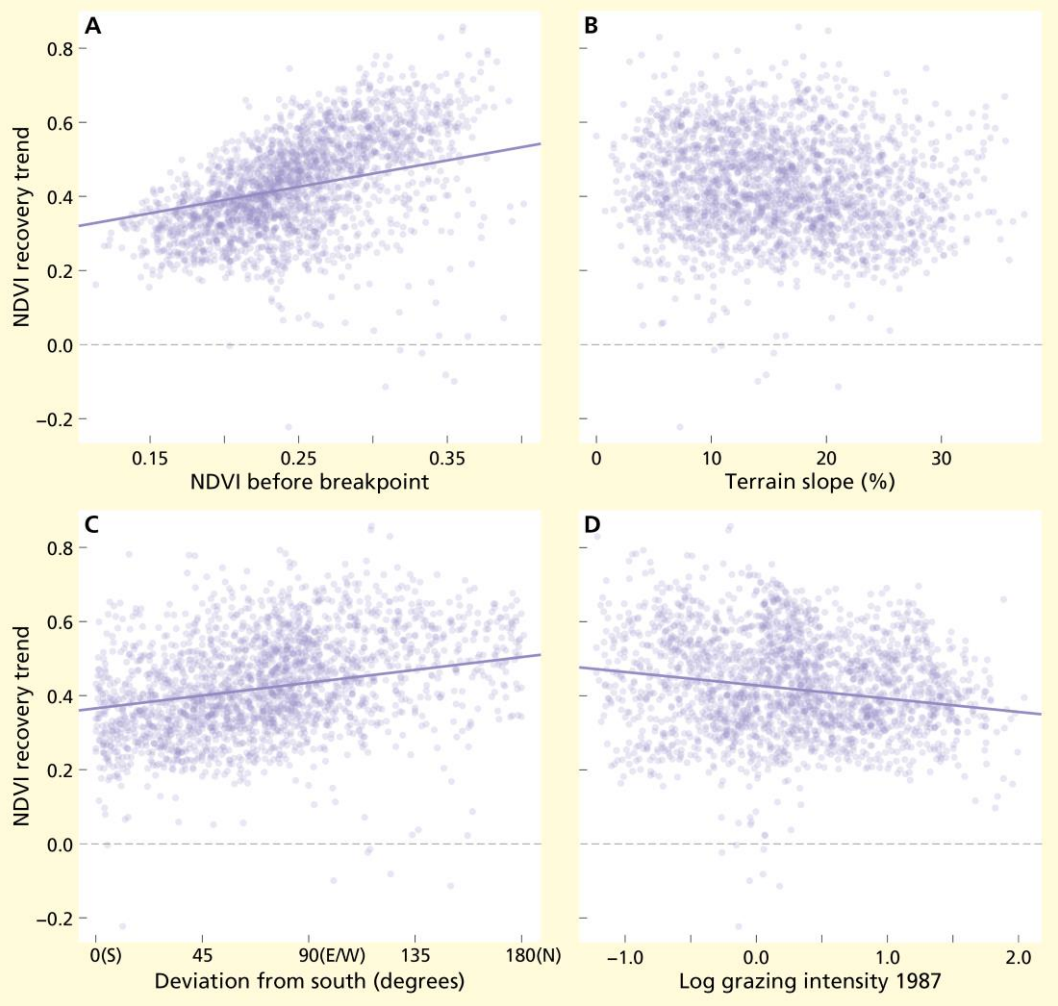

Figure 23[23]. Simple regression analysis between the NDVI recovery trend ($\frac{\Delta NDVI}{day} \times 10{,}000$) and A) NDVI before the breakpoint (β=0.278, p<0.001) B) terrain slope (β=-0.003, p=0.932) C) aspect measured as deviation from south (β=0.242, p<0.001), D) estimated grazing intensity in 1987 (β=-0.192, p=0.010). Regression lines are shown for significant relations (α=0.05).

Multiple regression analysis

When combining all factors that could explain the NDVI recovery trend after the breakpoint in one multiple regression model (using backward elimination), the relationships have a similar direction (Table 7). The variance inflation factor (VIF) was below 1.6 among factors, indicating that there is low multicollinearity between the explanatory factors. Interestingly, two significant interaction factors were found. The most significant interaction factor is between aspect (measured by deviation from south) and terrain slope. While the NDVI recovery trend was not significantly related to the terrain slope when using simple linear regression (Figure 23B), this relationship changed when including aspect (Figure 24A). The relationship between NDVI recovery trend and terrain slope is positive for northern-oriented slopes, while it is negative for southern-oriented slopes. Thus, on northern slopes, terrain slope had a positive effect on the NDVI recovery trend, while on southern slopes it had a negative effect. The second interaction factor is between deviation from south and the mean NDVI before the breakpoint. In the simple

[23] This figure appears in similar form in von Keyserlingk et al. (2021).

linear regression, there was a significant positive relationship between the deviation from south and the NDVI recovery trend (Figure 23C). Yet, when grouping the data based on the upper and lower 25% of NDVI values, this positive relationship was only significant for the group with the low NDVI data (Figure 24B).

Table 7[24]. Multiple regression between NDVI recovery trend and the independent variables including significant interactions.

Independent variable	β	p-value
Deviation from south (degrees)	0.295	< 0.001
NDVI before breakpoint	0.211	< 0.001
Log grazing intensity 1987 (livestock/m)	-0.121	0.042
Terrain slope (%)	-0.005	0.866
Deviation from south*Terrain slope	0.097	< 0.001
Deviation from south*NDVI before breakpoint	-0.059	0.012

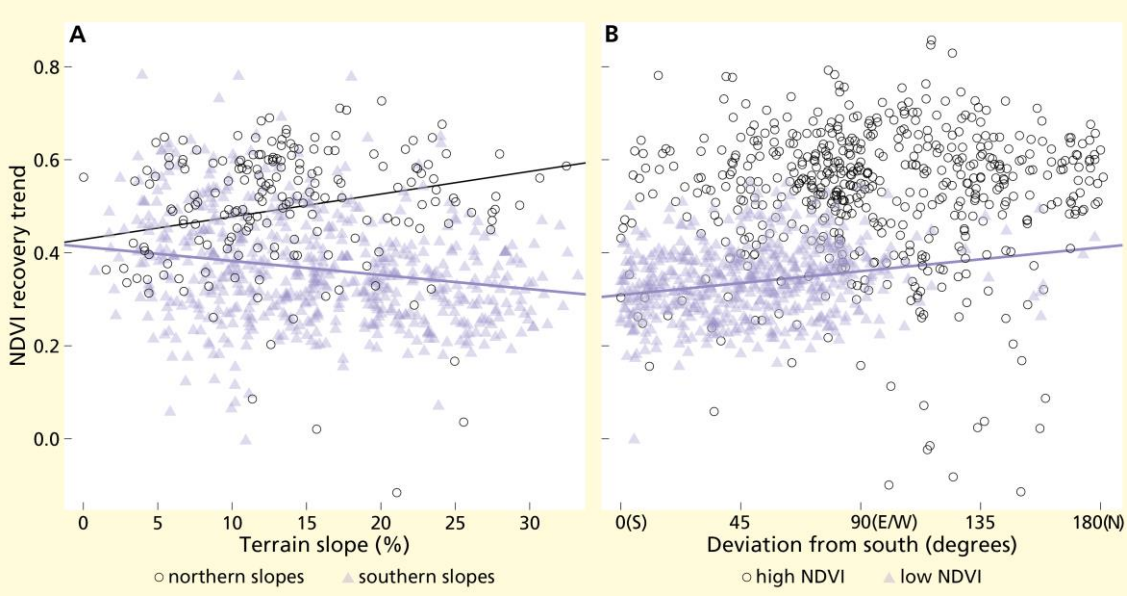

Figure 24[25]. Simple linear regression for significant interaction factors for the NDVI recovery trend ($\frac{\Delta NDVI}{day} \times 10{,}000$) after the drought breakpoint. A) Simple linear regression between the terrain slope and the recovery trend of the NDVI after the breakpoint. The relationship is positive for northern-oriented slopes (Aspect >315° or <45° indicated by black circles, β=0.251, p=0.012), while it is negative for southern-oriented slopes (135°>Aspect<225°, indicated with blue triangles, β=-0.191, p=0.001). B) Simple linear regression between aspect (measured as deviation from south) and the NDVI recovery trend. The relationship is not significant for the 25% of the data with the highest NDVI before the breakpoint (indicated by black circles, β=0.107, p=0.105), while it is significantly positive for the 25% of the data with the lowest NDVI before the breakpoint (indicated with blue triangles, β=0.231, p≤0.001). Regression lines are shown for significant relations (α=0.05).

4.3.2 Discussion

Regarding recovery from drought, the multiple regression analysis showed that the NDVI recovery trend was positively affected by, in order of importance: a northern orientation, high NDVI values before the breakpoint and low grazing intensities (Figure 23, Table 7). These results

[24] Table adapted from von Keyserlingk et al. (2021).
[25] This figure appears in similar form in von Keyserlingk et al. (2021).

indicate that, as expected, positive recovery rates of vegetation after drought are most pronounced in locations that are weakly stressed by grazing or solar radiation and/or where vegetation is already in a good condition, indicated by high NDVI values. This finding agrees with other studies: a remote sensing dryland study by Del Barrio et al. (2010) in a the Iberian Peninsula showed that improving vegetation trends are represented most in land of good or unusually good condition, while degrading or static trends of vegetation prevail in degraded or unusually degraded land. In a global modelling study based on remote sensing data, De Keersmaecker et al. (2015) found that in drought-sensitive areas (including semi-arid areas) vegetation types with a high fraction of bare soil displayed the strongest vegetation memory effects, resulting in particularly low recovery speed after a drought. This fits to the positive relationship I found between NDVI and the recovery trend after drought.

In a study on vegetation cover resilience in Italy (Simoniello et al., 2008), 'Sparsely Vegetated Areas' and 'Pastures' (i.e. potentially stressed lands) were the only Corine land cover type for which mean positive recovery trends did not exceed the negative trends during the period 1992–2003. Furthermore, the main clusters with a negative recovery potential were corresponding to areas at risk of desertification. Whitford et al. (1999) found that heavy grazing reduced the recovery rate from drought in a dry grassland ecosystem, which corresponds to my results. Contrary to this are results in Ruppert et al. (2015) on the effects of grazing on recovery from drought in drylands: in systems dominated by annual plants, the study found positive effects of grazing on recovery from drought (+72% compared to ungrazed system). The authors attribute this result to interactive effects between grazing, drought and dominant life history of the herbaceous layer. They argue that grazing might reduce perennials' fitness, leading to a competitive advantage of annuals that have often less nutritive value and are thus favoured in grazed systems (Sander et al., 1998). A higher proportion of annual compared to perennial plants might lead to an overall better recovery from drought, for Ruppert et al. (2015) found that annual systems specialized on fast recovery to buffer negative effects of drought, whereas perennial systems were specialized in higher resistance to drought, yet recovered more slowly. In dryland systems dominated by perennials, Ruppert et al. (2015) found no effect of grazing on recovery from drought. To interpret grazing effects on recovery in the Randi Forest study area in context with the dominant live history, complementary field-based research would be needed.

Terrain slope was neither related to resistance (see section 4.2) nor to the NDVI recovery trend, when studied individually. This was a surprising result, since steep slopes were expected to promote the unresponsive ecosystem state characterized by high resistance and low recovery rates. However, the multiple regression model of the NDVI recovery trend revealed that there was a significant interaction between terrain slope and orientation: on southern-oriented slopes, the NDVI recovery trend was indeed negatively related with terrain slope (Figure 24A, Table 7). This finding implies that the negative effects of southern orientation and steep terrain slope were synergetic. It agrees with the hypothesis that southern steep slopes have low recovery rates. However, for northern-oriented pixels, the relationship between NDVI recovery trend and terrain slope was positive. The reasons for this positive relationship remain unclear.

To resolve this issue, further research on slope/aspect interactions would be needed. However, my results indicate that steep terrain slope alone does not necessarily yield low recovery rates after drought, but that amplifying effects by other factors are needed.

A second interaction factor showed that the positive relationship between the NDVI recovery trend and deviation from south was stronger for pixels with lower mean NDVI before the drought breakpoint (Figure 24B, Table 7). Thus, regarding the recovery rate, pixels with low mean NDVI before the breakpoint benefit more from a northern orientation than pixels with high mean NDVI. Pixels with low mean NDVI before the breakpoint are associated with scarcer vegetation and thus are more susceptible to the negative effects of strong solar radiation. Interestingly, results revealed no interaction between grazing and terrain in their effect on recovery. I had expected that areas facing generally harsh conditions for vegetation, e.g. southern-oriented steep slopes, might be more sensitive to grazing pressure than flat areas. As a result effects of grazing and slope steepness and/or deviation to south could be expected to act synergetically on recovery from drought. A study by Riva et al. (2017), in an area in Cyprus partly overlapping with my study area in the Randi Forest, indeed found that slope steepness increased sensitivity to grazing pressure with regard to land degradation, except for very steep slopes that are difficult to reach for the animals. That I found no interaction between grazing and slope steepness may be due to the vertical friction factor implemented in the calculation of the grazing intensity index. Thereby, slope steepness increases the distance for goats if they have to walk up or downhill and thus limits grazing intensity on steep slopes. This might mask a synergetic effect of grazing and slope steepness, if present. In contrast, the study by Riva et al. (2017) did not account for slope steepness in their calculation of grazing intensity, which is simply based on the distance to farms. Regarding aspect, Riva et al. (2017) found that grazing predicted land degradation best on north-facing slopes. The authors argued that on south-, west- and east-facing slopes low water availability and poor soil fertility limit vegetation growth to such a degree that grazing has no additional effect.

4.3.3 Short conclusion

The analysis of the recovery rate after drought revealed that positive environmental conditions, namely a northern orientation and high NDVI values before the breakpoint, as well as low grazing intensities, positively affected recovery from drought. Further, on southern (but not on northern) oriented slopes, slope steepness was negatively related with recovery rate after drought, indicating a synergetic effect of slope steepness and southern orientation in their effect on recovery from drought. Finally, areas with low NDVI values before the drought were more sensitive to effects of a southern orientation than those with high NDVI values.

4.4 Derivation of a resilience score based on resistance and recovery

This chapter addresses objective 4: the derivation of an exemplary resilience score that can be related to land risk management, based on ecosystem resistance and recovery, followed by an assessment of the spatial dependencies of the discrete resilience classes.

This subchapter aims at integrating the previously obtained information on resistance and recovery in an applied context. For land users and managers, information on resilience to climatic disturbance – i.e. the likelihood of an ecosystem to reach a tipping point and flip into another, assumedly less desirable, state in the face of (climatic) disturbances – is of major importance. Especially in Mediterranean dryland ecosystems, which are exposed to a highly erratic climate with frequent droughts, a tendency that is predicted to be drastically exacerbated by climate change, this is highly relevant. Climate is a variable land users and managers cannot influence directly. However, they do have to cope with its effects on the ecosystem and can prepare themselves for upcoming risks. By adjusting their land management they can influence the resilience of the ecosystem to climatic disturbances, and thus mitigate the effects; they may even be able to prevent the ecosystem to reach a tipping point to a certain degree. Finally, they can put efforts into restoration measures. The different land risk management goals mentioned here can be captured by different phases of the classic risk management cycle (Figure 5), as commonly used in natural disaster risk management: 'prevention/mitigation', 'preparedness' and 'recovery'.

The resilience score was derived by combining spatial information on ecosystem resistance to climate variability and recovery rate from drought, which has been obtained in a previous analysis described in chapters 3.4 & 4.1. In a first step, the continuous variables for resistance and recovery were reclassified into discrete subclasses. Details about the reclassification procedure can be found in the methods (section 3.5.4). Results of the reclassification are presented in the first part of this chapter. In a second step, the resistance and recovery categories were combined into meaningful resilience classes that allow a linkage to land risk management goals. Finally, in the last part of this chapter, spatial dependencies between the resilience classes were assessed based on variogram analysis. Details on the variogram fitting can be found in the methods (section 3.5.5).

4.4.1 Results

Reclassification of resistance and recovery

In order to achieve a maximum of five distinct resilience classes, which can be linked to individual land risk management goals, the input variables for resistance and recovery were reclassified into discrete categories. Details on the reclassification procedure can be found in the method section (3.5.4).

Recovery from drought was measured as the linear trend of the NDVI fitted by the BFAST model after a drought breakpoint that occurred in the prolonged dry period 2005 to 2008 (h. years) (see sections 3.4 & 4.1). All pixels in the Randi Forest study area were reclassified into two categories, representing low and high recovery rates (Table 8). In case pixels did not show a drought breakpoint (37% of total) during this time period, recovery rate was approximated by using the mean NDVI over the years 1984 to 2011 (Table 8, Figure 26).

Results for the reclassification of recovery from drought are shown in Figure 25.

Table 8. Reclassification of recovery rate after drought

Pixels with drought breakpoint (NDVI drop ≥ 10%) in 2005–2008 (h. years)	Pixels without drought breakpoint (NDVI drop ≥ 10%) in 2005–2008 (h. years)	**Recovery category**
NDVI recovery trend after breakpoint in 2005–2008	**Mean NDVI 1984–2011**	
-0.22–0.44	0.1–0.23	**Low recovery**
0.45–0.86	0.24–0.37	**High recovery**

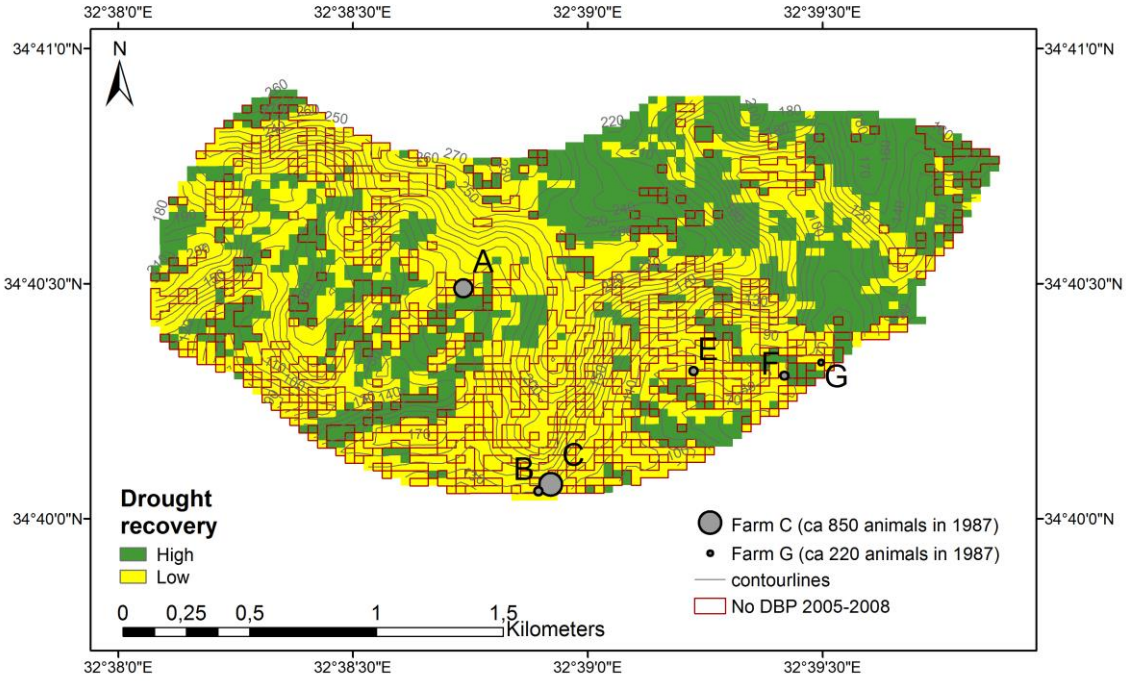

Figure 25. Reclassification of recovery rate after drought in the Randi Forest study area shown in two categories. Recovery rate was calculated as the slope of the modelled linear trend line of the NDVI succeeding a drought breakpoint, which occurred between the hydrological years 2005 to 2008. Areas encircled in red did not experience a drought breakpoint (DBP) during this time; for those pixels recovery rate was estimated by using the mean NDVI (1984–2011).

In chapters 4.1&4.2 resistance to climate variability was measured as the inverse of the overall number of breakpoints that were fitted by the change detection approach during the years 1984 to 2011. This idea was based on the assumption that the more resistant the ecosystem is to climatic disturbances, the less likely a breakpoint would occur in the climate-driven NDVI dynamics. It is an innovative approach that allows to get a proxy for the long-term resistance of an ecosystem to repeated disturbances. A different, more established way of measuring resistance is based on the direct damage caused by one distinct disturbance event. In the following, I used these two different approaches of measuring resistance as input for the resilience score: first, the long-term resistance (*lt*-resistance) to climate variability, and second an event-based (*eb*-resistance) approach. For the calculation of *lt*-resistance (Figure 27) the number of breakpoints that occurred during 1984 and 2011 were reclassified into three subclasses (Table 9). Pixels with one or two breakpoints were assigned to the 'high-resistance' class, pixels with three to five breakpoints to the 'low-resistance' class. Pixels with zero

breakpoints during the whole study period were considered to represent an 'unresponsive/stable' state. In most cases this state is assumed to be due to long-term degradation represented by an almost barren state, associated with an extremely low NDVI. This assumption is based on results from a previous analysis described in 4.2 that found these pixels to be overrepresented in areas with an extremely low NDVI (Figure 22F&J & red areas in Figure 26), as well as in strongly-grazed areas (Figure 22E&I). In the few cases where pixels with zero breakpoints were located in areas with a high NDVI (Figure 26), they were assumed to be in such a good condition that they were able to buffer and not be affected by climatic perturbations (see Table 10).

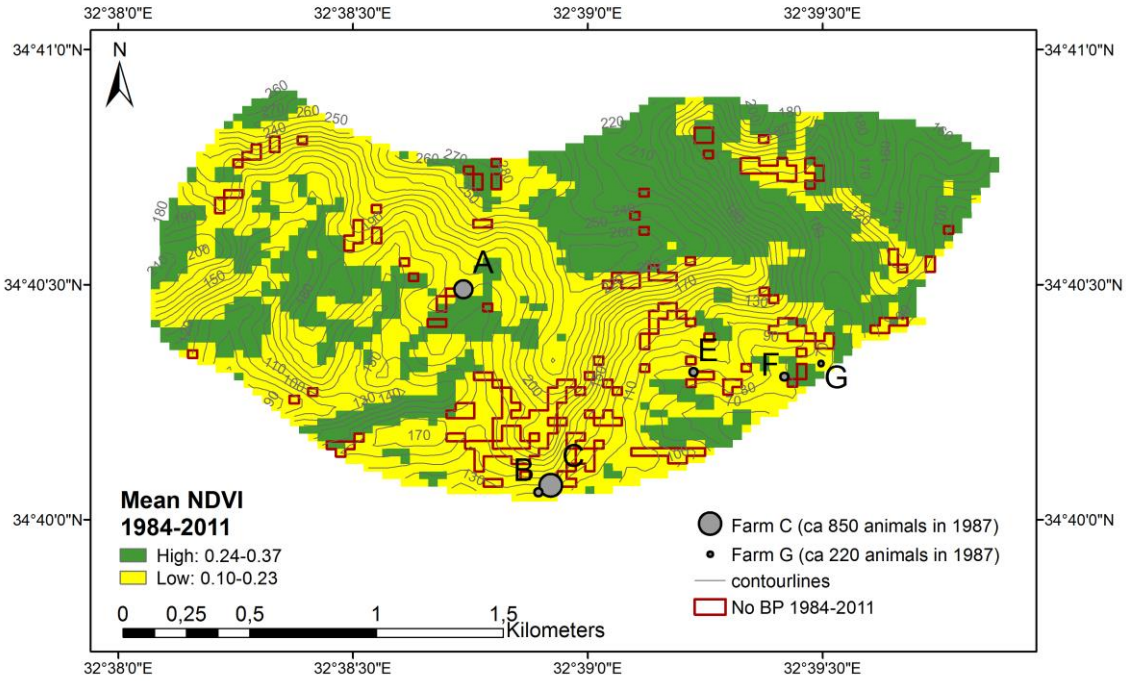

Figure 26. Mean NDVI (1984–2011) shown in two categories. The locations of the pixels with no breakpoint (BP) during the whole study period are encircled in red.

The *eb*-resistance to drought (Table 9, Figure 28) was measured as the relative difference in mean NDVI of the three years before and after a drought breakpoint, which occurred during the hydrological years 2005 to 2008. Pixels with a relative drop in NDVI of -63% to -22% were assigned to the 'low resistance' group. Pixels with a relative drop in NDVI of less than -0.22% were assigned to the 'high resistance' group. Pixels with no breakpoint during this time-period were assigned to the 'unresponsive/stable' category, with the same reasoning as explained in the paragraph above.

Table 9. Reclassification of resistance

Long-term resistance (number of breakpoints in the years 1984 to 2011)	**Event-based resistance** (relative change in NDVI around a breakpoint during the h. years 2005 to 2008	**Resistance category**
0	All pixels without breakpoint during 2005–2008	**Unresponsive/stable**
3–5	-0.63–(-0.22)	**Low resistance**
1 & 2	≥ -0.21	**High resistance**

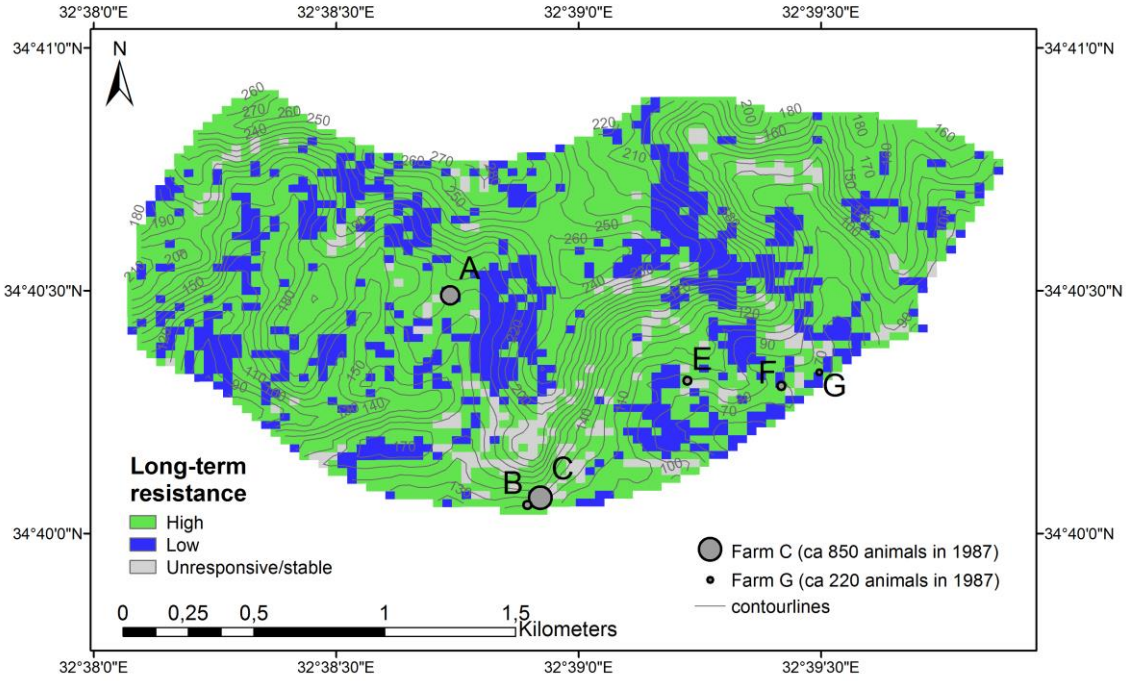

Figure 27. Long-term resistance to climate variability, based on the total number of breakpoints in 1984–2011, shown in three categories. Areas with no breakpoints during this time period were considered unresponsive/stable due to being permanently degraded.

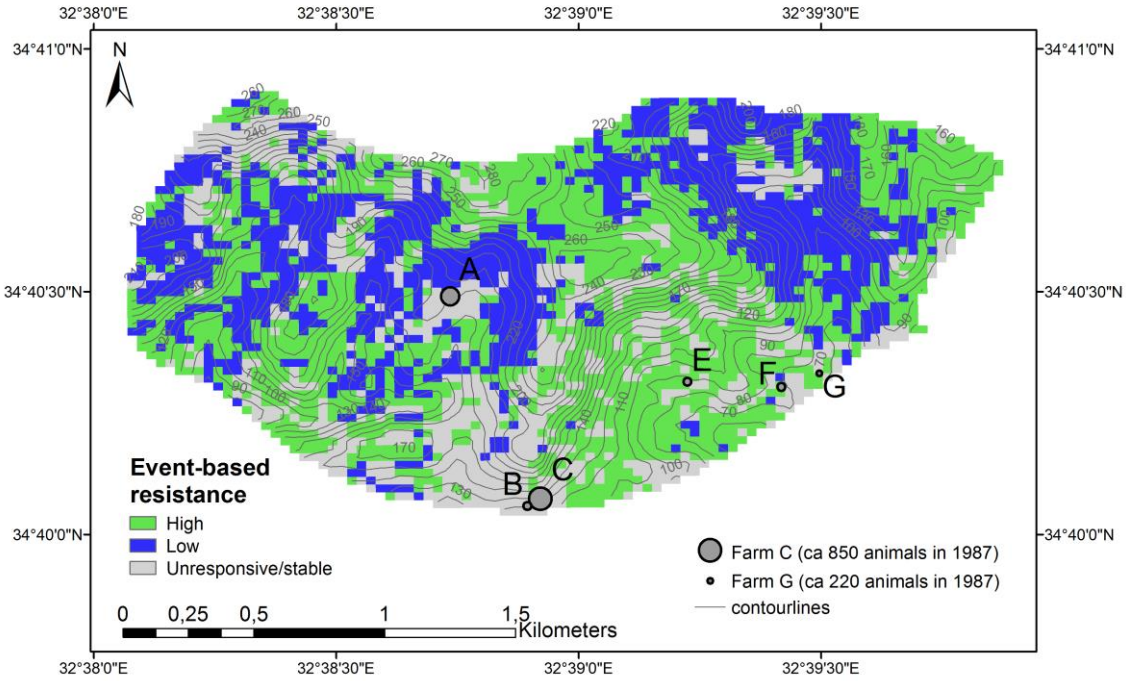

Figure 28. Event-based resistance to drought, based on the relative drop in NDVI around a drought breakpoint during the hydrological years 2005 to 2008, shown in three categories. Areas with no breakpoints during this time period were considered unresponsive/stable due to being permanently degraded.

Derivation of combined resilience score

Ecological resilience depends on the combination of resistance and recovery: an ecosystem can either be resilient, because it is very resistant to disturbance, or it may be resilient because it is very flexible (i.e. it has a low resistance), but can recover speedily after a disturbance, or both (see e.g. Ruppert et al., 2015). In the following, I combined the gathered information on resistance and recovery in such a way that may yield information on the overall resilience of the ecosystem and thus allow for a link to land risk management options. For land risk management purposes the different classes of the resilience score should be clearly distinguishable from each other and allow for a direct linkage to the risk-phases of the risk management cycle (Figure 5). Additionally, the location of the different resilience categories within the study area should be visualized in an easily interpretable map.

The classification system is described in Table 10. Related land risk management goals are suggested for each resilience category in the last column of the table. Maps showing the distribution of resilience categories in the Randi Forest study area are presented in Figure 29 & Figure 30. Since two alternative ways of measuring resistance (long-term and event-based) as described above were used as input for the resilience score, two different results were produced.

Table 10. Classification of resilience score based on resistance to climate variability and recovery after drought.

Resistance	Recovery	Ecological resilience category	Resilience score	Land risk management goals
High	High	**High resilience**: the ecosystem is resistant to climate variability and able to recover quickly after drought.	**1**	Prevention: preservation
Low	High	**Intermediate resilience 1**: the ecosystem is very **flexible**. It is easily affected by climatic perturbations, but able to recover fast.	**2**	Prevention: focus on maintaining recovery potential
High	Low	**Intermediate resilience 2**: the ecosystem is **stagnant**. It is very resistant to climate variability, yet if affected, it recovers slowly.	**3**	Prevention: focus on maintaining resistance
Low	Low	**Low resilience**: the ecosystem has probably reached a critically low resilience. It is easily affected by climatic perturbations and recovers slowly.	**4**	Preparedness: early-warning!
Unresponsive / stable	Low (based on NDVI)	**Permanently degraded**: the ecosystem does not react to climate variability any longer and is in an almost barren state.	**5**	Response: restoration
Unresponsive /stable	High (based on NDVI)	**High resilience**: the ecosystem is so stable that it can buffer climate variability well and recover fast (very few pixels).	**1**	Prevention: preservation

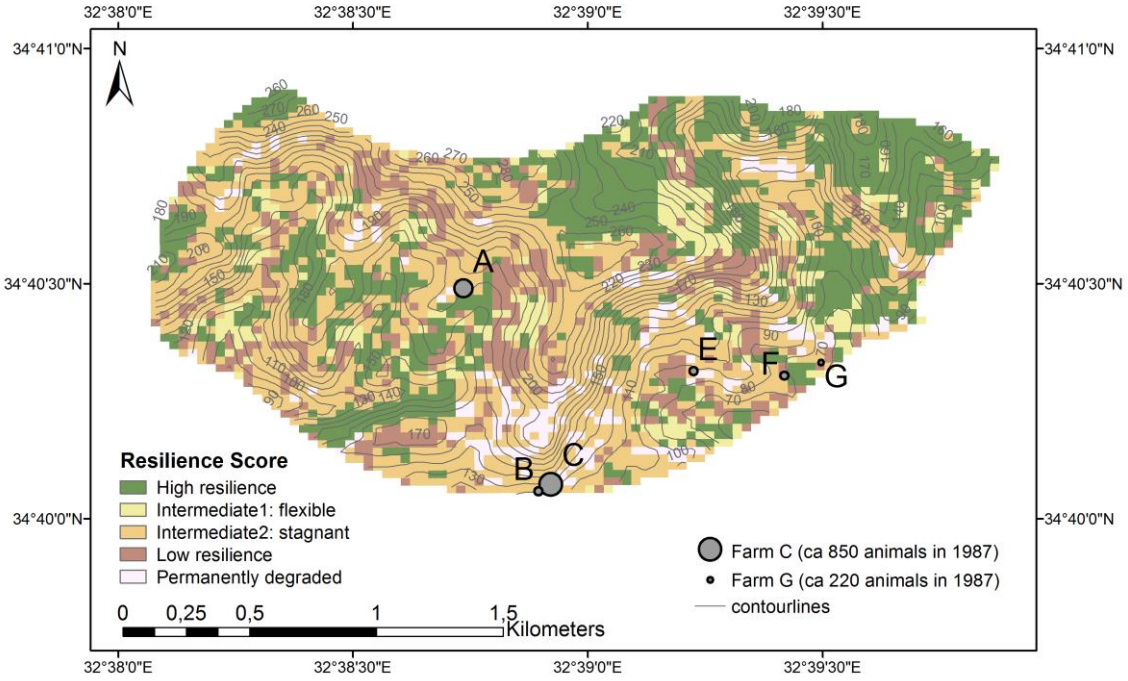

Figure 29. Resilience score. Results are based on recovery and long-term resistance. Resistance was quantified by the total number of breakpoints that occurred during the years 1984 to 2011. Recovery was quantified as the linear recovery trend after a drought breakpoint that occurred during the hydrological years 2005 to 2008. For pixels without a drought breakpoint during this time period, the general recovery potential was approximated by the mean NDVI (1984–2011).

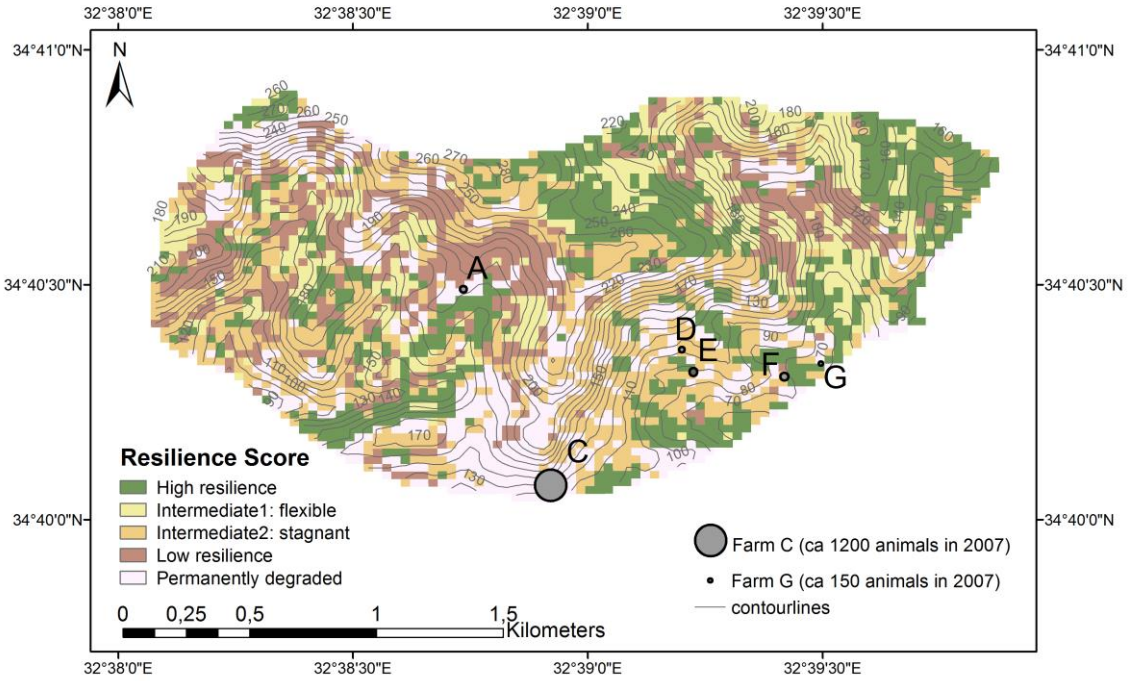

Figure 30. Resilience score. Results are based on recovery and event-based resistance. Resistance was quantified by the relative change in NDVI around a drought breakpoint during the hydrological years 2005 to 2008. Recovery was quantified as the linear recovery trend after this breakpoint. For pixels without a breakpoint during this time period the general recovery potential was approximated by the mean NDVI (1984–2011). Please note that between 1987 and

2007 farm B was integrated in farm C. Therefore farm B does not appear in this figure, which is based on the grazing intensity estimated for 2007.

The result maps of the resilience score (Figure 29 & Figure 30) show that the different resilience classes appear to be clustered in space: e.g. distinct hotspots of high, as well as critically low resilience can be identified. Larger connected areas with **high resilience** are particularly abundant in the north-east of our study area relatively far away from the farms and, to a smaller extent, in the south-west. They appear to be mainly limited to areas that have a high NDVI (compare Figure 26). Smaller patches of high resilience also appear in the vicinity of farms, e.g. south of farm A and close to farms F and G. Areas with a critically **low resilience** appear to be scattered all over the area. There is a larger distinct patch with a low resilience east and north-east of farm A, indicated by the classification based on *lt*-resistance (henceforth 'lt classification') and the classification based on *eb*-resistance (henceforth 'eb classification'), respectively. In the 'lt classification', several low resilient patches appear in the vicinity of farms E and F, but they also appear in other places. The '**flexible areas**', which are affected by climatic disturbances, but recover well, seem to be concentrated in the east of the study area, particularly in the 'eb classification'. The '**stagnant areas**' appear to be scattered over the whole area, with no clear pattern distinguishable for the human eye. The '**permanently degraded**' areas appear to be particularly concentrated in a strongly grazed area in the south of our study area, especially in the 'eb classification'. This area lies in a triangle between farms A, B, C and E and is visited by goats from all of these farms.

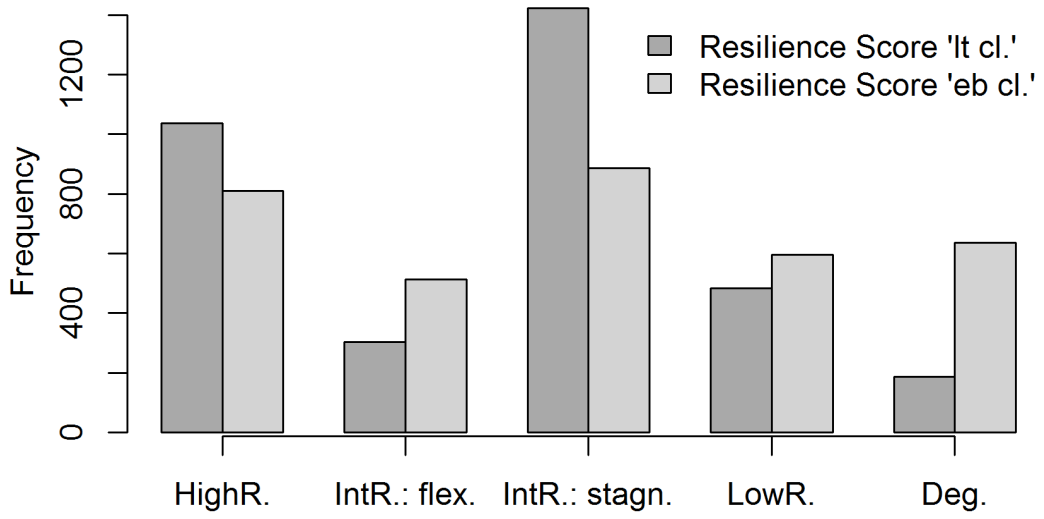

Figure 31. Frequency plot of resilience score based on the long-term ('lt') (dark grey) and event-based ('eb') (light grey) classification of resistance. Resilience categories from left to right: high resilience; intermediate resiilience1: flexible; intermediate resiilience2: stagnant; low resilience; permanently degraded.

The frequency plot of the resilience score (Figure 31) shows that most pixels (26–41% of total, depending on 'eb' or 'lt' classification) in the area were classified as intermediately resilient, with high resistance to climate variability and slow recovery after drought ('stagnant'). This category is particularly frequent in the 'lt classification' of resistance. Next most abundant is the

high resilience category (24–30% depending on 'eb' or 'lt' classification). The order of importance of the other three categories depends on the type of resistance classification. In the 'lt classification', the low resilience category is particularly abundant (14%), whereas only a small amount of pixels belong to the permanently degraded (5%) and the flexible (9%) category. In the 'eb classification', the permanently degraded category (18%), but also the low resilience (17%) and the flexible category (15%) are abundant.

Assessment of the spatial dependencies between resilience classes

This section studies the spatial dependencies of the resilience classes that have been derived by means of the resilience score in the previous section. The result maps (Figure 29 & Figure 30) show that the different resilience classes do not appear randomly distributed, but that spatial dependencies exist, causing clustering in the data. In the following, the extent of the spatial dependencies was evaluated by fitting variograms to the data. Details on the variogram fitting can be found in the methods (section 3.5.5).

Table 11 summarizes the model parameters used for fitting the variograms to the resilience data, based on the 'eb' and the 'lt' classification of resistance, respectively. Results for the experimental (dots) and modelled (broken lines) variograms are presented in Figure 32.

Table 11. Model parameters of variogram fit for the resilience classes based on the 'eb' and the 'lt' classification of resistance.

Input parameter	Model	Nugget	95%-sill	Effective range
Resilience score 'eb cl.'	Exponential	0.816	1.984	498.092
Resilience score 'lt cl.'	Exponential	0.621	1.359	409.353

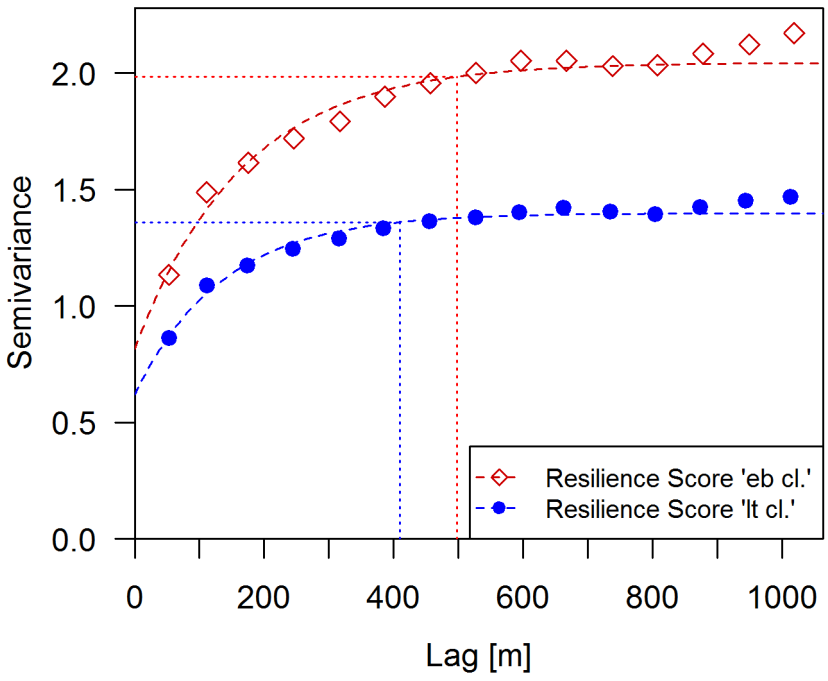

Figure 32. Experimental variograms (dots) and fitted exponential models (broken lines) for the resilience score based on the 'eb' (red) and the ' lt' (blue) classification of resistance. The dotted horizontal lines show the 95%-sill, the dotted vertical lines the effective range.

The resilience classes based on the 'eb', as well as on the 'lt' classification of resistance clearly show a spatial dependency that ranges up to 498 and 409 m, respectively. Within these distances the resilience classes are spatially autocorrelated, indicating that there are spatial sources of variation. Both datasets display a nugget effect, indicating that part of the spatial variation in the data cannot be explained by the inherent spatial dependencies.

4.4.2 Discussion

The objective of this chapter was a spatially explicit derivation of an exemplary resilience score that can be related to land risk management, based on ecosystem resistance and recovery; it is followed by an assessment of the spatial dependencies of the discrete resilience classes. A resilience score was designed based upon which resilience was classified into five categories: high, low, flexible, stagnant and permanently degraded. All of these classes enable a linkage to specific stages in the classic risk cycle, thereby potentially enabling land managers to take situation-adjusted actions. The specific actions depend on the particular properties of the land and the land use and are not the focus of this work.

Two different measures of ecosystem resistance were used as input for the calculation of the resilience score, resulting in two resilience classifications. First, long-term resistance to climate variability over 28 years (used in the 'lt classification'), and second, event-based resistance to a specific drought event (used in the 'eb classification'). Even though the frequency of the individual resilience categories differs based on classification of resistance, the overall spatial pattern of the resilience classes (compare Figure 27 & Figure 28) appears to conform to each other. Also, the range of the spatial dependency does not vary greatly between the two resilience classifications. While the overall number of breakpoints that occurred in a time series is an innovative approach of measuring resilience, quantifying the damage resulting from one disturbance event is a more established idea. That there does not appear considerable contradiction in the spatial variability of resilience derived from these two different resistance measures, supports the robustness of the number of breakpoints as a measure of resistance. However, further statistical analysis would be needed to confirm this impression. Using the number of breakpoints in a historical time series as a measure has the advantage of taking into account the long-term dynamics, which may promote the identification of permanently degraded areas that require restoration measures for improvement. In contrast, acutely, yet only momentarily degraded areas that were identified based on a single drought event (as in the 'eb classification'), may still be able to recover by themselves if land use stress (in our case grazing pressure) is reduced.

The spatially explicit results of the resilience classification revealed that resilience is not distributed uniformly within the Randi Forest study area. Spatial dependencies exist on scales up to 400 to 500 m (depending on 'lt' or 'eb' classification of resistance), leading to distinct clusters of the individual resilience categories. This result indicates that effective land risk management actions should focus on measures within this scale. A knowledge of the spatial

grain and characteristic range of spatial variability within an ecosystem is crucial for deciding on appropriate resilience-based management strategies (Chambers et al., 2019). The existence of a nugget effect shows that part of the spatial variation in the data cannot be explained by the spatial dependencies. Since the data used in this study were derived from satellite measurements, which are prone to measurement error, a nugget effect is to be expected. Furthermore, there are small-scale biotic and abiotic processes affecting resilience below the 30 m scale of Landsat imagery; e.g. plant-plant and plant-soil interactions on the plant scale, soil-compaction due to goat pathways, augmented surface run-off caused by local gully erosion, etc.

The spatial patterns of resilience classes is complex and the underlying sources for the spatial variation proved difficult to identify based on visual analysis alone. However, while in chapters 4.2 & 4.3 the spatial relationships between resistance, recovery and the environmental conditions as well as grazing intensity were studied in detail, this was not the aim of this section. Rather, an exemplary resilience score, which can be mapped and potentially linked to land risk management should be designed. Spatially explicit knowledge about ecological resilience at patch- to mesoscale allows land managers to prioritize areas for management actions and to determine effective strategies (Chambers et al., 2019). My results suggest that the Randi Forest area is dominated by intermediately resilient, stagnant, areas (26–41% of total, depending on 'eb' or 'lt' classification) that have a high resistance to climate variability yet recover only slowly after drought. Large parts (24–30%) of the area were classified as highly resilient (i.e. high resistance and fast recovery), 14 to 17% had 'low resilience' and only 5 to 18% were classified as permanently degraded. At first sight, these results are surprising, since the area is thought to be overall in a degraded state, showing few signs of recovery (Daliakopoulos and Tsanis, 2014; Riva et al., 2017). In a remotely sensed assessment of land degradation in Mediterranean drylands, Riva et al. (2017) studied among others an area partly corresponding to my area of interest in the Randi Forest. According to Riva, more than 40% of this area (area 'm' in Riva et al., 2017, Fig. 3) is 'heavily degraded' and the rest is mostly classified as 'degraded'. It has to be taken into account, however, that my analysis was an assessment of resilience, not of degradation status. Areas that I found to be 'stagnant' may at the same time be in a degraded state that is resilient within its boundaries. Resilience, as used in this work, is not a measure of ecosystem health. An exception is the 'permanently degraded' category, which I assumed to occur only in almost barren land. Since this state is characterised by a combination of high resistance with low recovery, it can be assumed to be in a state of degradation that is hard to reverse. The low percentage classified as 'permanently degraded' may be due to the strict classification rules applied to this category, especially in the 'lt classification'. Here, the area has to be unresponsive (indicated by zero breakpoints in the time series) to climate variability over a historical period of 28 years. In comparison, Riva et al. (2017) classified degradation based on spatial variation within one comparable landscape unit in mean annual NDVI of one single year (2015). Conforming to my results, north-eastern parts of Riva's area 'm' are classified as 'healthy'. Most of the highly resilient patches in my analysis were similarly located in this region. Further, highly resilient areas appeared to be mostly limited to areas that have a high NDVI,

which in the Randi Forest area is an indication of ecosystem health. This suggests that, as expected, highly resilient patches can be an indication of healthy areas.

It would be an interesting next step to study in detail the relationships between the different resilience categories assigned in my work and ecosystem state; for instance, the effects of vegetation composition on resilience, which are not captured by my purely NDVI driven approach. Ruppert et al. (2015) found that drylands with a vegetation dominated by perennial life forms were specialized on buffering negative effects of drought by a high resistance, yet recovered slowly. Annual dominated systems, on the other hand, had the opposite strategy: low resistance to drought, yet a fast recovery. My results suggest that the vegetation in the Randi forest study area has specialized predominantly on being resistant, for intermediately resilient, stagnant categories dominate the area. In contrast, the 'flexible' areas make up only a minor part. With regard to results by Ruppert et al. (2015) the high resistance in the area may be due to the vegetation composition in the Randi forest being dominated by perennial shrubs. However, to draw comprehensive conclusions, it would be necessary to compare vegetation composition between areas classified as 'flexible' and 'stagnant'. A detailed knowledge on the ecosystem's functioning related to its resilience characteristics in the end provides the foundation for deciding on informed land management actions. First of all, such knowledge is necessary in order to decide if the present state of the ecosystem is desirable from land users and/or ecological perspective. Is the preservation of resilience in the current ecosystem state desirable or not? Second, understanding the ecological features underlying the specific resilience characteristics allows for a purposeful modulation of resilience. Finally, in order to build management options on resilience categories suggested in my work, a detailed validation of resilience categories would be required. Validation of historical dynamics – which are the basis for my resilience indicator – is not directly possible. However, a comparison with historical high resolution satellite imagery at different time steps would be an option. Furthermore, the areas I classified as 'permanently degraded', but also those as 'highly resilient' are believed to be rather stable over time and to change only very slowly by themselves. A field-based comparison of these areas with the resilience maps produced in this work would be valuable. Such a step may also help to decide which measure of resistance is more suitable to distinguish between truly permanently degraded areas, and strongly degraded areas, that may have already changed since the end of my study period.

4.4.3 Short conclusion

This chapter presented an innovative approach to derive a spatially explicit ecological resilience index, based on joined information on resistance and recovery. The suggested resilience categories were directly linked to categories of the risk management cycle, which is a well-established tool for decision makers to deal with natural hazards. Results of the spatial resilience quantification in the Randi Forest study area suggest that large parts of the area is dominated by intermediately resilient, stagnant, areas that have a high resistance to climate variability yet recover only slowly after drought, followed by highly resilient, low resilient and permanently degraded parts. Spatial dependencies between resilience categories were found up to 400 to 500 m, leading to distinct resilience clusters in the area.

The main purpose of the chapter was to demonstrate a way how spatially explicit information about resilience on 30-m Landsat scale can be potentially employed by land managers to prioritize areas for management actions and to decide on appropriate strategies for disaster risk reduction (i.e. focussing on risk prevention/mitigation, response (restoration) or preparedness (early-warning)). To derive recommendation for effective management strategies however, further research, incorporating field-based validation of results, is crucially required.

5 CONCLUSIONS

5.1 MAIN FINDINGS AND CONCLUSIONS

The thesis aimed at creating a link between land degradation assessment and risk management. To this purpose, a systematic review on the discrepancies in existing land degradation risk assessment approaches was preformed (chapter 2.1). Ecological resilience, a system's ability to maintain its functional and structural integrity and persist without being pushed into an alternative stable state under the influence of disturbance (Holling, 1973, 1996), was identified as a key concept with high potential to link risk theory with land degradation research. Based on this understanding, the thesis then intended to develop an innovative approach to extract meaningful resilience metrics from satellite time series analysis in a spatially explicit manner, using a change detection method. This innovative approach has the advantage of being applicable even in otherwise data scarce areas, such as Mediterranean drylands. It allows to gain spatially explicit information on ecological resilience on a spatial scale that is relevant to land managers. Metrics for resistance to climate variability and recovery rate from drought were extracted for an exemplary dryland study area in southern Cyprus (chapter 4.1). How spatial variation of grazing – the main land use in that area – and other environmental factors were related to resistance and recovery was studied separately (chapters 4.2 & 4.3). Finally, the metrics for resistance and recovery from drought were combined to create a meaningful resilience score that allows a direct linkage to land risk management goals (chapter 4.4). Thus, coming back to the original intention of contributing to relating land degradation research more closely to land risk management.

In the following, the main results related to the four research objectives that were tackled are shortly summarized. Subsequently, main findings are discussed in the overall context of this thesis.

Objective 1: spatial quantification and mapping of ecosystem resistance to climate variability and recovery rate after drought in a dry rangeland of southern Cyprus, using proxies derived from satellite time series data by means of a change detection method and breakpoint analysis.

An innovative approach to spatiotemporally quantify two key resilience metrics, namely recovery rate after disturbance and long-term resistance was developed. Long-term time series of a vegetation index (NDVI) derived from Landsat satellite data were analysed by means of a change detection approach (BFAST), which I adapted specifically for this purpose. The approach was applied in a dry rangeland located in southern Cyprus (Randi Forest study area). As an inverse proxy for long-term resistance to climate variability, the number of breakpoints fitted by the change detection approach over 28 years was extracted in a spatially explicit manner. A low number of breakpoints, compared to the average, was interpreted as high resistance, which can either be due to a healthy ecosystem that is able to buffer climatic disturbance well, or due to a permanently degraded ecosystem that cannot react to climate variability any longer. A high number of breakpoints compared to the average was interpreted as low resistance, indicating a

flexible or transient ecosystem state. Recovery rate after a known drought event was likewise quantified spatially, using the linear trend of the BFAST model fitted after a drought associated breakpoint as a proxy for recovery rate after drought. Results suggest that the Randi Forest study area has overall a positive potential for recovery from drought and that areas with high resistance to climate variability exceed those with low resistance. Further, results revealed that resistance and recovery show large spatial variability in the Randi Forest study area. The spatial patterns are complex and could not visually be directly related to proximity to farms or the underlying terrain.

Objective 2: analysis of the spatial distribution of resistance to climate variability over spatial gradients of grazing intensity, mean NDVI and topographic properties in a dry rangeland in Cyprus.

Spatial density distributions of each breakpoint category were studied individually and compared to the spatial density distributions of possible underlying factors affecting resistance: grazing intensity, mean NDVI, terrain slope and aspect. Deviations from the spatial distributions of the underlying factors were tested individually for each breakpoint category, using a two-sample Kolmogorov-Smirnov test. Only if the underlying variable, or a mechanism related to that variable, had an effect on the spatial distribution of the studied breakpoint category, a deviation from the spatial distribution of the underlying variable was expected. Otherwise, the spatial distribution of the breakpoint category related to that variable should be random. Indeed, none of the breakpoint categories showed a significant deviation from the spatial distribution of terrain slope in the area. The other factors, however, had some effect on resistance: strong grazing as well as very low NDVI values were associated with high resistance, which may be an indication for a degraded, unresponsive ecosystem condition. Low grazing did not have a clear effect on resistance, while a high NDVI, as well as north-facing slopes promoted high resistance, which may be an indication of a healthy ecosystem state that is able to buffer climatic perturbations. Intermediate to high grazing levels as well as western/eastern orientation promoted the occurrence of patches with low resistance. The results are partly in line with my expectation of a bimodal pattern (see Figure 3) for the density distribution of resistance related to ecosystem state. High resistance was associated both with areas that are related to conditions promoting or indicating a healthy ecosystem state (northern orientation, high NDVI values), as well as with areas related to conditions promoting or indicating a degraded ecosystem state (high grazing, very low NDVI values). Low resistance was associated with intermediate to harsh conditions (western/eastern orientation of slopes, intermediate to high grazing). This suggests areas with reduced resilience that can easily shift either to a degraded or a healthy state. To draw comprehensive conclusion however, further research on the correlation between resistance and ecosystem state incorporating field-based validation is required.

Objective 3: analysis of the effects of grazing intensity, mean NDVI and topographic properties on the spatial variability of the recovery rate after drought in a dry rangeland in Cyprus.

A linear regression approach was applied to study the effects of environmental factors and grazing on recovery rate of vegetation after drought, both individually as well as jointly. Spatial autocorrelation between data points was taken into account. Results confirmed my hypothesis that overall favourable environmental conditions (northern orientation of hillslopes and high NDVI values before the drought) positively affected the recovery rate. Grazing intensity was negatively related with recovery from drought, confirming the hypothesis that strong grazing limits recovery rate after drought. Contrary to my expectations, terrain slope was of minor importance for recovery, and only became relevant in combination with aspect. On southern-oriented slopes terrain slope was as expected negatively related with recovery, indicating a synergetic interaction between slope and aspect. On northern-oriented slopes, however, the relationship was positive. The reason for the latter finding remains unclear and further research, including studies in other grazed rangelands, is required, to resolve this issue. Finally, areas with low NDVI values before the drought were more sensitive to effects of a southern orientation than those with high NDVI values.

Objective 4: derivation of an exemplary resilience score, based on ecosystem resistance and recovery, which can be related to land risk management goals, followed by an assessment of the spatial dependencies between resilience classes.

I illustrated an effective way to derive a spatially explicit ecological resilience index, based on joined information on resistance and recovery. The resilience categories were defined to the purpose of allowing a direct linkage to land risk management goals on a spatial scale of 30 that is relevant for land managers. The land risk management goals were directly related to different phases of the disaster risk management cycle (prevention, preparedness, response), which is a well-established tool for decision makers to deal with natural hazards. However, to my knowledge it has not previously been employed to deal with land degradation risk. Land degradation risk is often a consequence of a loss of ecological resilience, making transitions to a degraded state more likely. Thus, linking a resilience-based index to phases in the land risk management cycle is an important step towards an informed land degradation risk management. The here presented approach promotes an informed prioritization of areas that require specific prevention measures or that are already degraded and need restoration efforts. Finally, it facilitates the identification of areas with critically low resilience that may be at risk to shift to another, potentially degraded state. This is a valuable step towards developing early-warning tools for land degradation risk. However, linking information on resilience with the stability or sustainability of certain ecological states requires further research.

Results of the spatial resilience quantification suggest that the Randi Forest study area is dominated by intermediately resilient, stagnant parts that have a high resistance to climate variability yet recover only slowly after drought, followed by highly resilient, low resilient and permanently degraded parts. Spatial dependencies between resilience categories were found up to 400 to 500 m, leading to distinct resilience clusters in the area. The spatially explicit quantification of resilience categories in the Randi Forest area is an interesting result that can inspire future research in the area. However, for an interpretation of results in terms of

management recommendations, further research is crucially required that contains field-based validation of results. The same holds true if the approach is transferred to other dryland areas. An outlook into possible future research steps is given below (section 5.3).

5.2 METHODOLOGICAL LIMITATIONS[26]

5.2.1 Deriving proxies for resistance and recovery from breakpoint analysis of satellite time series data

Deriving information on ecological resilience from satellite NDVI time series data

The study is based on satellite data from the Landsat 5 and 7 missions acquired at a spatial resolution of 30 m. The TM and ETM+ instruments aboard these satellites have high inter-sensor comparability and were found to produce comparable results suitable for long-term monitoring of natural vegetation (Vogelmann et al., 2016). Great care was taken during pre-processing to surface reflectance so that all data have comparable high quality. To ensure geometrical consistency between all scenes, additional geometric correction was performed to achieve sub-pixel accuracy. Clouds and cloud shadows were masked on pixel level. As a result, spatial data availability was not uniform, which may have affected the spatial variation of the used measures of resistance and recovery. Despite the thorough pre-processing, satellite data can still be affected by insufficient atmospheric- or geometric correction, or cloud masking. This may have caused outliers in the NDVI time series. However, since the BFAST approach as applied in this thesis is based on a robust regression approach, which is particularly suitable for dealing with outliers, it is not likely that outliers affected breakpoint frequency or the linear slope fitted after a breakpoint. On the contrary, I believe that a particular strength of a statistical time series approach compared to approaches based on a comparison between individual scenes lies in its ability to deal with outliers, due to the large amount of data that are used for model fitting. Finally, temporal satellite data availability was not constant during the study period (Figure 19F), which may have affected overall temporal breakpoint frequency, yet should not have affected the spatial variability of the used proxies for resistance and recovery. For instance, low data availability in the hydrological year 1990 might be a reason why overall breakpoint frequency in the area was low during the dry period 1990–91, compared to the dry period 2005–08.

To capture vegetation response to climate variability in the Randi Forest study area, the Normalized Difference Vegetation Index (NDVI) was used. In areas with little vegetation cover, the NDVI is known to be affected by soil background, which may have affected my results. However, Weiss et al. (2004) demonstrated its effectiveness for capturing the intra- and interannual variation in dryland vegetation. Furthermore, in a dryland study by Gaitán et al. (2013), the NDVI was found to be the best predictor of ecosystem attributes, such as vegetation cover, species richness and infiltration, compared to several other vegetation indices, for instance the Enhanced Vegetation Index (EVI) or the Soil Adjusted Vegetation Index (SAVI). Regarding the effect of the choice of vegetation index on BFAST performance, a study by Watts

[26] Some text passages in this section appear with slight adaptions in von Keyserlingk et al. (2021).

and Laffan (2013), which used NDVI and the Enhanced Vegetation Index (EVI) in a BFAST time series analysis in a semi-arid environment, concluded that there was no clear advantage in using one particular index.

In this work, relatively low NDVI values are interpreted as an indicator of a degraded ecosystem state and trends and changes (breakpoints) in NDVI time series are interpreted in terms of ecological resilience. In areas as the Randi Forest study area, where land degradation is associated with a loss of natural vegetation cover, the NDVI can serve as a relative inverted proxy for degradation. However, the NDVI does not directly provide information on shifts in species composition, for example from perennial to annul life forms, which can also be a sign for a loss of ecological resilience and ongoing land degradation in drylands. A multisite grassland experiment by Mackie et al., 2019 showed that resistance to drought and recovery are sensitive to plant community composition. Particularly in context with grazing, a selective advantage of grazing resistant over drought resistant species can affect the ecological resilience to drought. Further, the NDVI does not directly capture signs of soil degradation, such as the frequency and intensity of gully erosion. Therefore, complementing field-based research is needed to strengthen the meaningfulness of interpreting NDVI dynamics in terms of land degradation processes and resilience. Riva et al. (2017) studied land degradation in an area partly overlapping with my study area in southern Cyprus, using a combination of remotely sensed NDVI data and field observations. The authors found that the distance of annual mean NDVI values from *potential* (maximal NDVI values in the area) within the same landscape unit was found to correlate significantly with degradation levels that have been assessed by visual field indicators (based on vegetation cover and structure, species richness, signs of erosion, soil compaction and litter cover). Interestingly, species richness was only reduced in the 'heavily degraded' class, but did not differ significantly between the classes 'degraded', 'healthy' and 'potential' (see Fig. 2 in Riva et al., 2017). These results indicate that in the Randi Forest study area, changes in vegetation species composition are less important compared to loss of total vegetation cover for predicting land degradation status. In conclusion, the findings by Riva et al. (2017) support the use of remotely sensed NDVI data to study land degradation dynamics in this area.

Number of breakpoints in a satellite time series as an inverse proxy for long-term resistance

First of all, I want to highlight again that resistance, as used in this work, is not a measure for ecosystem health or its sustainability. Rather, it depicts the resistance of an ecosystem when disturbed within the boundaries of its current state – which can be desirable or undesirable from land users' perspective.

The number of breakpoints in a NDVI time series depends to a large degree on the disturbance regime and the ecosystem type. In strongly fluctuating ecosystems, such as Mediterranean drylands that are driven by a high intra- and interannual variable climate regime, a much higher number of breakpoints can be expected within the same time period, compared to ecosystems that are likely fluctuating closely around a stable equilibrium state, such as agricultural plantations or evergreen forests. Thus, the number of breakpoints is a relative measure of resistance and not comparable between study regions. Its interpretability depends on the spatial frequency of breakpoints within one comparable area that is assumed to be driven by the same

environmental variability and disturbance regime. Only in such an area, spatial variability of breakpoints can be assumed to be related to ecosystem resistance to a specific disturbance and not to be due to substantial differences between ecosystems themselves.

In order to interpret the relative number of breakpoints as an inverse indicator of resistance towards a specific disturbance, it is necessary to identify the key disturbance factors in an area. The Randi Forest area is characterized by a highly variable climate with frequent summer droughts. Since the study area is small, with little elevation differences, climate was assumed to be similar in the area. Further, the ecosystem is stressed by a long history of intensive livestock grazing. The latter is assumed to be the main cause for land degradation in the area. Funded on the conceptualization of land degradation risk that I have proposed in chapter 2.1.5 of this work (compare Figure 6), I assumed that long-term grazing is a slow driver that promotes land degradation by reducing the ecological resilience of the land towards land degradation processes. Climatic perturbations such as drought on the other hand act as fast triggers of land degradation processes. Climatic events directly affect vegetation cover and greenness, especially in a water-limited environment. Thus, I assumed that breakpoints in NDVI time series are mainly climate driven. While I believe this to be a valid assumption, further testing of the relationship between climate variability and the occurrence of breakpoints would promote the robustness of the approach.

The Randi Forest study area was specifically selected for the purpose of this work, because it represents a typical Mediterranean rangeland, driven by the same climate regime, with comparable land cover type and land use (a grazed dryland with mosaics of vegetation patches). Through the cooperation with M. de Hoop and communication with local experts in the area during a field visit in 2017, I further learned that no major land use change or large scale disturbance had occurred during the study period. One major event was the construction of a highway between 2000 and 2006 south of the study area; this was taken into account by limiting the area of interest to the region north of this highway. The detailed knowledge on the disturbance history of the area allowed the assumption that breakpoints were mainly climate driven and can provide information about long-term resistance to climate variability.

Still, small-scale differences in land use, such as individual plantation of olive or carob trees, farm buildings or small roads may have affected results. In addition, small scale disturbances may have introduced additional breakpoints that were not related to climate variability. I accepted this possibility, firstly because no reliable spatially explicit data on past occurrence of such small-scale disturbances exist. Secondly, I believed the 30 m scale of Landsat imagery would yield mixed results for each pixel, thereby minimizing the effect of small scale effects. Thirdly, I assumed that the large number of pixels used for the analysis would even out such effects, for most of the area contains natural vegetation. For example, between 2003 and 2009 I observed a local land use change in the northeast of the study area (based on Quickbird imagery), appearing like the opening of a soil dumping site. Yet, this affected only 2% of more than 3000 pixels that were included in the analysis and was therefore treated as an outlier. Using a more detailed spatial scale would probably increase the effects of small-scale disturbances on the spatial occurrence of breakpoints.

Other factors might also have affected the overall number of breakpoints. Watts and Laffan (2014) found that the optimal value for the 'h' parameter, which sets the minimum number of observations between two breakpoints in the BFAST model, depends on vegetation type. In areas with little vegetation cover, the number of breakpoints might be overestimated. My results, however, revealed an overrepresentation of pixels with none or one breakpoint in areas with low NDVI, and therefore appear to be robust even with this limitation. The same holds true for potentially noise-induced breakpoints, which might have occurred in areas with low NDVI that have a low signal to noise ratio.

Next to study region, the number of breakpoints within a time series depends on the length of the time series, but also on the spatial scale, data availability and consistency between satellite instruments. The longer the time series, the more breakpoints can be expected. Further, a more detailed spatial scale makes the occurrence of breakpoints more likely, since the effects of small-scale disturbances are enhanced. The same holds true for data availability: a time series of high temporal resolution makes the occurrence of breakpoints more likely, for the distance between two breakpoints is limited by BFAST model-parameter 'h', which sets a minimal number of observations required between two breakpoints. The studied time series should therefore be of comparable length and based on datasets with similar spatial scale and temporal resolution. If data have been collected by different satellite instruments, comparability between sensors should be ensured to avoid artificial breakpoints in the time series. All of these criteria were taken into account when selecting and preparing the satellite data used in this work. However, measurement error or differences in spatial data availability due to clouds may have affected results on resistance (see first paragraph of section 5.2.1).

NDVI recovery trend as a proxy for vegetation recovery rate after drought

Interpreting the NDVI recovery trend as vegetation recovery rate after drought assumes that the negative breakpoint in the time series was related to drought effects. To make this assumption robust, great care was taken in the selection of the drought breakpoints. Only pixels that experienced a breakpoint during a known period of prolonged drought were included. Further, the breakpoint had to be associated with a drop in NDVI of at least 10%. The finding, that a majority of the area (63%) experienced such a breakpoint during the selected time period of drought, a unique case in the time series, supports the assumption that a large scale disturbance event affecting the whole area caused this response. To my knowledge (based on personal information received by local farmers), no alternative large-scale disturbance, except drought, affected the study area during this time period.

Using the linear NDVI recovery trend fitted by the adapted BFAST model after a drought breakpoint as an indicator for the recovery rate assumes a linear recovery behaviour. I am aware that this is a simplification, yet I believe it to be a good approximation, as long as the time period of the segment for which the recovery trend is fitted is comparable among pixels. In the case presented here this requirement is fulfilled, since the NDVI recovery trend is fitted to the last segment of the BFAST time series and almost none of the pixels experienced a second breakpoint before the end of the time series (Figure 19D). Focussing on the linear trend component of additive season-trend models fitted to a dense time series has the advantage that

seasonality is taken care of in a systematic manner. Compared to recovery estimations based on comparisons of individual snapshots in time, this time series based approach promotes a reliable separation of actual recovery trends from short-term differences in NDVI, which may arise due to seasonality effects or short-term effects of one rainy season.

5.2.2 Interpreting grazing effects on resistance and recovery

Spatial quantification of grazing intensity

Grazing intensity was measured indirectly through interviews with local farmers, which were input for calculations based on the distance to the farm, number of animals in farm and topography. Actual data about the grazing intensity (e.g. through GPS tracking) were not available for the study period. In general, it is very difficult to obtain the actual time, location and length of grazing, which can differ even for pastures with the same grazing season (e.g. summer or winter) (Wang et al., 2018). Therefore, the number of animals and the distance to the farm is commonly used as a proxy for grazing intensity (Manthey and Peper, 2010; Wang et al., 2018). To draw more general conclusions on grazing effects on resistance and recovery, future studies applying a consistent methodology on different ecosystems and comparing different spatial scales are needed.

Interpreting effects of grazing on resistance on recovery in dryland systems

The effects of grazing on resistance and recovery should be treated cautiously, since they depend on many factors: Maestre et al. (2016) pointed out that the effects of grazing on ecosystem structure and functioning in drylands vary with the intensity of grazing, the composition of herbivore assemblages, the shared evolutionary history of plants and herbivores, the way grazing pressure is measured and the spatial scale. The authors also found that grazing effects on resilience to climatic stresses are highly modulated by grazing interactions with species composition and richness. The latter is supported by Ruppert et al. (2015), who quantified resistance to drought and recovery using 174 long-term datasets from more than 30 dryland regions. They found that the effects of grazing on resistance to drought and recovery are modulated by the dominant life history of the herbaceous layer. Grazing and drought induced shifts in species composition and dominant life history may also have affected grazing effects on resistance to drought and recovery in the Randi Forest study area. During field studies my colleague M. de Hoop observed that in areas with higher grazing intensity, the number of unpalatable plant species increased. However, there was no clear shift in species composition from grasses to shrubs, for shrubs were the dominant vegetation type for all grazing levels (pers. comm. M. de Hoop). However, individual shrubs were affected by browsing effects, causing them to appear in unnatural bonsai-type shapes and dwarf forms. This is also reported from field observations conducted for the CASCADE project (see Daliakopoulos and Tsanis, 2014). Altogether, interpreting effects of grazing on vegetation resistance and recovery across different systems and studies remains challenging. Systematic field-based studies on grazing effects on vegetation composition and dominant plant life history in the Randi Forest area would be a valuable next step to gain more insight into functional effects of grazing on resistance to climate variability and recovery from drought.

5.3 OUTLOOK

The methodological approach presented in this work to spatially quantify ecological resilience from satellite derived NDVI time series, presents a valuable step towards assessing ecological resilience, particularly in otherwise data scarce areas. For historical and spatially explicit field-based information on vegetation dynamics is very scarce, particularly in global drylands. The methodology and results can inspire several lines of future research.

To promote the robustness of using the spatial variability of the number of breakpoints within an area as an inverse proxy for resistance to climate variability, studying the relationship between temporal breakpoint frequency and climate time series data would be an interesting next step. For instance, checking if breakpoint frequency can be related to the frequency of drought or other climatic anomalies in a corresponding climate time series. This could be done based on a drought index, for instance the Standardized Precipitation Evapotranspiration Index (SPEI), which captures not only the effects of rainfall, but also incorporates evaporation (World Meteorological Organization (WMO) and Global Water Partnership (GWP), 2016). The latter can be of high relevance in a Mediterranean dryland where vegetation is often stressed by heatwaves, in addition to lack of rainfall.

Another line of research could aim at testing the robustness of the used proxies for resistance and recovery against differences in spatial and temporal data availability. Further, including other satellite derived vegetation indices such as the Enhanced Vegetation Index (EVI) or the Soil Adjusted Vegetation Index (SAVI), could show if the results on breakpoint occurrence and NDVI recovery trend are sensitive to the chosen vegetation index particularly in sparsely vegetated areas.

For further disentangling the factors affecting spatial variability of resilience in drylands, a future line of research could be to combine all factors in a multivariate cluster analysis in space. Such an analysis could foster an understanding of the joined effects, including interactions. Such information is particularly valuable, when aiming at specific recommendation for land risk management.

The results of satellite-based resilience quantification can be used for a purposeful direction of subsequent field-based resilience or land degradation assessments. Results from such field-based research could promote validation of resistance, recovery and resilience categories that have been assigned based on the remote sensing approach. Effects of grazing on resistance and recovery could be studied in small-scale field experiments to corroborate or refute the results based on the remote-sensing assessment in the same area. In combination with such field-based research, the presented remote sensing approach to spatially quantify resilience is a valuable starting point for planning resilience-based land risk management options. The identification of areas that should be the focus of restoration measures, which areas are robust and suitable for continued land use, and which areas have critically low resilience, can be of major importance to land users. Areas with critically low resilience should receive particular attention (highlighted in red in Figure 29 & Figure 30). These areas can be at risk to shift into a hard to reverse degraded state due to minor stochastic climatic disturbances. Hence, critically low resilience can serve as

an early-warning tool for land managers to prevent or prepare for such a shift. However, according to Sietz et al. (2017), areas with reduced resilience can also present windows of opportunity for land management options designed to push the ecosystem towards the desired, healthy state. The management goal related to areas with low resilience thus depends on the present state of the ecosystem. In order to confirm the likelihood of an approaching shift in areas with low resilience, purposeful application of resilience-based metrics that have been specifically designed to identify approaching transitions, would be a valuable next step. Such metrics include for example an increase in spatial or temporal autocorrelation in NDVI indicating increased memory effects or repeated flickering between two distinct stable states observed in long-term time series (for a comprehensive overview of metrics indicating sudden transitions see e.g. Scheffer et al., 2012 & Kéfi et al., 2014).

Finally, testing the methodological approach to quantify resilience presented in this work in other dryland areas would help to test the reliability of the approach and promote its transferability.

5.4 Final remarks

This work promotes the use of ecological resilience to link land degradation research with quantitative risk assessment. Based on identified discrepancies in current land degradation risk assessment approaches, a conceptual risk-resilience model for land degradation risk assessment is proposed. A methodological approach to spatially quantify two aspects of resilience (resistance to climate variability and recovery rate after drought) was developed, using satellite derived NDVI time series data in combination with a change detection approach. Analysis of the spatial variation of resistance to climate variability and recovery after drought in a dry European rangeland revealed that resilience to climatic variation such as drought was modulated by grazing and environmental conditions. Finally, this thesis illuminates ways how spatially explicit information on resilience, based on joint knowledge on resistance and recovery, can be used to identify spatial resilience clusters. Based on spatial information on resilience, links to land risk management goals were proposed. Overall, this thesis contributes to advancing risk reduction strategies for land degradation, both on conceptual, as well as on methodological level.

6 ACKNOWLEDGEMENTS

First, I would like to thank my supervisors for their continuous support and guidance. To Eva Nora Paton I am particularly grateful for her often pragmatic advice that helped me structuring my work and for the fruitful scientific discussions. I thank Axel Bronstert for his kind and motivating words and for having the broader picture in mind. My special thanks go to Saskia Förster for her dedicated hands-on advice on all steps of the remote sensing analysis and for her always positive and encouraging manner, which helped to continue through the difficult parts of this thesis.

This work was made possible by the DFG-Research School NatRiskChange that provided funding and created a collegial, family friendly and structured working environment, supporting the individual and personal development of my research interests, which I highly appreciate.

I am very grateful for the experience I made during the three month at the Remote Sensing section of the German Research Centre for Geosciences (GFZ). The working environment, team spirit, and various scientific expertise were really inspiring and greatly promoted my working progress during the pre-analysis of all satellite imagery. I want to thank the GFZ for the provision of computational facilities and data storage, Daniel Scheffler for his assistance with the geometric co-registration with AROSIC and Sylvia Magnussen for her professional IT-support, without which I would have been stuck many times.

During a field visit in Southern Cyprus, Saskia, Eva and I were warmly welcomed and introduced to the on-site field ecology of the Randi Forest study area by Michalakis Christoforou, shown through the Kouris catchment by Athina Papatheodoulou and informed about the hydrology of the area by Gerald Dörflinger, who also assisted with the acquisition of all meteorological data. For all this generous support I am highly grateful.

Jan Verbesselt, Ben de Vries and Achim Zeileis gave valuable expert advice on the implementation and adaption of the BFAST algorithm, and Annegret Thieken on the topic of disaster risk research, which I highly appreciate. Further, I would like to thank NASA, ESA and USGS for providing the Landsat data as well as the digital elevation model used in this work.

Thanks go to all my colleagues at TU Berlin and Potsdam University, particularly Arne Reck, Loes van Schaik, Anna Smetanova and all my colleagues from NRC for the many helpful coffee-break discussions and for always having an open door. Further, to Lars Schulz for his very efficient assistance in implementing the LEDAPS algorithm. To all of my friends for staying close to me and also to the people in my online scientific writing group, who helped me to stay focused during the many hours of writing at home during this pandemic.

To Stefan C. Dekker, Max Rietkerk, Ángeles G. Mayor and Myrna de Hoop for the fruitful scientific discussions, the valuable feedback and the inspiring visit at Utrecht University that resulted in our joined paper. I really enjoyed the scientific cooperation with all of you. To Myrna I am especially grateful for the awesome team work and the moral support which made my work so much more enjoyable and strongly motivated me to keep going. I could not have achieved this task without you. Further, our scientific cooperation enabled me to analyse the satellite data in context with grazing, which greatly broadened the perspective of my work.

Finally, I am most grateful to my wonderful family for constantly being by my side. Thanks, Markus, for always believing in me and for your unconditional support that enabled me to finish this thesis. To Klara Elinor for always bringing a smile to my face. To my mother Grete, for having an open ear whenever needed and for proof reading large parts of this text. To my father Wolff, who, with his magic, inspired my deep-rooted curiosity to always find out how things work.

7 BIBLIOGRAPHY

Akbari, M., Ownegh, M., Asgari, H.R., Sadoddin, A., Khosravi, H., 2016. Desertification risk assessment and management program. Glob. J. Environ. Sci. Manag. 2, 365–380. https://doi.org/10.22034/gjesm.2016.02.04.006

Alcántara-Ayala, I., 2002. Geomorphology, natural hazards, vulnerability and prevention of natural disasters in developing countries. Geomorphology 47, 107–124.

Ali, R.R., Abdel Kawy, W.A.M., 2013. Land degradation risk assessment of El Fayoum depression, Egypt. Arab. J. Geosci. 6, 2767–2776. https://doi.org/10.1007/s12517-012-0524-7

Bai, J., Perron, P., 1998. Estimating and Testing Linear Models with Multiple Structural Changes. Econometrica 66, 47. https://doi.org/10.2307/2998540

Barrow, C.J., 1991. Land degradation: development and breakdown of terrestrial environments. Cambridge University Press, Cambridge.

Becerril-Piña, R., Mastachi-Loza, C.A., González-Sosa, E., Díaz-Delgado, C., Bâ, K.M., 2015. Assessing desertification risk in the semi-arid highlands of central Mexico. J. Arid Environ. 120, 4–13. https://doi.org/10.1016/j.jaridenv.2015.04.006

Ben Abbes, A., Bounouh, O., Farah, I.R., de Jong, R., Martínez, B., 2018. Comparative study of three satellite image time-series decomposition methods for vegetation change detection. Eur. J. Remote Sens. 51, 607–615. https://doi.org/10.1080/22797254.2018.1465360

Browning, D.M., Maynard, J.J., Karl, J.W., Peters, D.C., 2017. Breaks in MODIS time series portend vegetation change: verification using long-term data in an arid grassland ecosystem. Ecol. Appl. 27, 1677–1693. https://doi.org/10.1002/eap.1561

Cardona, O.D., 2003. The need for rethinking the concepts of vulnerability and risk from a holistic perspective: a necessary review and criticism for effective risk management, in: Mapping Vulnerability: Disasters, Development and People. Earthscan Publisher, London, Chapter 3.

Carpenter, S., Walker, B., Anderies, J.M., Abel, N., 2001. From metaphor to measurement: resilience of what to what? Ecosystems 4, 765–781. https://doi.org/10.1007/s10021-001-0045-9

Chambers, J.C., Allen, C.R., Cushman, S.A., 2019. Operationalizing Ecological Resilience Concepts for Managing Species and Ecosystems at Risk. Front. Ecol. Evol. 7, 241. https://doi.org/10.3389/fevo.2019.00241

Cumming, G.S., Barnes, G., Perz, S., Schmink, M., Sieving, K.E., Southworth, J., Binford, M., Holt, R.D., Stickler, C., Van Holt, T., 2005. An Exploratory Framework for the Empirical Measurement of Resilience. Ecosystems 8, 975–987. https://doi.org/10.1007/s10021-005-0129-z

Dakos, V., Carpenter, S.R., Brock, W.A., Ellison, A.M., Guttal, V., Ives, A.R., Kéfi, S., Livina, V., Seekell, D.A., van Nes, E.H., Scheffer, M., 2012. Methods for Detecting Early Warnings of Critical Transitions in Time Series Illustrated Using Simulated Ecological Data. PLoS ONE 7, e41010. https://doi.org/10.1371/journal.pone.0041010

Dakos, V., Carpenter, S.R., van Nes, E.H., Scheffer, M., 2014. Resilience indicators: prospects and limitations for early warnings of regime shifts. Philos. Trans. R. Soc. B Biol. Sci. 370, 20130263. https://doi.org/10.1098/rstb.2013.0263

Dakos, V., van Nes, E.H., Donangelo, R., Fort, H., Scheffer, M., 2010. Spatial correlation as leading indicator of catastrophic shifts. Theor. Ecol. 3, 163–174. https://doi.org/10.1007/s12080-009-0060-6

Daliakopoulos, I., Tsanis, I., 2014. Historical evolution of dryland ecosystems. CASCADE Project Deliverable 2.1. CASCADE Report 04. www.cascadis-project.eu/documents (accessed 31 January 2019).

de Jong, R., Verbesselt, J., Zeileis, A., Schaepman, M., 2013. Shifts in Global Vegetation Activity Trends. Remote Sens. 5, 1117–1133. https://doi.org/10.3390/rs5031117

De Keersmaecker, W., Lhermitte, S., Tits, L., Honnay, O., Somers, B., Coppin, P., 2015. A model quantifying global vegetation resistance and resilience to short-term climate anomalies and their relationship with vegetation cover: Global vegetation resistance and resilience. Glob. Ecol. Biogeogr. 24, 539–548. https://doi.org/10.1111/geb.12279

De Keersmaecker, W., van Rooijen, N., Lhermitte, S., Tits, L., Schaminee, J., Coppin, P., Honnay, O., Somers, B., 2016. Species-rich semi-natural grasslands have a higher resistance but a lower resilience than intensively managed agricultural grasslands in response to climate anomalies. J. Appl. Ecol. 53, 430–439. https://doi.org/10.1111/1365-2664.12595

del Barrio, G., Puigdefabregas, J., Sanjuan, M.E., Stellmes, M., Ruiz, A., 2010. Assessment and monitoring of land condition in the Iberian Peninsula, 1989–2000. Remote Sens. Environ. 114, 1817–1832. https://doi.org/10.1016/j.rse.2010.03.009

DeVries, B., Decuyper, M., Verbesselt, J., Zeileis, A., Herold, M., Joseph, S., 2015a. Tracking disturbance-regrowth dynamics in tropical forests using structural change detection and Landsat time series. Remote Sens. Environ. 169, 320–334. https://doi.org/10.1016/j.rse.2015.08.020

DeVries, B., Pratihast, A.K., Verbesselt, J., Kooistra, L., Herold, M., 2016. Characterizing Forest Change Using Community-Based Monitoring Data and Landsat Time Series. PLOS ONE 11, e0147121. https://doi.org/10.1371/journal.pone.0147121

DeVries, B., Verbesselt, J., Kooistra, L., Herold, M., 2015b. Robust monitoring of small-scale forest disturbances in a tropical montane forest using Landsat time series. Remote Sens. Environ. 161, 107–121. https://doi.org/10.1016/j.rse.2015.02.012

Dougill, A.J., Thomas, D.S.G., Heathwaite, A.L., 1999. Environmental change in the Kalahari: Integrated land degradation studies for nonequilibrium dryland environments. Ann. Assoc. Am. Geogr. 89, 420–442. https://doi.org/10.1111/0004-5608.00156

Dregne, H.E., 2002. Land degradation in the drylands. Arid Land Res. Manag. 16, 99–132. https://doi.org/10.1080/153249802317304422

Dutrieux, L.P., DeVries, B., 2004. bfastSpatial: Set of utilities and wrappers to perform change detection on satellite image time-series. https://github.com/loicdtx/bfastSpatial

Dutrieux, L.P., Verbesselt, J., Kooistra, L., Herold, M., 2015. Monitoring forest cover loss using multiple data streams, a case study of a tropical dry forest in Bolivia. ISPRS J. Photogramm. Remote Sens. 107, 112–125. https://doi.org/10.1016/j.isprsjprs.2015.03.015

Edwards, T.L., Challenor, P.G., 2013. Risk and unvertainty in hydrometeorological hazards, in: Rougier, J., Sparks, S., Hill, L.J. (Eds.), Risk and Uncertainty Assessment for Natural Hazards. Cambridge University Press, New York City, USA, pp. 100–150.

FAO, 2012. Livestock and Landscapes. Food and Agricultural Organization of the United Nations (FAO). www.fao.org/3/ar591e/ar591e.pdf (accessed 18 January 2021).

FAO, 1979. Report on the second meeting of the working group on soil degradation assessment methodology. Food and Agriculture Organization of the United Nations (FAO), Rome, Italy.

Felgentreff, C., Glade, T., 2007. Naturrisiken und Sozialkatastrophen.

Folke, C., 2016. Resilience (Republished). Ecol. Soc. 21, art44. https://doi.org/10.5751/ES-09088-210444

Folke, C., Carpenter, S., Walker, B., Scheffer, M., Elmqvist, T., Gunderson, L., Holling, C.S., 2004. Regime Shifts, Resilience, and Biodiversity in Ecosystem Management. Annu. Rev. Ecol. Evol. Syst. 35, 557–581. https://doi.org/10.1146/annurev.ecolsys.35.021103.105711

Frazier, A.E., Renschler, C.S., Miles, S.B., 2013. Evaluating post-disaster ecosystem resilience using MODIS GPP data. Int. J. Appl. Earth Obs. Geoinformation 21, 43–52. https://doi.org/10.1016/j.jag.2012.07.019

Gaitán, J.J., Bran, D., Oliva, G., Ciari, G., Nakamatsu, V., Salomone, J., Ferrante, D., Buono, G., Massara, V., Humano, G., Celdrán, D., Opazo, W., Maestre, F.T., 2013. Evaluating the performance of multiple remote sensing indices to predict the spatial variability of

ecosystem structure and functioning in Patagonian steppes. Ecol. Indic. 34, 181–191. https://doi.org/10.1016/j.ecolind.2013.05.007

Gamon, J.A., Field, C.B., Goulden, M.L., Griffin, K.L., Hartley, A.E., Joel, G., Penuelas, J., Valentini, R., 1995. Relationships between NDVI, canopy structure, and photosynthesis in three californian vegetation types. Ecol. Appl. 5, 28–41. https://doi.org/10.2307/1942049

Gao, Y., Zhong, B., Yue, H., Wu, B., Cao, S., 2011. A degradation threshold for irreversible loss of soil productivity: a long-term case study in China: Degradation threshold of soil productivity. J. Appl. Ecol. 48, 1145–1154. https://doi.org/10.1111/j.1365-2664.2011.02011.x

Garg, P.K., Harrison, A.R., 1992. Land degradation and erosion risk analysis in S.E. Spain: A geographic information system approach. CATENA 19, 411–425. https://doi.org/10.1016/0341-8162(92)90041-9

Geerken, R.A., 2009. An algorithm to classify and monitor seasonal variations in vegetation phenologies and their inter-annual change. ISPRS J. Photogramm. Remote Sens. 64, 422–431. https://doi.org/10.1016/j.isprsjprs.2009.03.001

Gill, J.C., Malamud, B.D., 2014. Reviewing and visualizing the interactions of natural hazards: Interactions of Natural Hazards. Rev. Geophys. 52, 680–722. https://doi.org/10.1002/2013RG000445

Goward, S., Arvidson, T., Williams, D., Faundeen, J., Irons, J., Franks, S., 2006. Historical Record of Landsat Global Coverage. Photogramm. Eng. Remote Sens. 72, 1155–1169. https://doi.org/10.14358/PERS.72.10.1155

Goward, S.N., Dye, D., Kerber, A., Kalb, V., 1987. Comparison of North and South American biomes from AVHRR observations. Geocarto Int. 2, 27–39. https://doi.org/10.1080/10106048709354079

Goward, S.N., Tucker, C.J., Dye, D.G., 1985. North American vegetation patterns observed with the NOAA-7 advanced very high resolution radiometer. Vegetatio 64, 3–14. https://doi.org/10.1007/BF00033449

Gräler, B., Pebesma, E., Heuvelink, G., 2016. Spatio-Temporal Interpolation using gstat. R J. 8, 204–218. https://doi.org/10.32614/RJ-2016-014

Gunderson, L.H., 2000. Ecological Resilience—In Theory and Application. Annu. Rev. Ecol. Syst. 31, 425–439. https://doi.org/10.1146/annurev.ecolsys.31.1.425

Hai, L.T., Gobin, A., Hens, L., 2013. Risk Assessment of Desertification for Binh Thuan Province, Vietnam. Hum. Ecol. Risk Assess. Int. J. 19, 1544–1556. https://doi.org/10.1080/10807039.2012.716688

Hansen, M.C., Loveland, T.R., 2012. A review of large area monitoring of land cover change using Landsat data. Remote Sens. Environ. 122, 66–74. https://doi.org/10.1016/j.rse.2011.08.024

Hastings, A., Wysham, D.B., 2010. Regime shifts in ecological systems can occur with no warning. Ecol. Lett. 13, 464–472. https://doi.org/10.1111/j.1461-0248.2010.01439.x

Haywood, J., Randall, J., 2008. Trending seasonal data with multiple structural breaks. NZ visitor arrivals and the minimal effects of 9/11 (Research report 08/10). University of Wellington, Victoria, New Zealand.

Hellmuth, M.E., Mason, S.J., Vaughan, C., van Aalst, M.K., Choularton, R. (Eds.), 2011. A better climate for disaster risk management. International Research Institute for Climate and Society (IRI), Columbia University, New York, USA.

Helman, D., Mussery, A., Lensky, I.M., Leu, S., 2014. Detecting changes in biomass productivity in a different land management regimes in drylands using satellite-derived vegetation index. Soil Use Manag. 30, 32–39. https://doi.org/10.1111/sum.12099

Henebry, G.M., 2019. Methodology II: Remote sensing of change in grasslands, in: Gibson, D.J., Newman, J.A. (Eds.), Grasslands and Climate Change. Cambridge University Press, pp. 40–64. https://doi.org/10.1017/9781108163941.005

Hirota, M., Holmgren, M., Van Nes, E.H., Scheffer, M., 2011. Global resilience of tropical forest and savanna to critical transitions. Science 334, 232–235. https://doi.org/10.1126/science.1210657

Hodgson, D., McDonald, J.L., Hosken, D.J., 2015. What do you mean, 'resilient'? Trends Ecol. Evol. 30, 503–506. https://doi.org/10.1016/j.tree.2015.06.010

Holling, C.S., 1996. Engineering resilience versus ecological resilience, in: Schulze, P.C. (Ed.), Engineering Within Ecological Constraints. The National Academies Press, Washington, DC, pp. 31–43.

Holling, C.S., 1973. Resilience and stability of ecological systems. Annu. Rev. Ecol. Syst. 4, 1–23. https://doi.org/10.1146/annurev.es.04.110173.000245

Huang, K., Zhou, T., Zhao, X., 2014. Extreme drought-induced trend changes in MODIS EVI time series in Yunnan, China. IOP Conf. Ser. Earth Environ. Sci. 17, 012070. https://doi.org/10.1088/1755-1315/17/1/012070

Ibáñez, J., Valderrama, J.M., Puigdefábregas, J., 2008. Assessing desertification risk using system stability condition analysis. Ecol. Model. 213, 180–190. https://doi.org/10.1016/j.ecolmodel.2007.11.017

İLseven, S., 2017. Analysis of maquis and garrigue communities on the island of cyprus and comparison with calabrian pine communities in terms of ecological characteristics. J. Environ. Biol. 38, 955–960. https://doi.org/10.22438/jeb/38/5(SI)/GM-12

Imeson, A., 2012. Desertification, Land Degradation and Sustainability. John Wiley & Sons, Inc., Chisester, West Sussex, UK.

Ingrisch, J., Bahn, M., 2018. Towards a Comparable Quantification of Resilience. Trends Ecol. Evol. 33, 251–259. https://doi.org/10.1016/j.tree.2018.01.013

IPCC, 2019: Olsson, L., H. Barbosa, S. Bhadwal, A. Cowie, K. Delusca, D. Flores-Renteria, K. Hermans, E. Jobbagy, W. Kurz, D. Li, D.J. Sonwa, L. Stringer, 2019: Land Degradation. In: Climate Change and Land: an IPCC special report on climate change, desertification, land degradation, sustainable land management, food security, and greenhouse gas fluxes in terrestrial ecosystems [P.R. Shukla, J. Skea, E. Calvo Buendia, V. Masson-Delmotte, H.-O. Pörtner, D. C. Roberts, P. Zhai, R. Slade, S. Connors, R. van Diemen, M. Ferrat, E. Haughey, S. Luz, S. Neogi, M. Pathak, J. Petzold, J. Portugal Pereira, P. Vyas, E. Huntley, K. Kissick, M. Belkacemi, J. Malley, (eds.)].

IPCC, 2014: Climate Change 2014: Impacts, Adaptation, and Vulnerability. Part B: Regional Aspects. Contribution of Working Group II to the Fifth Assessment Report of the Intergovernmental Panel on Climate Change [Barros, V.R., C.B. Field, D.J. Dokken, M.D. Mastrandrea, K.J. Mach, T.E. Bilir, M. Chatterjee, K.L. Ebi, Y.O. Estrada, R.C. Genova, B. Girma, E.S. Kissel, A.N. Levy, S. MacCracken, P.R. Mastrandrea, and L.L. White (eds.)]. Cambridge University Press, Cambridge, United Kingdom and New York, NY, USA, 688 pp.

IPCC, 2013: Climate Change 2013: The Physical Science Basis. Contribution of Working Group I to the Fifth Assessment Report of the Intergovernmental Panel on Climate Change [Stocker, T.F., D. Qin, G.-K. Plattner, M. Tignor, S.K. Allen, J. Boschung, A. Nauels, Y. Xia, V. Bex and P.M. Midgley (eds.)]. Cambridge University Press, Cambridge, United Kingdom and New York, NY, USA, 1535 pp.

IPCC, 2012: Managing the Risks of Extreme Events and Disasters to Advance Climate Change Adaptation. A Special Report of Working Groups I and II of the Intergovernmental Panel on Climate Change [Field, C.B., V. Barros, T.F. Stocker, D. Qin, D.J. Dokken, K.L. Ebi, M.D. Mastrandrea, K.J. Mach, G.-K. Plattner, S.K. Allen, M. Tignor, and P.M. Midgley (eds.)]. Cambridge University Press, Cambridge, UK, and New York, NY, USA, 582 pp.

IUSS Working Group WRB, 2015. World Reference Base for Soil Resources 2014, update 2015 International soil classification system for naming soils and creating legends for soil maps. World Soil Resources Reports No. 106, FAO, Rome. http://www.fao.org/3/i3794en/I3794en.pdf (accessed 12 November 2018).

Jenks, G.F., Caspall, F.C., 1971. Error on choroplethic maps: definition, measurement, reduction. Ann. Assoc. Am. Geogr. 61, 217–244. https://doi.org/10.1111/j.1467-8306.1971.tb00779.x

Kaplan, S., Garrick, B.J., 1981. On the quantitative definition of risk. Risk Anal. 1, 11–27.

Karssenberg, D., Bierkens, M.F.P., 2012. Early-warning signals (potentially) reduce uncertainty in forecasted timing of critical shifts. Ecosphere 3, art15. https://doi.org/10.1890/ES11-00293.1

Karssenberg, D., Bierkens, M.F.P., Rietkerk, M., 2017. Catastrophic Shifts in Semiarid Vegetation-Soil Systems May Unfold Rapidly or Slowly. Am. Nat. E000–E000. https://doi.org/10.1086/694413

Katagis, T., Gitas, I.Z., Toukiloglou, P., Veraverbeke, S., Goossens, R., 2014. Trend analysis of medium- and coarse-resolution time series image data for burned area mapping in a Mediterranean ecosystem. Int. J. Wildland Fire 23, 668–677. https://doi.org/10.1071/WF12055

Kawamura, K., Akiyama, T., Yokota, H., Tsutsumi, M., Yasuda, T., Watanabe, O., Wang, S., 2005. Quantifying grazing intensities using geographic information systems and satellite remote sensing in the Xilingol steppe region, Inner Mongolia, China. Agric. Ecosyst. Environ. 107, 83–93. https://doi.org/10.1016/j.agee.2004.09.008

Kéfi, S., Dakos, V., Scheffer, M., Van Nes, E.H., Rietkerk, M., 2013. Early warning signals also precede non-catastrophic transitions. Oikos 122, 641–648.

Kéfi, S., Guttal, V., Brock, W.A., Carpenter, S.R., Ellison, A.M., Livina, V.N., Seekell, D.A., Scheffer, M., van Nes, E.H., Dakos, V., 2014. Early warning signals of ecological transitions: Methods for spatial patterns. PLoS ONE 9, 1–13. https://doi.org/10.1371/journal.pone.0092097

Kéfi, S., Rietkerk, M., Alados, C.L., Pueyo, Y., Papanastasis, V.P., ElAich, A., de Ruiter, P.C., 2007. Spatial vegetation patterns and imminent desertification in Mediterranean arid ecosystems. Nature 449, 213–217. https://doi.org/10.1038/nature06111

Kennedy, R.E., Andréfouët, S., Cohen, W.B., Gómez, C., Griffiths, P., Hais, M., Healey, S.P., Helmer, E.H., Hostert, P., Lyons, M.B., Meigs, G.W., Pflugmacher, D., Phinn, S.R., Powell, S.L., Scarth, P., Sen, S., Schroeder, T.A., Schneider, A., Sonnenschein, R., Vogelmann, J.E., Wulder, M.A., Zhu, Z., 2014. Bringing an ecological view of change to Landsat-based remote sensing. Front. Ecol. Environ. 12, 339–346. https://doi.org/10.1890/130066

Kraaij, T., Ward, D., 2006. Effects of Rain, Nitrogen, Fire and Grazing on Tree Recruitment and Early Survival in Bush-Encroached Savanna, South Africa. Plant Ecol. 186, 235–246. https://doi.org/10.1007/s11258-006-9125-4

Kwon, H.-Y., Nkonya, E., Johnson, T., Graw, V., Kato, E., Kihiu, E., 2016. Global estimates of the impacts of grassland segradation on livestock productivity from 2001 to 2011, in: Nkonya, E., Mirzabaev, A., von Braun, J. (Eds.), Economics of Land Degradation and Improvement – A Global Assessment for Sustainable Development. Springer International Publishing, Cham, pp. 197–214.

LADA, 2011: Biancalani, R., Nachtergaele, F., Petri, M., Bunning, S., 2011. Land Degradation Assessment in Drylands (LADA) - Methodology and Results. Food and Agriculture Organization of the United Nations (FAO), Rome, Italy.

Ladisa, G., Todorovic, M., Trisorio Liuzzi, G., 2012. A GIS-based approach for desertification risk assessment in Apulia region, SE Italy. Phys. Chem. Earth Parts ABC 49, 103–113. https://doi.org/10.1016/j.pce.2011.05.007

Le, Q.B., Nkonya, E., Mirzabaev, A., 2016. Biomass productivity-based mapping of global degradation hotspots, in: Nkonya, E., Mirzabaev, A., von Braun, J. (Eds.), Economics of Land Degradation and Improvement – A Global Assessment for Sustainable Development. Springer International Publishing, Cham, pp. 55–84. https://doi.org/10.1007/978-3-319-19168-3_6

Leopold, L.B., Clarke, F.E., Hanshaw, B.B., Balsley, J.R., 1971. A procedure for evaluating environmental impact (Report No. 645), Circular. Washington, D.C. https://doi.org/10.3133/cir645

López, D.R., Brizuela, M.A., Willems, P., Aguiar, M.R., Siffredi, G., Bran, D., 2013. Linking ecosystem resistance, resilience, and stability in steppes of North Patagonia. Ecol. Indic. 24, 1–11. https://doi.org/10.1016/j.ecolind.2012.05.014

Mackie, K.A., Zeiter, M., Bloor, J.M.G., Stampfli, A., 2019. Plant functional groups mediate drought resistance and recovery in a multisite grassland experiment. J. Ecol. 107, 937–949. https://doi.org/10.1111/1365-2745.13102

Maestre, F.T., Eldridge, D.J., Soliveres, S., Kéfi, S., Delgado-Baquerizo, M., Bowker, M.A., García-Palacios, P., Gaitán, J., Gallardo, A., Lázaro, R., Berdugo, M., 2016. Structure and Functioning of Dryland Ecosystems in a Changing World. Annu. Rev. Ecol. Evol. Syst. 47, 215–237. https://doi.org/10.1146/annurev-ecolsys-121415-032311

Mäler, K.-G., 2000. Development, ecological resources and their management: A study of complex dynamic systems. Eur. Econ. Rev. 44, 645–665. https://doi.org/10.1016/S0014-2921(00)00043-X

Manthey, M., Peper, J., 2010. Estimation of grazing intensity along grazing gradients – the bias of nonlinearity. J. Arid Environ. 74, 1351–1354. https://doi.org/10.1016/j.jaridenv.2010.05.007

Masek, J.G., Vermote, E.F., Saleous, N.E., Wolfe, R., Hall, F.G., Huemmrich, K.F., Gao, F., Kutler, J., Lim, T.-K., 2006. A Landsat Surface Reflectance Dataset for North America, 1990–2000. IEEE Geosci. Remote Sens. Lett. 3, 68–72. https://doi.org/10.1109/LGRS.2005.857030

Mayor, Á.G., Kéfi, S., Bautista, S., Rodríguez, F., Cartení, F., Rietkerk, M., 2013. Feedbacks between vegetation pattern and resource loss dramatically decrease ecosystem resilience and restoration potential in a simple dryland model. Landsc. Ecol. 28, 931–942. https://doi.org/10.1007/s10980-013-9870-4

McLeman, R.A., Dupre, J., Berrang Ford, L., Ford, J., Gajewski, K., Marchildon, G., 2014. What we learned from the Dust Bowl: lessons in science, policy, and adaptation. Popul. Environ. 35, 417–440. https://doi.org/10.1007/s11111-013-0190-z

MEA, 2005a. Ecosystems and Human Well-being: Synthesis. Millennium Ecosystem Assessment (MEA). Island Press, Washington, DC.

MEA, 2005b. Ecosystems and Human Well-being: Desertification Synthesis. World Resources Institute. Millennium Ecosystem Assessment (MEA), Washington, D.C.

Merz, B., Thieken, A.H., 2004. Flood Risk Analysis: Concepts and Challenges. Springer Austria. Östereichische Wasser- Abfallwirtsch. 56, 27–34.

Merz, B., Thieken, A.H., Gocht, M., 2007. Flood risk mapping at the local scale: Concepts and challenges, in: Begum, S., Stive, M.J.F., Hall, J.W. (Eds.), Flood Risk Management in Europe. Springer Netherlands, Dordrecht, pp. 231–251. https://doi.org/10.1007/978-1-4020-4200-3_13

Michaelides, S., Pashiardis, S., 2008. Monitoring drought in Cyprus during the 2007-2008 hydrometeorological year by using the Standardized Precipitation Index (SPI). Eur. Water 23/24, 123–131.

Myneni, R., Hall, F., Sellers, P., Marshak, A., 1995. The Interpretation of Spectral Vegetation Indexes. Ieee Trans. Geosci. Remote Sens. 33, 481–486. https://doi.org/10.1109/36.377948

Nachtergaele, F., Biancalani, R., Bunning, S., George, H., 2010. Land degradation assessment: the LADA approach, in: 19th World Congress of Soil Science, Brisbane, Australia.

Nimmo, D.G., Mac Nally, R., Cunningham, S.C., Haslem, A., Bennett, A.F., 2015. Vive la résistance: reviving resistance for 21st century conservation. Trends Ecol. Evol. 30, 516–523. https://doi.org/10.1016/j.tree.2015.07.008

Nkonya, E., Anderson, W., Kato, E., Koo, J., Mirzabaev, A., von Braun, J., Meyer, S., 2016. Global cost of land degradation, in: Nkonya, E., Mirzabaev, A., von Braun, J. (Eds.), Economics

of Land Degradation and Improvement – A Global Assessment for Sustainable Development. Springer International Publishing, Cham, pp. 117–165. https://doi.org/10.1007/978-3-319-19168-3_6

O'Connor, T.G., 1995. Acacia karroo invasion of grassland: environmental and biotic effects influencing seedling emergence and establishment. Oecologia 103, 214–223. https://doi.org/10.1007/BF00329083

Olofsson, P., Eklundh, L., Lagergren, F., Jönsson, P., Lindroth, A., 2007. Estimating net primary production for Scandinavian forests using data from Terra/MODIS. Adv. Space Res. 39, 125–130. https://doi.org/10.1016/j.asr.2006.02.031

Pebesma, E.J., 2004. Multivariable geostatistics in S: the gstat package. Comput. Geosci. 30, 683–691. https://doi.org/10.1016/j.cageo.2004.03.012

Pebesma, E.J., 1992. Gstat user's manual 108.

Pettorelli, N., Vik, J.O., Mysterud, A., Gaillard, J.-M., Tucker, C.J., Stenseth, N.Chr., 2005. Using the satellite-derived NDVI to assess ecological responses to environmental change. Trends Ecol. Evol. 20, 503–510. https://doi.org/10.1016/j.tree.2005.05.011

Pimm, S.L., 1984. The complexity and stability of ecosystems. Nature 307, 321–326. https://doi.org/10.1038/307321a0

Pinheiro, J., Bates, D., DebRoy, S., Sarkar, D., 2018. Nlme: Linear and nonlinear mixed effects models. R package version 3.1-137. https://CRAN.R-project.org/package=nlme.

Plate, E.J., Merz, B. (Eds.), 2001. Naturkatastrophen: Ursachen, Auswirkungen, Vorsorge. E. Schweizerbart'sche Verlagsbuchhandlung (Nägele u. Obermüller).

Popkin, G., 2014. On the edge. Science 345, 1552–1554. https://doi.org/10.1126/science.345.6204.1552

R Core Team, 2019. A language and environment for statistical computing. R Foundation for Statistical Computing, Vienna, Austria.

R Core Team, 2017. A language and environment for statistical computing. R Foundation for Statistical Computing, Vienna, Austria. http://www.R-project.org/.

Republic of Cyprus: Department of Meteorology, 2019. Meteorological Reports, Precipitation Statistics Pafos, 1991-2005. http://www.moa.gov.cy/moa/ms/ms.nsf/DMLclimet_reports_en/DMLclimet_reports_en?opendocument (accessed 22 August 2019).

Republic of Cyprus: Meteorological Service, 2019. Climate of Cyprus. http://www.moa.gov.cy/moa/ms/ms.nsf/DMLcyclimate_en/DMLcyclimate_en?OpenDocument (accessed 22 August 2019).

Reynolds, J.F., Stafford Smith, D.M., Lambin, E.F., Turner, B.L., Mortimore, M., Batterbury, S.P.J., Downing, T.E., Dowlatabadi, H., Fernandez, R.J., Herrick, J.E., Huber-Sannwald, E., Jiang, H., Leemans, R., Lynam, T., Maestre, F.T., Ayarza, M., Walker, B., 2007. Global desertification: Building a science for dryland development. Science 316, 847–851. https://doi.org/10.1126/science.1131634

Rietkerk, M., van de Koppel, J., 1997. Alternate stable states and threshold effects in semi-arid grazing systems. Oikos 79, 69. https://doi.org/10.2307/3546091

Riva, M.J., Daliakopoulos, I.N., Eckert, S., Hodel, E., Liniger, H., 2017. Assessment of land degradation in Mediterranean forests and grazing lands using a landscape unit approach and the normalized difference vegetation index. Appl. Geogr. 86, 8–21. https://doi.org/10.1016/j.apgeog.2017.06.017

Rohde, R.F., Hoffman, M.T., 2012. The historical ecology of Namibian rangelands: Vegetation change since 1876 in response to local and global drivers. Sci. Total Environ. 416, 276–288. https://doi.org/10.1016/j.scitotenv.2011.10.067

Roques, K.G., O'Connor, T.G., Watkinson, A.R., 2001. Dynamics of shrub encroachment in an African savanna: relative influences of fire, herbivory, rainfall and density dependence. J. Appl. Ecol. 38, 268–280. https://doi.org/10.1046/j.1365-2664.2001.00567.x

Rouse, J.W., Haas, R.H., Schell, J.A., Deering, D., Deering, W., 1974. Monitoring vegetation systems in the Great Plains with ERTS. NASA, Goddard Space Flight Center. 3d ERTS-1

Symp., Vol.1, Sect. A., paper A 20, 309–317. https://ntrs.nasa.gov/citations/19740022614

Rubio, J.L., Bochet, E., 1998. Desertification indicators as diagnosis criteria for desertification risk assessment in Europe. J. Arid Environ. 39, 113–120. https://doi.org/10.1006/jare.1998.0402

Ruppert, J.C., Harmoney, K., Henkin, Z., Snyman, H.A., Sternberg, M., Willms, W., Linstaedter, A., 2015. Quantifying drylands' drought resistance and recovery: the importance of drought intensity, dominant life history and grazing regime. Glob. Change Biol. 21, 1258–1270. https://doi.org/10.1111/gcb.12777

Safriel, U.N., 2006. Dryland development, desertification and security in the Mediterranean, in: Kepner, W.G., Rubio, J.L., Mouat, D.A., Pedrazzini, F. (Eds.), Desertification in the Mediterranean Region. A Security Issue. Springer Netherlands, Dordrecht, pp. 227–250.

Salvati, L., Kosmas, C., Kairis, O., Karavitis, C., Acikalin, S., Belgacem, A., Solé-Benet, A., Chaker, M., Fassouli, V., Gokceoglu, C., Gungor, H., Hessel, R., Khatteli, H., Kounalaki, A., Laouina, A., Ocakoglu, F., Ouessar, M., Ritsema, C., Sghaier, M., Sonmez, H., Taamallah, H., Tezcan, L., de Vente, J., 2015. Unveiling soil degradation and desertification risk in the Mediterranean basin: a data mining analysis of the relationships between biophysical and socioeconomic factors in agro-forest landscapes. J. Environ. Plan. Manag. 58, 1789–1803. https://doi.org/10.1080/09640568.2014.958609

Salvati, L., Zitti, M., 2009. Convergence or divergence in desertification risk? Scale-based assessment and policy implications in a Mediterranean country. J. Environ. Plan. Manag. 52, 957–971. https://doi.org/10.1080/09640560903181220

Salvati, L., Zitti, M., Ceccarelli, T., 2008. Integrating economic and environmental indicators in the assessment of desertification risk: a case study. Appl. Ecol. Environ. Res. 6, 129–138. https://doi.org/10.15666/aeer/0601_129138

Sander, H., Bollig, M., Linstädter, A., 1998. Himba paradise lost: Stability, degradation, and pastoralist management of the Omuhonga Basin (Namibia). Erde Z. Ges. Für Erdkd. Zu Berl. 129, 301–315.

Santini, M., Caccamo, G., Laurenti, A., Noce, S., Valentini, R., 2010. A multi-component GIS framework for desertification risk assessment by an integrated index. Appl. Geogr. 30, 394–415. https://doi.org/10.1016/j.apgeog.2009.11.003

Saruul, K., Jiangwen, L., Jianming, N., Qing, Z., Xuefeng, Z., Guodong, H., Mengli, Z., Haifeng, B., 2019. Typical steppe ecosystems maintain high stability by decreasing the connections among recovery, resistance, and variability under high grazing pressure. Sci. Total Environ. 659, 1146–1157. https://doi.org/10.1016/j.scitotenv.2018.12.447

Sauvage, C., 1961. Recherches géobotanique sur les Subéraies marocaines., Serie Botanique. Travoux de l'Institute Scientifique Chérifien.

Scheffer, M., 1990. Multiplicity of stable states in freshwater systems. Hydrobiologia 200–201, 475–486. https://doi.org/10.1007/BF02530365

Scheffer, M., Carpenter, S., Foley, J.A., Folke, C., Walker, B., 2001. Catastrophic shifts in ecosystems. Nature 413, 591–596. https://doi.org/10.1038/35098000

Scheffer, M., Carpenter, S.R., 2003. Catastrophic regime shifts in ecosystems: linking theory to observation. Trends Ecol. Evol. 18, 648–656. https://doi.org/10.1016/j.tree.2003.09.002

Scheffer, M., Carpenter, S.R., Dakos, V., van Nes, E.H., 2015. Generic indicators of ecological resilience: Inferring the chance of a critical transition. Annu. Rev. Ecol. Evol. Syst. 46, 145–167. https://doi.org/10.1146/annurev-ecolsys-112414-054242

Scheffer, M., Carpenter, S.R., Lenton, T.M., Bascompte, J., Brock, W., Dakos, V., van de Koppel, J., van de Leemput, I.A., Levin, S.A., van Nes, E.H., Pascual, M., Vandermeer, J., 2012. Anticipating critical transitions. Science 338, 344–348. https://doi.org/10.1126/science.1225244

Scheffer, M., Hosper, S.H., Meijer, M.-L., B. Moss, Jeppesen, E., 1993. Alternative equilibria in shallow lakes. Trends Ecol. Evol. 8, 275–279. https://doi.org/10.1016/0169-5347(93)90254-M

Scheffler, D., Hollstein, A., Diedrich, H., Segl, K., Hostert, P., 2017. AROSICS: An automated and robust open-source image co-registration software for multi-sensor satellite data. Remote Sens. 9, 676. https://doi.org/10.3390/rs9070676

Schelske, C., Brezonik, P., 1992. , in: Maurizi, S., Poillon, F. (Eds.), Restoration of Aquatic Ecosystems. National Academic Press, Washington DC, pp. 393–398.

Schmidt, G., Jenkerson, C.B., Masek, J., Vermote, E., Gao, F., 2013. Landsat ecosystem disturbance adaptive processing system (LEDAPS) algorithm description (Report No. 2013–1057), Open-File Report. Reston, VA. https://doi.org/10.3133/ofr20131057

Schneider, F.D., Kéfi, S., 2016. Spatially heterogeneous pressure raises risk of catastrophic shifts. Theor. Ecol. 9, 207–217. https://doi.org/10.1007/s12080-015-0289-1

Scholes, R.J., Archer, S.R., 1997. Tree-grass interactions in savannas. Annu. Rev. Ecol. Syst. 28, 517–544.

Schwalm, C.R., Anderegg, W.R.L., Michalak, A.M., Fisher, J.B., Biondi, F., Koch, G., Litvak, M., Ogle, K., Shaw, J.D., Wolf, A., Huntzinger, D.N., Schaefer, K., Cook, R., Wei, Y., Fang, Y., Hayes, D., Huang, M., Jain, A., Tian, H., 2017. Global patterns of drought recovery. Nature 548, 202–205. https://doi.org/10.1038/nature23021

Showers, K.B., 2005. Imperial gullies: Soil erosion and conservation in Lesotho. Ohio University Press, Athens, Ohio, USA.

Sietz, D., Fleskens, L., Stringer, L.C., 2017. Learning from non-linear ecosystem dynamics is vital for achieving land degradation neutrality. Land Degrad. Dev. 28, 2308–2314. https://doi.org/10.1002/ldr.2732

Simoniello, T., Lanfredi, M., Liberti, M., Coppola, R., Macchiato, M., 2008. Estimation of vegetation cover resilience from satellite time series. Hydrol. Earth Syst. Sci. 12, 1053–1064. https://doi.org/10.5194/hess-12-1053-2008

Strogatz, S.H., 1994. Nonlinear dynamics and chaos: With applications to physics, biology, chemistry and engineering. Addison-Wesley, Reading, Massachusetts.

Taguas, E.V., Carpintero, E., Ayuso, J.L., 2013. Assessing land degradation risk through the long-term analysis of erosivity: a case study in southern Spain. Land Degrad. Dev. 24, 179–187. https://doi.org/10.1002/ldr.1119

Thieken, A.H., Cammerer, H., Dobler, C., Lammel, J., Schöberl, F., 2016. Estimating changes in flood risks and benefits of non-structural adaptation strategies - a case study from Tyrol, Austria. Mitig. Adapt. Strateg. Glob. Change 21, 343–376. https://doi.org/10.1007/s11027-014-9602-3

Tietjen, B., Zehe, E., Jeltsch, F., 2009. Simulating plant water availability in dry lands under climate change: A generic model of two soil layers. Water Resour. Res. 45, n/a-n/a. https://doi.org/10.1029/2007WR006589

Tomaselli, R., 1977. The degradation of the Mediterranean maquis. Ambio, The Mediterranean: A Special Issue 6, 356–362.

Tombolini, I., Colantoni, A., Renzi, G., Sateriano, A., Sabbi, A., Morrow, N., Salvati, L., 2016. Lost in convergence, found in vulnerability: A spatially-dynamic model for desertification risk assessment in Mediterranean agro-forest districts. Sci. Total Environ. 569–570, 973–981. https://doi.org/10.1016/j.scitotenv.2016.06.049

Tucker, C.J., 1979. Red and photographic infrared linear combinations for monitoring vegetation. Remote Sens. Environ. 8, 127–150. https://doi.org/10.1016/0034-4257(79)90013-0

Turnbull, L., Wainwright, J., Brazier, R.E., 2008. A conceptual framework for understanding semi-arid land degradation: ecohydrological interactions across multiple-space and time scales. Ecohydrology 1, 23–34. https://doi.org/10.1002/eco.4

Turner, B.L., Kasperson, R.E., Matson, P.A., McCarthy, J.J., Corell, R.W., Christensen, L., Eckley, N., Kasperson, J.X., Luers, A., Martello, M.L., others, 2003. A framework for vulnerability analysis in sustainability science. Proc. Natl. Acad. Sci. 100, 8074–8079.

Turner, D.P., Ritts, W.D., Maosheng Zhao, Kurc, S.A., Dunn, A.L., Wofsy, S.C., Small, E.E., Running, S.W., 2006. Assessing interannual variation in MODIS-based estimates of gross primary production. IEEE Trans. Geosci. Remote Sens. 44, 1899–1907. https://doi.org/10.1109/TGRS.2006.876027

Ubugunov, L.L., Kulikov, A.I., Kulikov, M.A., 2011. On the application of risk analysis technology for assessment of the ecological hazard of desertification (by the example of Republic of Buryatia). Contemp. Probl. Ecol. 4, 178–185. https://doi.org/10.1134/S1995425511020093

UNCCD, 2020. United Nations Convention to Combat Desertification (UNCCD). Official website. https://www.unccd.int (accessed 24 April 2020).

UNCCD, 2013: Low, P.S. (ed) (2013) Economic and Social impacts of desertification, land degradation and drought. White Paper I. UNCCD 2nd Scientific Conference, prepared with the contributions of an international group of scientists.

UNCCD, 2009. Factsheets about the United Nations Convention to Combat Desertification. UNCCD publications, Bonn, Germany.

UNCCD, 1994. United Nations Convention to Combat Desertification. United Nations General Assembly, Paris, France.

UNDRR, 2019. Global Assessment Report on Disaster Risk Reduction. United Nations Office for Disaster Risk Reduction (UNDRR), Geneva, Switzerland.

UNISDR, 2015. Sendai Framework for Disaster Risk Reduction 2015-2030. United Nations International Strategy for Disaster Risk Reduction (UNISDR). The Framework was adopted at the Third UN World Conference on Disaster Risk Reduction in Sendai, Japan, on March 18, 2015.

UNISDR, 2009. 2009 UNISDR terminology on disaster risk reduction. United Nations International Strategy for Disaster Risk Reduction (UNISDR), Geneva, Switzerland.

Vallejo, V.R., Valdecantos, A., Mayor, Á.G., Christoforou, M., Geeson, N., 2014. Overgrazing in Cyprus - adaptions and degradation processes. CASCADE report series: Catastrophic Shifts in drylands: how can we prevent ecosystem degradation? https://esdac.jrc.ec.europa.eu/projects/CASCADE/Resources/RandiFinal_120814.pdf (accessed 19 January 2021).

van de Leemput, I.A., Dakos, V., Scheffer, M., van Nes, E.H., 2018. Slow recovery from local disturbances as an indicator for loss of ecosystem resilience. Ecosystems 21, 141–152. https://doi.org/10.1007/s10021-017-0154-8

van Nes, E.H., Scheffer, M., 2007. Slow Recovery from Perturbations as a Generic Indicator of a Nearby Catastrophic Shift. Am. Nat. 169, 738–747. https://doi.org/10.1086/516845

Verbesselt, J., Hyndman, R., Newnham, G., Culvenor, D., 2010a. Detecting trend and seasonal changes in satellite image time series. Remote Sens. Environ. 114, 106–115. https://doi.org/10.1016/j.rse.2009.08.014

Verbesselt, J., Hyndman, R., Zeileis, A., Culvenor, D., 2010b. Phenological change detection while accounting for abrupt and gradual trends in satellite image time series. Remote Sens. Environ. 114, 2970–2980. https://doi.org/10.1016/j.rse.2010.08.003

Verbesselt, J., Umlauf, N., Hirota, M., Holmgren, M., Van Nes, E.H., Herold, M., Zeileis, A., Scheffer, M., 2016. Remotely sensed resilience of tropical forests. Nat. Clim. Change 6, 1028–1031. https://doi.org/10.1038/nclimate3108

Verbesselt, J., Zeileis, A., Herold, M., 2012. Near real-time disturbance detection using satellite image time series. Remote Sens. Environ. 123, 98–108. https://doi.org/10.1016/j.rse.2012.02.022

Vetter, S., 2009. Drought, change and resilience in South Africa's arid and semi-arid rangelands. South Afr. J. Sci. 105, 29–33.

Vicente-Serrano, S.M., Gouveia, C., Camarero, J.J., Begueria, S., Trigo, R., Lopez-Moreno, J.I., Azorin-Molina, C., Pasho, E., Lorenzo-Lacruz, J., Revuelto, J., Moran-Tejeda, E., Sanchez-Lorenzo, A., 2013. Response of vegetation to drought time-scales across global land biomes. Proc. Natl. Acad. Sci. 110, 52–57. https://doi.org/10.1073/pnas.1207068110

Vogelmann, J.E., Gallant, A.L., Shi, H., Zhu, Z., 2016. Perspectives on monitoring gradual change across the continuity of Landsat sensors using time-series data. Remote Sens. Environ. https://doi.org/10.1016/j.rse.2016.02.060

von Keyserlingk, J., de Hoop, M., Mayor, A.G., Dekker, S.C., Rietkerk, M., Foerster, S., 2021. Resilience of vegetation to drought: Studying the effect of grazing in a Mediterranean rangeland using satellite time series. Remote Sens. Environ. 255, 112270. https://doi.org/10.1016/j.rse.2020.112270

Vorovencii, I., 2016. Assessing and monitoring the risk of land degradation in Baragan Plain, Romania, using spectral mixture analysis and Landsat imagery. Environ. Monit. Assess. 188. https://doi.org/10.1007/s10661-016-5446-5

Vorovencii, I., 2015. Assessing and monitoring the risk of desertification in Dobrogea, Romania, using Landsat data and decision tree classifier. Environ. Monit. Assess. 187. https://doi.org/10.1007/s10661-015-4428-3

Walker, B., Holling, C.S., Carpenter, S.R., Kinzig, A., 2004. Resilience, adaptability and transformability in social– ecological systems. Ecol. Soc. 9(2).

Wang, Y., Lehnert, L.W., Holzapfel, M., Schultz, R., Heberling, G., Görzen, E., Meyer, H., Seeber, E., Pinkert, S., Ritz, M., Fu, Y., Ansorge, H., Bendix, J., Seifert, B., Miehe, G., Long, R.-J., Yang, Y.-P., Wesche, K., 2018. Multiple indicators yield diverging results on grazing degradation and climate controls across Tibetan pastures. Ecol. Indic. 93, 1199–1208. https://doi.org/10.1016/j.ecolind.2018.06.021

Wang, Y., Zhang, J., Guo, E., Sun, Z., 2015. Fuzzy Comprehensive Evaluation-Based Disaster Risk Assessment of Desertification in Horqin Sand Land, China. Int. J. Environ. Res. Public. Health 12, 1703–1725. https://doi.org/10.3390/ijerph120201703

Washington-Allen, R., Ramsey, R., West, N., Norton, B., 2008. Quantification of the ecological resilience of drylands using digital remote sensing. Ecol. Soc. 13. https://doi.org/10.5751/ES-02489-130133

Watts, L.M., Laffan, S.W., 2014. Effectiveness of the BFAST algorithm for detecting vegetation response patterns in a semi-arid region. Remote Sens. Environ. 154, 234–245. https://doi.org/10.1016/j.rse.2014.08.023

Watts, L.M., Laffan, S.W., 2013. Sensitivity of the BFAST algorithm to MODIS satellite and vegetation index, in: Piantadosi, J., Anderssen, R.S., Boland, J. (Eds.), Presented at the 20th International Congress on Modelling and Simulation, Modelling & Simulation Soc Australia & New Zealand Inc, Adelaide, Australia.

Weinzierl, T., Wehberg, J., Böhner, J., Conrad, O., 2016. Spatial assessment of land degradation risk for the Okavango River catchment, Southern Africa. Land Degrad. Dev. 27, 281–294. https://doi.org/10.1002/ldr.2426

Weiss, J.L., Gutzler, D.S., Coonrod, J.E.A., Dahm, C.N., 2004. Long-term vegetation monitoring with NDVI in a diverse semi-arid setting, central New Mexico, USA. J. Arid Environ. 58, 249–272. https://doi.org/10.1016/j.jaridenv.2003.07.001

Whitford, W.G., Rapport, D.J., deSoyza, A.G., 1999. Using resistance and resilience measurements for “fitness” tests in ecosystem health. J. Environ. Manage. 57, 21–29. https://doi.org/10.1006/jema.1999.0287

World Meteorological Organization (WMO), 2021. Official Website. https://www.wmo.int/pages/prog/wcp/ccl/faqs.php#q3 (accessed 22 January 2021).

World Meteorological Organization (WMO) and Global Water Partnership (GWP), 2016: Handbook of Drought Indicators and Indices (M. Svoboda and B.A. Fuchs). Integrated Drought Management Programme (IDMP), Integrated Drought Management Tools and Guidelines Series 2. Geneva.

Zeileis, A., Kleiber, C., Krämer, W., Hornik, K., 2003. Testing and dating of structural changes in practice. Comput. Stat. Data Anal. 44, 109–123. https://doi.org/10.1016/S0167-9473(03)00030-6

Zeileis, A., Leisch, F., Hornik, K., Kleiber, C., 2002. strucchange. An R package for testing for structural change in linear regression models. J. Stat. Softw. 7, 1–38. https://doi.org/10.18637/jss.v007.i02

Zewdie, W., Csaplovics, E., Inostroza, L., 2017. Monitoring ecosystem dynamics in northwestern Ethiopia using NDVI and climate variables to assess long term trends in dryland vegetation variability. Appl. Geogr. 79, 167–178. https://doi.org/10.1016/j.apgeog.2016.12.019

Zhou, Z.C., Gan, Z.T., Shangguan, Z.P., Dong, Z.B., 2010. Effects of grazing on soil physical properties and soil erodibility in semiarid grassland of the Northern Loess Plateau (China). CATENA 82, 87–91. https://doi.org/10.1016/j.catena.2010.05.005

Zhu, Z., Woodcock, C.E., 2014. Continuous change detection and classification of land cover using all available Landsat data. Remote Sens. Environ. 144, 152–171. https://doi.org/10.1016/j.rse.2014.01.011

8 LIST OF ABBREVIATIONS

BFAST	Breaks for Additive Seasonal and Trend
BP	Breakpoint
DBP	Drought breakpoint
'eb classification' of resistance	Reclassification of resistance values based on *eb*-resistance
eb-resistance	Event-based resistance
ESA	European Space Agency
ETM+	Enhanced Thematic Mapper Plus instrument aboard the Landsat 7 satellite
FAO	Food and Agriculture Organization of the United Nations
GIS	Geographic information system (software)
H. year	Hydrological year
IPCC	Intergovernmental Panel on Climate Change
LADA	Land Degradation Assessment in Drylands (LADA)
LEDAPS	Landsat Ecosystem Disturbance Adaptive Processing System
'lt classification' of resistance	Reclassification of resistance values based on *lt*-resistance
lt-resistance	Long-term resistance
MEA	Millennium Ecosystem Assessment
NASA	National Aeronautics and Space Administration
NDVI	Normalized Difference Vegetation Index
NIR	Near Infrared
SD	Standard deviation
SRTM	Shuttle Radar Topography Mission
TM	Thematic Mapper instrument aboard the Landsat 4 and 5 satellites
UN	United Nations
UNCCD	United Nations Convention to Combat Desertification
UNDRR	United Nations Office for Disaster Risk Reduction
UNISDR	United Nations International Strategy for Disaster Risk Reduction
USGS	U.S. Geological Survey

9 GLOSSARY

Term	Description	References
Breakpoint	In the BFAST approach, breakpoints in NDVI time series indicate abrupt changes in additive seasonal and trend models, indicating effects of disturbance or land cover change. Methodologically, a breakpoint indicates a significant deviation from structural stability in a time series (assessed by a residuals-based Moving Sum (MOSUM) test).	Bai and Perron, 1998; Verbesselt et al., 2010a
Climate variability	"Variations in the mean state and other statistics of the climate on all temporal and spatial scales, beyond individual weather events." In this work the term climate variability is used to describe intra- and interannual variability in precipitation and drought events.	World Meteorological Organization (WMO), 2021
Desertification	Desertification means land degradation in arid, semi-arid, and dry sub-humid areas resulting from various factors, including climatic variations and human activities.	UNCCD, 1994
Disaster	A serious disruption of the functioning of a community or a society involving widespread human, material, economic or environmental losses and impacts, which exceeds the ability of the affected community or society to cope using its own resources.	UNISDR, 2009
Disaster mitigation	The lessening or limitation of the adverse impacts of hazards and related disasters.	UNISDR, 2009
Disaster preparedness	The knowledge and capacities developed by governments, professional response and recovery organizations, communities and individuals to effectively anticipate, respond to, and recover from, the impacts of likely, imminent or current hazard events or conditions.	UNISDR, 2009
Disaster prevention	The outright avoidance of adverse impacts of hazards and related disasters.	UNISDR, 2009
Disaster recovery	The restoration, and improvement where appropriate, of facilities, livelihoods and living conditions of disaster-affected communities, including efforts to reduce disaster risk factors.	UNISDR, 2009
Disaster response	The provision of emergency services and public assistance during or immediately after a disaster in order to save lives, reduce health impacts, ensure public safety and meet the basic subsistence needs of the people affected.	UNISDR, 2009
Disaster risk	The potential disaster losses, in lives, health status, livelihoods, assets and services, which	UNISDR, 2009

	could occur to a particular community or a society over some specified future time period.	
Disaster risk management	The systematic process of using administrative directives, organizations, and operational skills and capacities to implement strategies, policies and improved coping capacities in order to lessen the adverse impacts of hazards and the possibility of disaster.	UNISDR, 2009
Disaster risk reduction	The concept and practice of reducing disaster risks through systematic efforts to analyse and manage the causal factors of disasters, including through reduced exposure to hazards, lessened vulnerability of people and property, wise management of land and the environment, and improved preparedness for adverse events.	UNISDR, 2009
Drought breakpoint (DBP)	A breakpoint fitted by the BFAST approach to the NDVI-time series during the prolonged dry period 31.09.2004–01.10.2008 (h. years 2005–2008), if this breakpoint was associated with a drop in NDVI of at least 10% (calculated from mean NDVI 3 years before and after the breakpoint).	Own definition of term as used within this thesis
Drylands	Dry submhumid, semi-arid, arid or hyper-arid ecosystems; water-limited ecosystesm with low soil moisture due to a combination of low rainfall and high evaporation rate.	MEA, 2005; Safriel, 2006
Event-based resistance (*eb*-resistance)	Proxy for event-based resistance eb-resistance) to drought used in this thesis. Calculated as the relative difference in mean NDVI of the three years before and after the drought breakpoint, which occurred during the prolonged dry period 31.09.2004–01.10.2008.	Own definition of terms as used within this thesis
Ecological regime shift	A shift between alternative stable states in ecosystems. Accompanied by drastic changes in dynamic system behaviour.	Scheffer 2003; Hastings and Wysham, 2010
Ecological resilience	A system's ability to maintain its functional and structural integrity and persist without being pushed into an alternative stable state (basin of attraction) under the influence of disturbance.	Holling, 1996; 1973;
Exposure	People, property, systems, or other elements, present in hazard zones that are thereby subject to potential losses.	UNISDR, 2009
Hydrological year ('h. years')	In Cyprus (and generally the northern hemisphere): 1 October to 30 September; "the annual cycle that is associated with the natural progression of the hydrologic seasons. It commences with the start of the season of soil moisture recharge, includes the season of maximum runoff (or season of maximum groundwater recharge), if any, and concludes with the completion of the season of maximum	https://www.pik-potsdam.de/cigrasp-2/bg/glossary.html#H (accessed 20 January 2021)

	evapotranspiration (or season of maximum soil moisture utilization).” The hydrological year is designated by the calendar year in which it ends.	
Land degradation	Land degradation is a negative trend in land condition, caused by direct or indirect human-induced processes including anthropogenic climate change, expressed as long-term reduction or loss of at least one of the following: biological productivity, ecological integrity or value to humans.	IPCC, 2019
Long-term resistance (*lt*-resistance)	Proxy for long-term resistance eb-resistance) to climate variability used in this thesis. Measure based on the inverse of the total number of breakpoints fitted by BFAST during the study period (1984–2011).	Own definition of terms as used within this thesis
Natural disaster risk research	Natural disaster risk research based on the risk concept established within the UN Sendai Framework of Disaster Risk Reduction. Risk is composed of Hazard, Exposure and Vulnerability.	UNISDR, 2015
Natural hazard	Natural process or phenomenon that may cause loss of life, injury or other health impacts, property damage, loss of livelihoods and services, social and economic disruption, or environmental damage.	UNISDR, 2009
NDVI recovery trend	Proxy for the recovery rate of the vegetation after a drought event used in this thesis. Calculated as the slope of the linear trend component (parameter β) fitted by the BFAST model to the segment following the drought breakpoint occurring between 31.09.2004 and 01.10.2008 (h. years 2005–2008).	Own definition of terms as used within this thesis
Recovery rate	The return rate to equilibrium after a disturbance; also referred to as speed of recovery.	Pimm, 1984
Resistance	The instantaneous impact of exogenous disturbances on the system state.	Hodgson et al., 2015
Risk	The combination of the probability of an event and its negative consequences. Risk is composed of Hazard, Exposure and Vulnerability.	UNISDR, 2009
Risk assessment	A methodology to determine the nature and extent of risk by analysing potential hazards and evaluating existing conditions of vulnerability that together could potentially harm exposed people, property, services, livelihoods and the environment on which they depend.	UNISDR, 2009
Tipping point	A point where the system rapidly reorganizes into an alternative system state, represented by the hill tops in the ‘ball-in-a-cup’ model (see Figure 6 & Figure 7).	Kéfi et al., 2014; Scheffer et al., 2015

Vulnerability	The characteristics and circumstances of a community, system or asset that make it susceptible to the damaging effects of a hazard.	UNISDR, 2009